AD-A052 839 PENNSYLVANIA STATE UNIV UNIVERSITY PARK APPLIED RESE--ETC F/G 20/4
TABULATION AND SUMMARY OF THERMODYNAMIC EFFECTS DATA FOR DEVELO--ETC(U)
JAN 78 J W HOLL, M L BILLET, D S WEIR N00017-73-C-1418

UNCLASSIFIED TM-78-18 NL

1 OF 2

AD
A052839

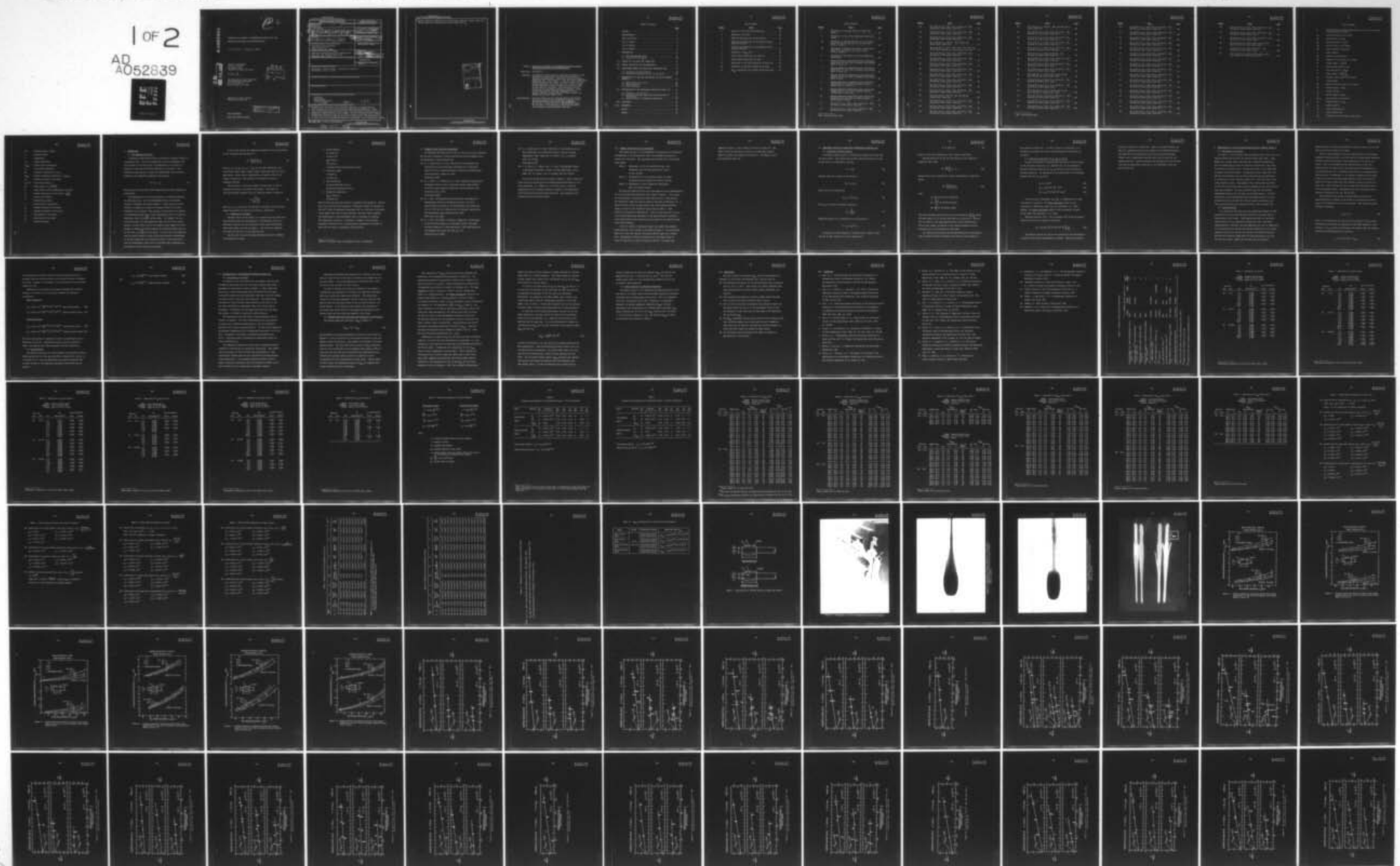

AD A052839

12

TABULATION AND SUMMARY OF THERMODYNAMIC EFFECTS DATA FOR

DEVELOPED CAVITATION ON OGIVE-NOSED BODIES

J. W. Holl, M. L. Billet, D. S. Weir

AD No.
DDC FILE COPY

Technical Memorandum
File No. TM 78-18
30 January 1978
Contract No. N00017-73-C-1418

Copy No. 9

The Pennsylvania State University
APPLIED RESEARCH LABORATORY
Post Office Box 30
State College, PA 16801

Approved for Public Release
Distribution Unlimited

NAVY DEPARTMENT

NAVAL SEA SYSTEMS COMMAND

UNCLASSIFIED

SECURITY CLASSIFICATION OF THIS PAGE (When Data Entered)

REPORT DOCUMENTATION PAGE		READ INSTRUCTIONS BEFORE COMPLETING FORM
1. REPORT NUMBER 14 TM-78-18	2. GOVT ACCESSION NO.	3. RECIPIENT'S CATALOG NUMBER
4. TITLE (and Subtitle) 6 TABULATION AND SUMMARY OF THERMODYNAMIC EFFECTS DATA FOR DEVELOPED CAVITATION ON OGIVE-NOSED BODIES,		5. TYPE OF REPORT & PERIOD COVERED 9 Technical Memo[redacted]m, 6. PERFORMING ORG. REPORT NUMBER
7. AUTHOR(s) 10 J. W. Holl, M. L. Billet D. S. Weir		8. CONTRACT OR GRANT NUMBER(s) 15 N00017-73-C-1418, NGL-39-009-001
9. PERFORMING ORGANIZATION NAME AND ADDRESS Applied Research Laboratory Post Office Box 30 State College, PA 16801		10. PROGRAM ELEMENT, PROJECT, TASK AREA & WORK UNIT NUMBERS
11. CONTROLLING OFFICE NAME AND ADDRESS National Aeronautics and Space Administration Mail Stop 5-9, 21000 Brookpark Road Cleveland, Ohio 44135		12. REPORT DATE 11 30 Jan[redacted]978 13. NUMBER OF PAGES 127 12 130p.
14. MONITORING AGENCY NAME & ADDRESS(if different from Controlling Office)		15. SECURITY CLASS. (of this report) UNCLASSIFIED 15a. DECLASSIFICATION/DOWNGRADING SCHEDULE

16. DISTRIBUTION STATEMENT (of this Report)

Approved for public release. Distribution unlimited.
Per NAVSEA - April 3, 1978

17. DISTRIBUTION STATEMENT (of the abstract entered in Block 20, if different from Report)

18. SUPPLEMENTARY NOTES

19. KEY WORDS (Continue on reverse side if necessary and identify by block number)

cavitation
hydrodynamics
thermodynamic effects

(T sub infinity) (Delta T) (C sub Q)

20. ABSTRACT (Continue on reverse side if necessary and identify by block number)

Thermodynamic effects data for developed cavitation on zero and quarter caliber ogives in Freon 113 and water are tabulated and summarized. These data include temperature depression (ΔT), flow coefficient (C_Q) and various geometrical characteristics of the cavity. For the ΔT tests, the free-stream temperature (T_∞) varied from 35°C to 95°C in Freon 113 and from 60°C to 125°C in water for a velocity range of 19.5 m/sec to 36.6 m/sec. Two correlations of the ΔT data by the entrainment method are presented. These correlations Over

DD FORM 1 JAN 73 1473 EDITION OF 1 NOV 65 IS OBSOLETE

UNCLASSIFIED

SECURITY CLASSIFICATION OF THIS PAGE (When Data Entered)

391 007 JOB

involve different combinations of the Nusselt, Reynolds, Froude, Weber and Péclet numbers and dimensionless cavity length (L/D).

Subject: Tabulation and Summary of Thermodynamic Effects Data for Developed Cavitation on Ogive-Nosed Bodies

References: See page 32.

Abstract: Thermodynamic effects data for developed cavitation on zero and quarter caliber ogives in Freon 113 and water are tabulated and summarized. These data include temperature depression (ΔT), flow coefficient (C_Q) and various geometrical characteristics of the cavity. For the ΔT tests, the free-stream temperature (T_∞) varied from 35°C to 95°C in Freon 113 and from 60°C to 125°C in water for a velocity range of 19.5 m/sec to 36.6 m/sec. Two correlations of the ΔT data by the entrainment method are presented. These correlations involve different combinations of the Nusselt, Reynolds, Froude, Weber and Péclet numbers and dimensionless cavity length (L/D).

Acknowledgments: The major portion of the technical work on the research program was sponsored by the National Aeronautics and Space Administration under Grant NGL 39-009-001. Mr. Werner R. Britsch of NASA is the technical monitor of this grant. All reports as a result of this grant do not require security clearance from NASA.

Table of Contents

List of Tables

List of Figures

*QCO = Quarter-Caliber Ogive

*ZCO = Zero-Caliber Ogive

List of Symbols

A	- axial distance from the leading edge of the cavity to location of maximum cavity diameter
A_v	- cross-sectional area of cavity
A_w	- surface area of cavity
C_A	- area coefficient $\equiv A_w/D^2$
Cp_L	- specific heat of the liquid
C_Q	- flow coefficient $\equiv \dot{Q}_v/V_\infty D^2$
D	- model diameter
D_m	- maximum cavity diameter
D_T	- diameter of the tunnel test section
Fr	- Froude number $\equiv V_\infty/\sqrt{g\ D}$
g	- gravitational acceleration
h	- film coefficient $\equiv \dot{q}/A_w \Delta T$
J	- Jakob number $\equiv \Delta T / \frac{\rho_v}{\rho_L} \frac{\lambda}{Cp_L}$
K_L	- thermal conductivity of the liquid
L	- cavity length
$\dot{m}_v$	- mass flow rate of vapor in the cavity
Nu	- Nusselt number $\equiv hD/K_L$
P_c	- cavity pressure
Pe	- Péclet number $\equiv V_\infty D/\alpha_L$
P_{G-S}	- gas pressure at saturation
Pr	- Prandtl number $\equiv \nu_L/\alpha_L$
P_v	- vapor pressure
P_∞	- free-stream pressure
$\dot{q}$	- heat transfer rate
$\dot{Q}_v$	- volume flow rate of vapor in the cavity

Re	- Reynolds number $\equiv V_\infty D/\nu_L$
S	- surface tension
T	- temperature
T_c	- cavity temperature
$T_{c_{min}}$	- minimum cavity temperature
T_∞	- free-stream temperature
ΔT	- temperature depression $\equiv T_\infty - T_c$
ΔT_{max}	- maximum temperature depression $\equiv T_\infty - T_{c_{min}}$
V_v	- velocity of vapor in the cavity
V_∞ or V	- free-stream velocity
We	- Weber number $\equiv V_\infty \sqrt{D}/\sqrt{S/\rho_L}$
X	- axial distance from leading edge of the body
α_L	- thermal diffusivity of the liquid = $\dfrac{K_L}{C_{P_L}\ \rho_L}$
β	- Henry's law constant
γ	- dissolved gas content
λ	- latent heat of vaporization
μ_L	- dynamic viscosity of the liquid
ν_L	- kinematic viscosity of the liquid
ρ_L	- mass density of the liquid
ρ_v	- mass density of the vapor
σ	- cavitation number

I. INTRODUCTION

1.1 The Thermodynamic Effect

A continuous vaporization process is required to sustain a cavity in a cavitating flow. Since this vaporization process is dependent upon heat transfer at the cavity wall, the temperature in the cavity is always less than that of the bulk temperature of the fluid. This localized cooling process is called the thermodynamic effect which is measured by the temperature depression (ΔT) given by

$$\Delta T = T_\infty - T_c \tag{1}$$

where T_∞ and T_c are the bulk liquid temperature and cavity temperature, respectively.

The determination of the cavity pressure is of primary importance in cavitating flows. Thus the thermodynamic effect is important because it influences the cavity pressure. In many cases the cavity pressure is assumed to be equal to the vapor pressure at the bulk temperature of the liquid. This estimate is quite good in the absence of noncondensable gases and at states significantly below the critical temperature where P_v and $\frac{dP_v}{dT}$ are both small. For example, this is a very good estimate for room temperature water with a low gas content. However, for many fluids such as the cryogens liquid oxygen and liquid hydrogen as employed in rockets engines the operating temperatures can be such that P_v and $\frac{dP_v}{dT}$ are both large. In these cases, the assumption that the cavity pressure is equal to the vapor pressure corresponding to the bulk temperature of the liquid can lead to very large errors. Thus the thermodynamic effect must be considered when determining the net-positive suction head for rocket pumps.

In this investigation the temperature depression has been correlated by the entrainment equation given by

$$\Delta T = \frac{C_Q}{C_A} \frac{Pe}{Nu} \frac{\rho_v}{\rho_L} \frac{\lambda}{Cp_L} \tag{2}$$

where C_Q, C_A, Pe, Nu, ρ_v, ρ_L, λ, Cp_L are the flow coefficient, area coefficient, Péclét number, Nusselt number, vapor mass density, liquid mass density, latent heat of vaporization, and specific heat of the liquid, respectively. This equation is discussed in detail in subsequent sections.

The flow state of particular concern in this report is that of developed cavitation or so-called cavity flows. The extent of cavitation depends primarily upon the cavitation number (σ) given by

$$\sigma = \frac{P_\infty - P_c}{\frac{1}{2} \rho_L V_\infty^2} \tag{3}$$

where P_∞, P_c, ρ_L, and V_∞ are the pressure at infinity, cavity pressure, liquid mass density and velocity at infinity, respectively.

1.2 Objective of the Report

The major intent of this report is to organize the data which have been obtained during the investigations of thermodynamic effects in developed cavitation on zero and quarter caliber ogive nosed bodies. These model shapes are shown in Figure 1. The tests were conducted with Freon 113 and water as the working fluids.

The data fall into the following categories (see list of symbols for definition of terms):

1. Cavity geometry

   C_A versus L/D

   σ versus L/D

   D_M/D versus σ

   A/D versus σ

   σ versus L/D for various values of D/D_T

2. Cavitation number

   σ versus T_∞

   σ versus X/L

3. Flow coefficient

   C_Q (with diffusion) versus σ

   C_Q (without diffusion) versus σ

4. Temperature depression

   ΔT_{max} versus T_∞

   ΔT versus X/L

Most of these data have been reported in graphical form elsewhere. However, none of the data have been tabulated. Furthermore, except for examples in Weir [1]*, plots of temperature depression (ΔT) as a function of fractional cavity length (X/L) have not been reported. Thus this report completes the documentation of the experimental data by providing the necessary data tabulations and plots. In addition, a summary of the necessary background information such as description of experiments is provided in order that the report is reasonably self sufficient.

---

*Numbers in brackets refer to documents in list of references.

II. SOURCES OF DATA PLOTS AND TABULATIONS

As indicated previously plots of most of the data are given elsewhere. The six basic references in which these data are plotted together with an abbreviation of each reference are:

(1) M. L. Billet and D. S. Weir, "The Effect of Gas Diffusion and Vaporization on the Entrainment Coefficient for a Ventilated Cavity," TM 74-15, Applied Research Laboratory, The Pennsylvania State University, January 24, 1974.
Abbreviation BW74

(2) M. L. Billet, J. W. Holl and D. S. Weir, "Geometric Description of Developed Cavities on Zero- and Quarter-Caliber Ogive Bodies," TM 74-136, Applied Research Laboratory, The Pennsylvania State University, May 6, 1974.
Abbreviation BHW74

(3) D. S. Weir, "An Experimental and Theoretical Investigation of Thermodynamic Effects on Developed Cavitation," TM 75-34, Applied Research Laboratory, The Pennsylvania State University, Feb. 21, 1975 (or M. S. Thesis, Dept. of Aerospace Engineering, The Pennsylvania State University, May 1975).
Abbreviation W75 (ARL)

(4) D. S. Weir, "The Effect of Velcoity, Temperature, and Blockage on the Cavitation Number for a Developed Cavity," 1975 ASME Cavitation Number for a Developed Cavity," 1975 ASME Cavitation and Polyphase Flow Forum, May 1975, pp. 7-9.
Abbreviation W75 (ASME)

(5) M. L. Billet and D. S. Weir, "The Effect of Gas Diffusion on the Flow Coefficient for a Ventilated Cavity," Journal of Fluids Engineering, Trans. ASME, Vol. 97, Series 1, No. 4, December 1975, pp. 501-506.

Abbreviation BW75

(6) J. W. Holl, M. L. Billet, and D. S. Weir, "Thermodynamic Effects on Developed Cavitation," Journal of Fluids Engineering, Trans. ASME, Vol. 97, Series 1, No. 4, December 1975, pp. 507-513.

The sources of data plots are listed in Table 1. First, second and third sources are given using the aforementioned abbreviations for the basic references, i.e., HBW75, etc. The first source is the most comprehensive of the indicated sources in regard to the completeness of the plotted data and associated discussion. Data tabulations are presented at the end of this report.

III. GENERAL DESCRIPTION OF THE EXPERIMENTS

The primary purpose of the experimental investigation was to determine the magnitude of the thermodynamic effect on developed cavitation for various flow conditions. The experiments were divided into the following three phases:

Phase I — Measurement of the flow coefficient (C_Q), area coefficient (C_A) and other geometrical aspects of the cavities.

Phase II — Determination of the cavitation number (σ) based on measured cavity pressure for natural cavities.

Phase III — Measurement of cavity temperature depressions (ΔT) for natural cavities.

The principal facility used in this investigation was the NASA-sponsored 3.8 cm ultra-high speed cavitation tunnel shown in Figure 2. This tunnel has the capability of operating at high velocities over a wide pressure and temperature range with various fluids as described in Reference [2]. A second facility, a 30.5 cm water tunnel with a more limited operating range, was used for the ventilated cavity tests in Phase I. This facility is described in Reference [3]. Both of these facilities are part of the Fluids Engineering Department of the Applied Research Laboratory of The Pennsylvania State University and are housed in the Garfield Thomas Water Tunnel Building.

A total of fourteen sting-mounted ogive test models were employed having two basic nose contours as described in Figure 1. The zero-caliber ogive has a blunt nose whereas the quarter-caliber ogive has a rounded nose. Photographs of natural cavitation on a zero-caliber ogive in Freon 113 and water are shown in Figures 3A and 3B. Six models were

employed in Phase I, four in Phase II and four in Phase III. The Phase I tests are described in Section V of this report whereas Phase III results are presented in Section VI. The Phase II tests are discussed by Weir [1].

IV. ENTRAINMENT METHOD FOR CORRELATING TEMPERATURE DEPRESSION DATA

4.1 Derivation of Basic Equation

A developed vaporous cavity is continuously supplied with vapor from the cavity walls. This vaporization process requires energy in the form of heat which is transferred at the rate

$$\dot{q} = \lambda \dot{m}_v \quad . \tag{4}$$

The mass flow rate of vapor in the cavity is

$$\dot{m}_v = \rho_v V_v A_v \tag{5}$$

which can also be expressed as

$$\dot{m}_v = \rho_v D^2 V_\infty C_Q \tag{6}$$

where C_Q is the flow coefficient defined as

$$C_Q \equiv \frac{\dot{Q}_v}{D^2 V_\infty} \quad . \tag{7}$$

Employing Equation (6) in Equation (4) for $\dot{m}_v$ results in

$$\dot{q} = \rho_v \lambda C_Q D^2 V_\infty \quad . \tag{8}$$

Following the method employed in convective heat transfer theory the rate of heat transfer can also be expressed as

$$\dot{q} = h\ A_w(T_\infty - T_c) \tag{9}$$

where h is the film coefficient or heat transfer coefficient.

Equating Equations (8) and (9) and solving for the temperature depression (ΔT) yields

$$\Delta T = \frac{C_Q}{h} \frac{D^2}{A_w} V_\infty\ \lambda\ \rho_v \quad . \tag{10}$$

Equation (10) can be expressed in terms of dimensionless coefficients namely

$$\Delta T = \frac{C_Q}{C_A} \frac{Pe}{Nu} \frac{\rho_v}{\rho_L} \frac{\lambda}{Cp_L} \tag{11}$$

where

$$C_A = \frac{A}{D^2} \text{ is the area coefficient}$$

$$Pe = \frac{V_\infty\ D}{\alpha_L} \text{ is the Péclet number}$$

$$Nu = \frac{hD}{K_L} \text{ is the Nusselt number} \quad .$$

(Note that dividing Equation (11) by the fluid properties $\frac{\rho_v}{\rho_L} \frac{\lambda}{Cp_L}$ yields the Jakob number (J) on the left hand side of the equation.) Equation (11) is similar to the relationship derived by Holl and Wislicenus [4] but more closely corresponds to the relation proposed by Acosta and Parkin [5] in the discussion of that paper.

All temperature depression data obtained during this investigation were correlated by means of Equation (11) which was first applied to

this problem by Billet [6]. In order to obtain a correlation, it is necessary to determine the form of the dimensionless coefficients C_Q, C_A and Nu.

4.2 Correlation Equations for C_A, C_Q, Nu and ΔT

In order to determine an equation which correlates ΔT data by means of the entrainment equation, i.e., Equation (11), it is necessary to determine empirical equations for C_A, C_Q and Nu in terms of pertinent physical parameters. An examination of the problem led to the following general forms for C_A, C_Q and Nu:

$$C_A = C_1 \{L/D\}^a \tag{12}$$

$$C_Q = C_2 \, Re^b \, Fr^c \, We^d \, \{L/D\}^e \tag{13}$$

$$Nu = C_3 \, Re^f \, Fr^g \, We^h \, Pr^i \, \{L/D\}^j \quad . \tag{14}$$

As will be seen in subsequent sections, two combinations of terms were tried for C_Q and Nu. The <u>first correlation</u> refers to that correlation in which Weber number was not considered, i.e., d=h=0. Whereas, the <u>second correlation</u> refers to that correlation in which Froude number was eliminated, i.e., c=g=0.

Employing Equations (12) - (14) in Equation (11) yields the general empirical form for the temperature depression

$$\Delta T = C_4 (L/D)^k \, Re^\ell \, Fr^m \, We^n \, Pr^p \, Pe \, \frac{\rho_v}{\rho_L} \frac{\lambda}{c_{p_L}} \quad . \tag{15}$$

The unknown constants for all of the correlations were determined by a modified least-squares approximation technique. Taking the logarithm

reduces the equation to linear form. Then, as outlined by Becket and Hunt [7], minimizing the sum of the squares of the difference between the logarithm of the measured data and the correlative expression yields a set of simultaneous equations which can be solved for the unknown constants. Details concerning the application of this modified least-square approximation technique to the entrainment theory are given by Weir [1].

V. DETERMINATION OF THE FLOW COEFFICIENT AND CAVITY GEOMETRY (PHASE I)

5.1 Description of the Tests

For Phase I, six test models were used namely 0.318, 0.635, and 1.27 cm diameter models with both zero and quarter-caliber ogive noses. These models have a hollow center from which air is injected through holes near the leading edge to form the ventilated cavities and a tube along the surface of the model with a pressure port close to the leading edge to measure the cavity pressure. By measuring the gas volume flow rate ($\dot{Q}$) and cavity pressure (P_c) the flow coefficient (C_Q) was determined as a function of σ for a velocity range of 9.1 - 18.3 m/sec and various cavity lengths in water. Photographs of the cavities were also taken so that the cavity profile shape could be measured and the cavity surface area (A_w) determined. The area coefficient (C_A) was then found by nondimensionalizing A_w by the square of the model diameter. Detailed descriptions of the experimental method and resulting data for C_Q are presented by Billet and Weir [8], [9] and details concerning C_A and other geometrical data are presented by Billet, Holl, and Weir [10].

5.2 Flow Coefficient

It is well known that there are many similarities between the characteristics of natural and ventilated cavities for the same value of dimensionless cavity length. (This applies only when the ventilated cavity operates in the reentrant jet regime [8], [9].) The German hydrodynamicist H. Reichardt [11] was apparently the first to demonstrate this characteristic by showing that the drag coefficient for an axially symmetric body was the same for both natural and ventilated cavities provided the cavitation number based on cavity pressure was the same for both flow states. Billet [6] has shown that the geometric

characteristics of natural and ventilated cavities on ogives are the same when the cavitation number is the same.

Early in the development of the entrainment theory for correlating temperature depression data it was felt that the aforementioned similarity principle would be applicable to the volume flow rate of gas in the cavity. Thus it was assumed that the characteristics of the flow coefficient for the vapor flow in the cavity would be approximated by the flow coefficient for a ventilated cavity having the same geometrical characteristics. Furthermore, it was decided to minimize the diffusion of gas at the cavity wall and thereby produce a value of C_Q which was based on the entire volume flow rate required to sustain a cavity of a given size. Billet [6] was the first to apply the similarity concept to the entrainment theory. Subsequently this work was improved and is reported in References [1], [8], [9] and [12].

The diffusion of air across the cavity wall was minimized by maintaining the air pressure in the cavity at the saturation pressure (P_{G-S}) of the dissolved gas in the free stream. This pressure is given by Henry's law namely

$$P_{G-S} = \gamma\beta \tag{16}$$

where γ is the dissolved air content and β is the Henry's law constant. The dissolved air content was measured by a Van Slyke apparatus. Since we have $P_c = P_{G-S}$ to assure no diffusion, this implies that the reference pressure (P_∞) from Equation (3) is given by

$$P_\infty = 1/2\ \rho_L V_\infty^2 \sigma + P_{G-S} \quad . \tag{17}$$

It is apparent that diffusion cannot be entirely eliminated by this procedure since the cavity pressure is not precisely constant throughout the cavity. However, it does appear to yield satisfactory and consistent results [8], [9].

Application of the modified least-square approximation technique referred to in Section 4.2 to the C_Q data produced the following correlations:

First Correlation

$$C_Q = 0.424 \times 10^{-2} \left(\frac{L}{D}\right)^{0.69} Re^{0.16} Fr^{0.13} \quad \text{(zero-caliber ogive)} \quad (18)$$

$$C_Q = 0.320 \times 10^{-4} \left(\frac{L}{D}\right)^{0.74} Re^{0.46} Fr^{0.26} \quad \text{(quarter-caliber ogive)} \quad (19)$$

Second Correlation

$$C_Q = 0.225 \times 10^{-1} \left(\frac{L}{D}\right)^{0.69} Re^{-0.10} We^{0.40} \quad \text{(zero-caliber ogive)} \quad (20)$$

$$C_Q = 0.836 \times 10^{-3} \left(\frac{L}{D}\right)^{0.74} Re^{-0.06} We^{0.79} \quad \text{(quarter-caliber ogive)} \quad (21)$$

The first correlations are compared with plots of experimental data in References [8] and [9]. Experimental values of C_Q are tabulated in Table 2 and compared with values calculated from the correlations.

5.3 Cavity Geometry

The empirical equations for cavity geometry are tabulated in Table 3. These equations are for L/D, D_M/D, and A/D as a function of σ and C_A as a function of L/D. The area coefficient (C_A) empirical equations are of major interest in the temperature depression correlations and are given by

$$C_A = 4.59 \left(\frac{L}{D}\right)^{1.19} \quad \text{(zero-caliber ogives)} \tag{22}$$

and

$$C_A = 2.06 \left(\frac{L}{D}\right)^{1.18} \quad \text{(quarter-caliber ogives)} \quad . \tag{23}$$

VI. DETERMINATION OF THE TEMPERATURE DEPRESSION (PHASE III)

6.1 Description of the Tests

For Phase III, four test models were used namely 0.318 and 0.635 cm diameter models with both zero- and quarter-caliber ogive noses. A photograph of these models is shown in Figure 4. These models have three ports in which thermocouple beads are mounted in epoxy cement on the model surface and the thermocouple leads exit the tunnel through the hollow center of the model and sting mount. The thermocouples are mounted at three different axial positions on the model so that the axial distribution of temperature within the cavity could be determined. In addition, the two larger models have one tube along the surface of the model to monitor the cavity pressure.

The thermocouple wires were made of copper-constantan and were 0.010 cm in diameter. The cavity thermocouples were each connected in series with a downstream thermocouple so that the temperature depression (ΔT) could be measured directly. The free stream temperature was measured independently with a thermocouple references to a 0°C ice bath. In general, the accuracy of temperature measurements was ±0.3°C. Additional details concerning the thermocouple system are given in Reference [1].

All temperature readings were taken with an integrating digital voltmeter to time average any temperature fluctuations. This differs from the procedure of Billet [6] who used a galvanometer to take instantaneous readings and then only considered the minimum measured cavity temperatures. The averaging technique therefore produces smaller temperature depressions than those measured by Billet, but is more consistent with the steady-state entrainment analysis.

Temperature depressions were determined as a function of T_∞ for a velocity range of 19.5 to 36.6 m/sec at various cavity lengths for the flow test models. Free stream temperatures varied from 35°C to 95°C in Freon 113 and from 60°C to 125°C in water.

In order to minimize the effects of variations in the amount of noncondensable gas dissolved in the liquid, all temperature depression tests were run with the liquid near saturation. The saturated air content at 22°C and one atmosphere is about 14 ppm for water and 1200 ppm for Freon 113 where ppm is moles of air per million moles of the liquid solvent. It has been shown [13] however that variations in air content have little effect on the temperature depression for the fluids, models and flow conditions examined in this study.

6.2 Maximum Temperature Depression and Discussion of Correlations

The maximum temperature depression (ΔT_{max}) defined as

$$\Delta T_{max} = T_\infty - T_{c_{min}} \tag{24}$$

was determined by the method described in Section 6.3 and is shown in Figures 5 - 10 as a function of T_∞ for various velocities for the four models in Freon 113 and water. Each symbol is the average of at least ten data points. The solid lines are the values of ΔT_{max} calculated from the first correlation by the entrainment theory given in Table 4. Since both the first and second correlations were determined by the modified least-squares method referred to in Section 4.2 both correlations will give approximately the same result. This is shown in Table 6 where the experimental values of ΔT_{max} are compared with values calculated by both correlations.

The correlations of ΔT_{max} with the various flow parameters was obtained by the entrainment method presented in Section 4.2. The resulting correlations are presented in Tables 4 and 5 together with the correlations for C_Q and Nu. These correlations are compared with corresponding correlations for venturis in Reference [14]. The first correlation, which is presented in Table 4, did not include Weber number as a scaling parameter. The second correlation, which did not include Froude number as a scaling parameter, is given in Table 5. As indicated previously, values of ΔT_{max} calculated from the correlations are compared with the experimental values of ΔT_{max} in Table 6. The first correlation is the same as that given in References [1] and [12] except that small adjustments in the constants were made to account for the use of more recent thermodynamic properties of Freon 113. The empirical equations for the properties of Freon 113 and water are given in Tables 7 and 8, respectively. These equations were used in the process of finding correlation #1 and #2 for ΔT_{max}. Freon 113 and water fluid properties are tabulated in Tables 9 and 10. These data were obtained from References [17] - [22].

Referring to the data for C_Q, Nu, and ΔT for the first correlation (Table 4), it is seen that the correlations are consistent, i.e., the exponents of like terms have the same sign in corresponding correlations for the two ogives. Furthermore, the correlations for the ΔT_{max} data are nearly independent of Froude number. This is perhaps not surprising since the Froude number was rather high in these tests. This result suggested the possibility that Froude number could be eliminated in the expressions for C_Q, Nu and ΔT_{max} and that other parameters could be considered. Since the entrainment mechanism may

depend upon surface tension effects, it seemed reasonable to consider Weber number as a scaling parameter. Thus Froude number was replaced by Weber number and a second set of correlations for C_Q, Nu and ΔT_{max} were obtained as shown in Table 5.

Referring to the ogive data for C_Q, Nu, and ΔT_{max} in Table 5, it is seen that the exponents of like terms have the same sign and thus corresponding correlations for the two ogives are consistent. Furthermore, the exponents on the Weber number terms in Table 5 are consistently higher than the corresponding exponents on the Froude number terms in Table 4. Perhaps this indicates that in this instance the Weber number is better than Froude number as a scaling parameter.

As indicated in the foregoing discussion, the data for the two ogive families are consistent within the context of the entrainment theory for both correlations, i.e., exponents of like terms in the equations have the same sign. It is also interesting to compare the correlations for ΔT_{max} for the case of constant fluid properties where ΔT_{max} has the form

$$\Delta T_{max} = C\left(\frac{L}{D}\right)^{M_1} V_\infty^{M_2} D^{M_3} \tag{25}$$

in which the constants C, M_1, M_2, and M_3 are in general different for each configuration. These correlations are shown in Table 11 for the two ogives and two correlations. For a given model shape it is seen that the two correlations give nearly the same exponents for like terms. For the quarter-caliber ogives, ΔT_{max} increases with velocity (V_∞) and size (D) whereas the opposite trend is displayed by the zero-caliber ogives. As shown in Reference [14] in which data for

venturi, hydrofoils and ogives are compared, ΔT_{max} for venturis and hydrofoils also tend to increase with V_∞ and D. Thus the zero-caliber ogive tends to be the exception when examined for the case of constant fluid properties.

6.3 Axial Variation of Temperature Depression

The axial variation of the temperature depression along the cavity was found to be roughly linear with the maximum temperature depression occurring near the leading edge of the cavity. This is in agreement with other investigators [15], [16]. Therefore, to consistently determine the maximum temperature depression (ΔT_{max}) the axial distribution was extrapolated to the leading edge to determine ΔT_{max}. These extrapolations for all of the ΔT_{max} values plotted in Figures 5 - 10 are given in Figures 11 - 68. The indicated ΔT_{max} is shown in each figure and tabulated in Table 6.

VII. CONCLUSIONS

The major conclusions regarding ΔT_{max} from this investigation as documented in this report and References [1], [12] and [14] are:

(1) The temperature depression for the quarter-caliber ogives increases with T_∞, L/D, V_∞, and D. This result is in general agreement with other investigations of quarter-caliber ogives, hydrofoils, and venturis.

(2) The temperature depression for the zero-caliber ogives increases with T_∞ and L/D but tends to decrease with V_∞ and D.

(3) Both the first and second correlations show consistent results for the ogives within the context of the entrainment theory in that the exponents of like terms have the same sign in the expressions for C_Q, Nu and ΔT_{max}.

(4) The ΔT_{max} expressions for the ogives from the first correlation show that the Froude number term is very small and can be neglected. This result was the basis for obtaining the second correlation in which the Froude number was replaced by Weber number.

(5) For additional related conclusions the reader is referred to References [1], [12] and [14].

VIII. REFERENCES

1. Weir, D. S., "An Experimental and Theoretical Investigation of Thermodynamic Effects on Developed Cavitation," M.S. Thesis, The Pennsylvania State University, May 1975 (or ARL Technical Memorandum 75-34).

2. Weir, D. S., Billet, M. L. and Holl, J. W., "The 1.5-Inch Ultra-High-Speed Cavitation Tunnel at the Applied Research Laboratory of The Pennsylvania State University," ARL Technical Memorandum 75-188, July 10, 1975.

3. Holl, J. W., "Cavitation Research Facilities of the Ordnance Research Laboratory of The Pennsylvania State University," Proceedings of the Symposium on Cavitation Research Facilities and Techniques, ASME, May 18-20, 1964, pp. 11-18.

4. Holl, J. W. and Wislicenus, G. F., "Scale Effects on Cavitation," Journal of Basic Engineering, Trans. ASME, Vol. 83, Sept. 1961, pp. 385-398.

5. Acosta, A. J and Parkin, B. R., Discussion of Reference 4, Journal of Basic Engineering, Trans. ASME, Vol. 83, Sept. 1961, pp. 395-396.

6. Billet, M. L., "Thermodynamic Effects on Developed Cavitation in Water and Freon 113," M.S. Thesis, The Pennsylvania State University, March 1970.

7. Becket, R. and Hunt, J., "Numerical Calculations and Algarithms," McGraw-Hill, 1967.

8. Billet, M. L. and Weir, D. S., "The Effect of Gas Diffusion and Vaporization on the Entrainment Coefficient for a Ventilated Cavity," ARL Technical Memorandum 74-15, January 24, 1974.

9. Billet, M. L. and Weir, D. S., "The Effect of Gas Diffusion on the Flow Coefficient for a Ventilated Cavity," Journal of Fluids Engineering, Trans. ASME, Vol. 97, December 1975, pp. 501-506.

10. Billet, M. L., Holl, J. W., and Weir, D. S., "Geometric Description of Developed Cavities on Zero- and Quarter-Caliber Ogive Bodies," ARL Technical Memorandum 74-136, May 6, 1974.

11. Reichardt, H., "The Laws of Cavitation Bubbles at Axially Symmetrical Bodies in a Flow," Reports and Translations No. 766, Office of Naval Research, October 1947.

12. Holl, J. W., Billet, M. L., and Weir, D. S., "Thermodynamic Effects on Developed Cavitation," Journal of Fluids Engineering, Trans. ASME, Vol. 97, December 1975, pp. 507-514.

13. Fricks, E. E., "The Influence of Temperature, Velocity, Size, and Boundary Form on the Thermodynamic Effect in Developed Cavitation in Freon 113," M.S. Thesis, The Pennsylvania State University, March 1974.

14. Billet, M. L., Holl, J. W., and Weir, D. S., "Correlations by the Entrainment Theory of Thermodynamic Effects for Developed Cavitation in Venturis and Comparisons with Ogive Data," ARL Technical Memorandum 75-291, December 11, 1975 (or NASA CR-135018).

15. Gelder, T. F., Ruggeri, R. S., and Moore, R. D., "Cavitation Similarity Considerations Based on Measured Pressure and Temperature Depressions in Cavitated Regions of Freon 114," NASA TN D-3509, April 17, 1966.

16. Hord, J., Anderson, L. M., and Hall, W. J., "Cavitation in Liquid Cryogens I-Venturi," NASA CR-2054, May 1972.

17. Bennington, A. F. and McHarness, R. C. "The Thermodynamic Properties of Freon 113," Report T113A, E. I. duPont de Nemours and Company, Wilmington, Delaware, 1938.

18. "Transport Properties of Freon Fluorocarbons," Report C-30, E. I. duPont de Nemours and Company, Wilmington, Delaware, 1973.

19. "Surface Tension of the Freon Compounds," Report D-27, E. I. duPont de Nemours and Company, Wilmington, Delaware, 1967.

20. Keenan, J. H and Keyes, F. G., "Thermodynamic Properties of Steam," John Wiley, 1936.

21. Gebhart, B., "Heat Transfer," McGraw-Hill, 1961.

22. Vargaftik, N. B., "Tables on the Thermophysical Properties of Liquids and Gases," John Wiley, 2nd Edition, 1975.

Table 1 - Sources of Data Plots and Tabulations

	← SOURCES FOR DATA PLOTS	→		
	First	Second	Third	Table* Number
Area coefficient (C_A) versus dimensionless cavity length (L/D)	BHW74	W75(ARL)		3^+
Cavitation number (σ)** versus dimensionless cavity length (L/D)	BHW74	W75(ARL)		3^+
Dimensionless maximum cavity diameter (D_M/D) versus σ**	BHW74			3^+
Dimensionless location of maximum cavity diameter (A/D) versus σ**	BHW74			3^+
σ** versus L/D for various ratios of model to tunnel diameter (D/D_T)	W75(ARL)	W75(ASME)		--
σ** versus temperature at infinity (T_∞)	W75(ARL)	HBW75	W75(ASME)	--
σ*** versus X/L	W75(ARL)			--
C_Q (with diffusion) versus σ**	BW74	BW75		--
C_Q (without diffusion) versus σ**	BW74	BW75	W75(ARL)	2
Maximum temperature depression (ΔT_{max}) versus T_∞	This report	W75(ARL)	HBW75	6
Temperature depression (ΔT) versus X/L	This report	W75(ARL)		--

*This is the table number for data tabulations in this report.

**σ based on cavity pressure at first tap.

***σ based on local cavity pressure corresponding to X/L.

Table 2 - Tabulation of C_Q Data

MODEL: Quarter-Caliber Ogive
DIAMETER: 0.318 cm (0.125 inch)
FLUID: Water at 21.1°C (70°F)

Velocity			C_Q	C_Q Correlations	
fps	mps	L/D	Experimental*	First	Second
30	9.15	3.5	0.030	0.026	0.029
		3.5	0.028	"	"
		5.0	0.034	0.033	0.038
		5.0	0.033	"	"
		7.0	0.038	0.043	0.049
		7.0	0.037	"	"
		10.0	0.040	0.056	0.063
		10.0	0.040	"	"
45	13.725	3.5	0.050	0.034	0.039
		3.5	0.044	"	"
		5.0	0.052	0.045	0.051
		5.0	0.054	"	"
		7.0	0.060	0.058	0.065
		7.0	0.057	"	"
		10.0	0.057	0.075	0.085
		10.0	0.061	"	"
60	18.300	3.5	0.069	0.042	0.048
		3.5	0.071	"	"
		5.0	0.075	0.055	0.063
		5.0	0.078	"	"
		7.0	0.088	0.071	0.081
		7.0	0.087	"	"
		10.0	0.096	0.092	0.105
		10.0	0.095	"	"

*Experiments conducted in 30.5 cm (12 inch) water tunnel.

Table 2 - Tabulation of C_Q Data (Cont.)

MODEL: Quarter-Caliber Ogive
DIAMETER: 0.635 cm (0.25 inch)
FLUID: Water at 21.1°C (70°F)

Velocity fps	Velocity mps	L/D	C_Q Experimental*	C_Q Correlations First	C_Q Correlations Second
30	9.15	2.0	0.022	0.021	0.024
		2.0	0.030	"	"
		3.5	0.042	0.032	0.037
		3.5	0.046	"	"
		5.0	0.055	0.042	0.048
		5.0	0.058	"	"
		8.0	0.060	0.060	0.068
		8.0	0.064	"	"
		10.0	0.068	0.070	0.080
		10.0	0.070	"	"
45	13.725	2.0	0.034	0.029	0.033
		2.0	0.035	"	"
		3.5	0.055	0.043	0.049
		3.5	0.058	"	"
		5.0	0.071	0.056	0.064
		5.0	0.075	"	"
		8.0	0.085	0.080	0.091
		8.0	0.090	"	"
		10.0	0.100	0.094	0.107
		10.0	0.108	"	"
60	18.300	2.0	0.037	0.035	0.040
		2.0	0.040	"	"
		3.5	0.065	0.053	0.061
		3.5	0.069	"	"
		5.0	0.085	0.069	0.079
		5.0	0.087	"	"
		8.0	0.110	0.098	0.112
		10.0	0.134	0.116	0.132

*Experiments conducted in 30.5 cm (12 inch) water tunnel.

Table 2 - Tabulation of C_Q Data (Cont.)

MODEL: Quarter-Caliber Ogive
DIAMETER: 1.27 cm (0.50 inch)
FLUID: Water at 21.1°C (70°F)

Velocity			C_Q	C_Q Correlations	
fps	mps	L/D	Experimental*	First	Second
30	9.15	1.0	0.017	0.016	0.018
		1.0	0.017	"	"
		1.75	0.029	0.024	0.028
		1.75	0.030	"	"
		2.5	0.040	0.032	0.036
		2.5	0.039	"	"
		3.5	0.054	0.041	0.046
		3.5	0.057	"	"
		5.0	0.070	0.053	0.060
		5.0	0.070	"	"
45	13.725	1.0	0.019	0.022	0.025
		1.0	0.018	"	"
		1.75	0.035	0.032	0.037
		1.75	0.036	"	"
		2.5	0.050	0.042	0.049
		2.5	0.053	"	"
		3.5	0.070	0.054	0.062
		3.5	0.073	"	"
		5.0	0.090	0.071	0.082
		5.0	0.098	"	"
60	18.300	1.0	0.017	0.026	0.030
		1.0	0.017	"	"
		1.75	0.036	0.040	0.046
		1.75	0.037	"	"
		2.5	0.054	0.052	0.060
		2.5	0.055	"	"
		3.5	0.075	0.067	0.077
		3.5	0.078	"	"

*Experiments conducted in 30.5 cm (12 inch) water tunnel.

Table 2 - Tabulation of C_Q Data (Cont.)

MODEL: Zero-Caliber Ogive
DIAMETER: 0.318 cm (0.125 inch)
FLUID: Water at 21.1°C (70°F)

Velocity			C_Q	C_Q Correlations	
fps	mps	L/D	Experimental*	First	Second
30	9.15	3.5	0.092	0.087	0.098
		3.5	0.095	"	"
		5.0	0.126	0.112	0.126
		5.0	0.128	"	"
		7.0	0.135	0.141	0.159
		7.0	0.138	"	"
		7.0	0.143	"	"
45	13.725	3.5	0.112	0.098	0.111
		3.5	0.113	"	"
		5.0	0.151	0.126	0.142
		5.0	0.155	"	"
		7.0	0.167	0.158	0.179
		7.0	0.170	"	"
60	18.300	3.5	0.120	0.107	0.121
		3.5	0.123	"	"
		5.0	0.150	0.137	0.155
		5.0	0.158	"	"
		7.0	0.182	0.172	0.196
		7.0	0.187	"	"

*Experiments conducted in 30.5 cm (12 inch) water tunnel.

Table 2 - Tabulation of C_Q Data (Cont.)

MODEL: Zero-Caliber Ogive
DIAMETER: 0.635 cm (0.25 inch)
FLUID: Water at 21.1°C (70°F)

Velocity fps	Velocity mps	L/D	C_Q Experimental*	C_Q Correlations First	C_Q Correlations Second
30	9.15	2.0	0.061	0.063	0.072
		2.0	0.062	"	"
		3.5	0.100	0.093	0.106
		3.5	0.103	"	"
		5.0	0.131	0.119	0.135
		5.0	0.135	"	"
		8.0	0.170	0.165	0.187
		8.0	0.175	"	"
		10.0	0.200	0.192	0.218
		10.0	0.203	"	"
45	13.725	2.0	0.048	0.071	0.081
		2.0	0.053	"	"
		3.5	0.105	0.105	0.119
		3.5	0.110	"	"
		5.0	0.158	0.134	0.152
		5.0	0.160	"	"
		8.0	0.203	0.186	0.211
		8.0	0.214	"	"
		10.0	0.228	0.216	0.246
		10.0	0.236	"	"
60	18.300	2.0	0.040	0.077	0.088
		2.0	0.040	"	"
		3.5	0.113	0.114	0.130
		3.5	0.115	"	"
		5.0	0.160	0.146	0.166
		5.0	0.163	"	"

*Experiments conducted in 30.5 cm (12 inch) water tunnel.

Table 2 - Tabulation of C_Q Data (Cont.)

MODEL: Zero-Caliber Ogive
DIAMETER: 1.27 cm (0.5 inch)
FLUID: Water at 21.1°C (70°F)

Velocity			C_Q	C_Q Correlations	
fps	mps	L/D	Experimental*	First	Second
30	9.15	1.25	0.080	0.049	0.056
		1.25	0.085	"	"
		1.25	0.085	"	"
		1.25	0.085	"	"
		1.80	0.107	0.063	0.071
		1.80	0.110	"	"
		1.80	0.113	"	"
		1.80	0.115	"	"
		1.80	0.119	"	"
		2.5	0.148	0.079	0.090
		2.5	0.155	"	"
		2.5	0.165	"	"

*Experiments conducted in 30.5 cm (12 inch) water tunnel.

Table 3 - Empirical Equations for Cavity Geometry

Zero-Caliber Ogive	Quarter-Caliber Ogive
$\sigma = 0.751 \left(\frac{L}{D}\right)^{-0.75}$	$\sigma = 0.460 \left(\frac{L}{D}\right)^{-0.66}$
$\frac{D_M}{D} = 1.43\ \sigma^{-0.34}$	$\frac{D_M}{D} = 1.02\ \sigma^{-0.36}$
$\frac{A}{D} = 0.557\ \sigma^{-1.22}$	$\frac{A}{D} = 0.196\ \sigma^{-1.47}$
$C_A = 4.59 \left(\frac{L}{D}\right)^{1.19}$	$C_A = 2.06 \left(\frac{L}{D}\right)^{1.18}$

where

σ = cavitation number based on cavity pressure

L = length of cavity

D = maximum body diameter

D_M = maximum diameter of the cavity

A = axial distance from the leading edge of the cavity to the location of maximum cavity diameter

$C_A = \frac{A_w}{D^2}$ = area coefficient

A_w = surface area of cavity.

Table 4

Constants and Exponents for Entrainment Theory - First Correlation

Model	Quantity	Eq. No.	Constant C_2, C_3 or C_4	L/D Exp.	Re Exp.	Fr Exp.	We Exp.	Pr Exp.	Pe Exp.
Zero-Caliber Ogive	C_Q	13	0.424×10^{-2}	0.69	0.16	0.13	0	----	----
	Nu^*	14	0.148×10^{-3}	-1.33	1.39	0.15	0	0.85	----
	ΔT^*_{max}	15	6.221	0.83	-1.23	-0.02	0	-0.85	1.0
Quarter-Caliber Ogive	C_Q	13	0.320×10^{-4}	0.74	0.46	0.26	0	----	----
	Nu^*	14	0.464×10^{-2}	-0.70	1.03	0.30	0	0.41	----
	ΔT^*_{max}	15	0.335×10^{-2}	0.26	-0.57	-0.04	0	-0.41	1.0

Zero-Caliber Ogives: $C_A = 4.59\ (L/D)^{1.19}$

Quarter-Caliber Ogives: $C_A = 2.06\ (L/D)^{1.18}$

*These correlations are the same as those given in References [1] and [12] except for small adjustments in the constants due to the use of new fluid property data for Freon 113.

Table 5

Constants and Exponents for Entrainment Theory - Second Correlation

Model	Quantity	Eq. No.	Constant C_2, C_3 or C_4	L/D Exp.	Re Exp.	Fr Exp.	We Exp.	Pr Exp.	Pe Exp.
Zero-Caliber Ogive	C_Q	13	0.225×10^{-1}	0.69	-0.10	0	0.40	----	----
	Nu	14	0.415×10^{-2}	-1.37	0.90	0	0.68	0.64	----
	ΔT_{max}	15	1.183	0.87	-1.00	0	-0.28	-0.64	1.0
Quarter-Caliber Ogive	C_Q	13	0.836×10^{-3}	0.74	-0.06	0	0.79	----	----
	Nu	14	0.271	-0.70	0.41	0	0.93	0.31	----
	ΔT_{max}	15	1.498×10^{-3}	0.26	-0.47	0	-0.14	-0.31	1.0

Zero-Caliber Ogives: $C_A = 4.59\ (L/D)^{1.19}$

Quarter-Caliber Ogives: $C_A = 2.06\ (L/D)^{1.18}$

Table 6 - Tabulation of ΔT_{max} Data

MODEL: Quarter-Caliber Ogive
DIAMETER: 0.635 cm (0.25 inch)
FLUID: Freon 113

Velocity		Temperature			ΔT_{max} Experimental		Figure*	ΔT_{max} 1st Corr.**		ΔT_{max} 2nd Corr.***	
fps	mps	°F	°C	L/D	°F	°C	Number	°F	°C	°F	°C
64	19.5	103.6	39.8	2.0	3.1	1.72	11	2.57	1.43	2.59	1.44
		103.8	39.9	3.5	3.4	1.89	11	3.00	1.67	3.02	1.68
		104.5	40.3	5.0	3.7	2.06	11	3.34	1.86	3.36	1.87
		120.6	49.2	2.0	3.8	2.11	12	3.43	1.91	3.44	1.91
		122.5	50.2	3.5	4.1	2.27	12	4.12	2.29	4.12	2.29
		122.4	50.2	5.0	4.2	2.33	12	4.51	2.51	4.53	2.52
		140.2	60.1	2.0	5.6	3.11	13	4.66	2.59	4.66	2.59
		141.9	61.1	3.5	5.9	3.28	13	5.55	3.08	5.55	3.08
		142.0	61.1	5.0	6.2	3.44	13	6.02	3.34	6.03	3.35
		158.6	70.3	2.0	7.2	4.00	14	6.08	3.38	6.07	3.37
		160.5	71.4	3.5	7.7	4.27	14	7.25	4.03	7.24	4.02
		161.7	72.1	5.0	8.1	4.50	14	8.10	4.50	8.09	4.49
		179.4	81.9	2.0	9.4	5.22	15	8.00	4.44	8.04	4.47
		181.6	83.1	3.5	10.0	5.56	15	9.60	5.33	9.55	5.31
		180.8	82.7	5.0	10.0	5.56	15	10.45	5.81	10.41	5.78
		199.9	93.3	2.0	11.6	6.44	16	10.35	5.75	10.24	5.69
120	36.6	120.5	49.2	2.0	3.6	2.00	17	4.35	2.42	4.37	2.43
		127.9	53.3	2.0	4.3	2.39	17	4.90	2.72	4.92	2.73
		115.5	46.4	3.5	4.0	2.22	17	4.65	2.58	4.68	2.60
		124.6	51.4	3.5	4.9	2.72	17	5.39	2.99	5.43	3.02
		110.2	43.4	5.0	4.9	2.72	17	4.68	2.60	4.72	2.62
		122.2	50.1	5.0	5.9	3.28	17	5.71	3.17	5.75	3.19
		147.2	64.0	2.0	5.9	3.28	18	6.56	3.64	6.57	3.65
		144.3	62.4	3.5	7.0	3.88	18	7.30	4.06	7.32	4.07
		141.2	60.7	5.0	7.4	4.11	18	7.67	4.26	7.70	4.28
		165.2	74.0	2.0	7.9	4.39	19	8.46	4.70	8.45	4.69
		162.5	72.5	3.5	8.4	4.67	19	7.67	4.27	7.68	4.27
		160.4	71.3	5.0	9.3	5.17	19	10.11	5.62	10.21	5.67
		182.6	83.7	2.0	11.2	6.22	20	10.63	5.91	10.60	5.89
		181.0	82.8	3.5	11.6	6.44	20	12.09	6.72	12.07	6.71
		179.4	81.9	5.0	12.3	6.83	20	13.03	7.24	13.01	7.23
		202.4	94.7	2.0	12.8	7.11	21	13.53	7.52	13.41	7.45
		201.9	94.4	3.5	13.4	7.44	21	15.61	8.67	15.50	8.61
		201.0	93.9	5.0	15.9	8.83	21	16.99	9.44	16.88	9.38

*Figure number for ΔT versus X/L plot.

**The first correlation involves the dimensionless parameters Fr, Re, Pr, Pe, L/D.

***The second correlation involves the dimensionless parameters We, Re, Pr, Pe, L/D.

Table 6 - Tabulation of ΔT_{max} Data (Cont.)

MODEL: Quarter-Caliber Ogive
DIAMETER: 0.318 cm (0.125 inch)
FLUID: Freon 113

Velocity		Temperature			ΔT_{max} Experimental		Figure*	ΔT_{max} 1st Corr.		ΔT_{max} 2nd Corr.	
fps	mps	°F	°C	L/D	°F	°C	Number	°F	°C	°F	°C
64	19.5	118.8	48.2	4.0	2.6	1.44	22	2.93	1.63	2.93	1.63
		121.9	49.9	5.2	2.9	1.61	22	3.30	1.83	3.31	1.84
		125.7	52.1	7.0	3.0	1.67	22	3.80	2.11	3.81	2.12
		135.2	57.3	4.0	3.1	1.72	23	3.80	2.11	3.79	2.11
		139.5	59.7	5.2	3.6	2.00	23	4.35	2.42	4.34	2.41
		144.1	62.3	7.0	3.9	2.17	23	3.82	2.12	3.82	2.12
		154.2	67.9	4.0	4.6	2.55	24	5.01	2.78	5.01	2.78
		163.9	73.3	5.2	5.2	2.89	24	7.11	3.95	7.07	3.93
		162.7	72.6	7.0	5.8	3.22	24	6.57	3.65	6.54	3.63
		180.2	82.3	4.0	7.0	3.89	25	7.14	3.97	7.09	3.94
		174.5	79.2	5.2	8.3	4.61	25	7.11	3.95	7.07	3.93
		180.0	82.2	7.0	8.6	4.78	25	8.27	4.59	8.22	4.57
		198.4	92.4	4.0	8.2	4.56	26	8.94	4.97	8.84	4.91
90	27.4	118.0	47.8	4.0	3.1	1.72	27	3.30	1.83	3.30	1.83
		117.1	47.3	5.2	3.2	1.78	27	3.48	1.93	3.46	1.92
		115.9	46.6	7.0	3.8	2.11	27	3.69	2.05	3.70	2.06
		130.8	54.9	4.0	4.0	2.22	28	4.04	2.24	4.04	2.24
		130.3	54.6	5.2	4.4	2.44	28	4.30	2.39	4.30	2.39
		130.6	54.8	7.0	4.4	2.44	28	4.67	2.59	4.68	2.60
		153.7	67.6	4.0	6.2	3.44	29	5.67	3.15	5.67	3.15
		155.5	68.6	5.2	6.8	3.78	29	6.25	3.47	6.24	3.47
		158.8	70.4	7.0	8.2	4.56	29	7.08	3.93	7.07	3.93
		180.1	82.3	4.0	10.6	5.89	30	8.12	4.51	8.07	4.48
120	36.6	131.4	55.2	4.0	4.6	2.56	31	4.55	2.53	4.56	2.54
		128.4	53.6	5.2	4.8	2.67	31	4.65	2.58	4.66	2.59
		125.5	51.9	7.0	5.1	2.83	31	4.81	2.67	4.83	2.68
		144.0	62.2	4.0	5.6	3.11	32	5.50	3.06	5.51	3.06
		141.7	60.9	5.2	6.2	3.44	32	5.70	3.17	5.71	3.17
		137.6	58.7	7.0	6.6	3.67	32	5.80	3.22	5.82	3.23
		162.6	72.6	4.0	7.6	4.22	33	7.17	3.98	7.16	3.98
		162.6	72.6	5.2	8.4	4.67	33	7.69	4.27	7.68	4.27
		161.4	71.9	7.0	8.8	4.89	33	8.19	4.55	8.18	4.54
		183.2	84.0	4.0	8.8	4.89	34	9.42	5.23	9.37	5.21
		181.2	82.9	5.2	9.8	5.44	34	9.85	5.47	9.80	5.44
		178.3	81.3	7.0	11.1	6.17	34	10.27	5.71	10.23	5.68

*Figure number for ΔT versus X/L plot.

Table 6 - Tabulation of ΔT_{max} Data (Cont.)

MODEL: Quarter-Caliber Ogive
DIAMETER: 0.318 cm (0.125 inch)
FLUID: Freon 113

Velocity		Temperature			ΔT_{max} Experimental		Figure*	ΔT_{max} 1st Corr.		2nd Corr.	
fps	mps	°F	°C	L/D	°F	°C	Number	°F	°C	°F	°C
120	36.6	188.0	86.7	4.0	10.2	5.67	35	10.00	5.56	9.94	5.52
		187.1	86.2	5.2	11.4	6.33	35	10.61	5.89	10.55	5.86
		195.5	90.8	4.0	11.2	6.22	36	10.96	6.09	10.88	6.04
		200.8	93.8	5.2	13.3	7.39	36	12.52	6.96	12.41	6.89
		201.9	94.4	7.0	14.0	7.78	36	13.72	7.62	13.60	7.56

MODEL: Quarter-Caliber Ogive
DIAMETER: 0.635 cm (0.25 inch)
FLUID: Water

Velocity		Temperature			ΔT_{max} Experimental		Figure*	ΔT_{max} 1st Corr.		2nd Corr.	
fps	mps	°F	°C	L/D	°F	°C	Number	°F	°C	°F	°C
64	19.5	149.1	65.1	2.0	0.2	0.11	37	0.21	0.12	0.21	0.12
		150.4	65.8	3.5	0.3	0.17	37	0.25	0.14	0.25	0.14
		151.9	66.6	5.0	0.3	0.17	37	0.28	0.16	0.28	0.16
		200.4	93.6	2.0	0.5	0.28	38	0.56	0.31	0.56	0.31
		202.6	94.8	3.5	0.6	0.33	38	0.68	0.38	0.68	0.38
		204.5	95.8	5.0	0.7	0.39	38	0.77	0.43	0.77	0.43
		245.0	118.3	2.0	1.2	0.67	39	1.17	0.65	1.16	0.64
		247.8	119.9	3.5	1.4	0.78	39	1.42	0.79	1.41	0.78
		250.3	121.3	5.0	1.5	0.83	39	1.85	1.03	1.85	1.03
120	36.6	148.6	64.8	2.0	0.16	0.09	40	0.21	0.12	0.20	0.11
		148.5	64.7	3.5	0.2	0.11	40	0.25	0.14	0.24	0.13
		148.2	64.6	5.0	0.4	0.22	40	0.43	0.24	0.43	0.24
		196.9	91.6	2.0	0.6	0.33	41	0.67	0.37	0.67	0.37
		196.3	91.3	3.5	1.0	0.56	41	0.77	0.43	0.78	0.43
		194.8	90.4	5.0	1.3	0.72	41	0.85	0.47	0.85	0.47
		251.8	122.1	2.0	1.6	0.89	42	1.65	0.92	1.64	0.91
		249.5	120.8	3.5	1.9	1.06	42	1.84	1.02	1.84	1.02
		247.0	119.4	5.0	2.0	1.11	42	1.96	1.09	1.96	1.09

*Figure number for ΔT versus X/L plot.

Table 6 - Tabulation of ΔT_{max} Data (Cont.)

MODEL: Zero-Caliber Ogive
DIAMETER: 0.635 cm (0.25 inch)
FLUID: Freon 113

Velocity		Temperature			ΔT_{max} Experimental		Figure*	ΔT_{max} 1st Corr.		ΔT_{max} 2nd Corr.	
fps	mps	°F	°C	L/D	°F	°C	Number	°F	°C	°F	°C
64	19.5	121.6	49.8	2.0	1.0	0.56	43	0.92	0.51	0.94	0.52
		122.6	50.3	3.5	1.7	0.94	43	1.50	0.83	1.55	0.86
		123.2	50.7	5.0	2.3	1.28	43	2.04	1.13	2.14	1.19
		142.0	61.1	2.0	1.2	0.67	44	1.23	0.68	1.24	0.69
		143.0	61.7	3.5	1.9	1.06	44	1.99	1.11	2.05	1.14
		142.5	61.4	5.0	2.9	1.61	44	2.66	1.48	2.78	1.54
		158.0	70.0	2.0	1.5	0.83	45	1.51	0.84	1.52	0.85
		159.9	71.1	3.5	2.5	1.39	45	2.45	1.36	2.53	1.41
		160.9	71.6	5.0	3.8	2.11	45	3.34	1.86	3.47	1.93
		177.7	80.9	2.0	1.5	0.83	46	1.90	1.06	1.91	1.07
		179.5	81.9	3.5	2.8	1.56	46	3.11	1.73	3.19	1.77
		180.4	82.4	5.0	4.6	2.56	46	4.26	2.37	4.41	2.45
		195.3	90.7	2.0	2.0	1.11	47	2.31	1.28	2.31	1.28
		199.1	92.8	3.5	3.5	1.94	47	3.81	2.12	3.90	2.17
		201.9	94.4	5.0	5.2	2.89	47	5.32	2.96	5.47	3.04
120	36.6	125.6	52.0	2.0	0.9	0.50	48	0.83	0.46	0.82	0.45
		123.5	50.8	3.5	1.2	0.67	48	1.29	0.72	1.31	0.73
		121.6	49.8	5.0	1.7	0.94	48	1.69	0.94	1.74	0.97
		144.3	62.4	2.0	1.0	0.56	49	1.02	0.57	1.01	0.56
		142.6	61.4	3.5	1.4	0.78	49	1.68	0.93	1.69	0.94
		141.4	60.8	5.0	2.7	1.50	49	2.22	1.23	2.28	1.27
		159.1	70.6	2.0	1.3	0.72	50	1.29	0.72	1.28	0.71
		158.1	70.1	3.5	2.3	1.28	50	2.05	1.14	2.06	1.15
		157.1	69.5	5.0	3.6	2.00	50	2.73	1.52	2.78	1.54
		184.0	84.4	2.0	1.3	0.72	51	1.74	0.97	1.71	0.95
		177.2	80.7	3.5	2.4	1.33	51	2.57	1.43	2.58	1.44
		176.3	80.2	5.0	4.7	2.61	51	3.34	1.91	3.49	1.94
		198.5	92.5	2.0	1.8	1.00	52	2.03	1.13	1.98	1.10
		197.8	92.1	3.5	3.0	1.67	52	3.22	1.79	3.21	1.78
		197.2	91.8	5.0	4.8	2.67	52	4.31	2.39	4.35	2.42

*Figure number for ΔT versus X/L plot.

Table 6 - Tabulation of ΔT_{max} Data (Cont.)

MODEL: Zero-Caliber Ogive
DIAMETER: 0.318 cm (0.125 inch)
FLUID: Freon 113

Velocity		Temperature			ΔT_{max} Experimental		Figure*	ΔT_{max} 1st Corr.		2nd Corr.	
fps	mps	°F	°C	L/D	°F	°C	Number	°F	°C	°F	°C
64	19.5	102.0	38.9	4.0	2.1	1.17	53	1.43	0.79	1.81	1.01
		106.0	41.1	5.2	2.2	1.22	53	1.90	1.06	1.90	1.06
		110.0	43.3	7.0	2.3	1.28	53	2.59	1.44	2.62	1.46
		118.5	48.1	4.0	2.0	1.11	54	1.91	1.06	1.93	1.07
		119.6	48.7	5.2	2.2	1.22	54	2.00	1.11	2.00	1.11
		120.6	49.2	7.0	2.5	1.39	54	2.41	1.34	2.42	1.34
		137.5	58.6	4.0	2.4	1.33	55	2.40	1.33	2.38	1.32
		140.3	60.2	5.2	2.8	1.56	55	3.11	1.73	3.10	1.72
		140.8	60.4	7.0	3.1	1.72	55	2.89	1.61	2.78	1.54
		158.3	70.2	4.0	3.1	1.72	56	3.14	1.74	3.10	1.72
		159.2	70.7	5.2	3.7	2.06	56	3.96	2.20	3.94	2.19
		161.9	72.2	7.0	4.0	2.22	56	4.62	2.57	4.54	2.52
		173.9	78.8	4.0	3.6	2.00	57	3.79	2.11	3.73	2.07
		178.3	81.3	5.2	4.6	2.56	57	4.94	2.74	4.94	2.74
		177.8	81.0	7.0	5.2	2.89	57	6.33	3.52	6.33	3.52
		191.5	88.6	4.0	4.0	2.22	58	4.62	2.57	4.52	2.51
		200.0	93.3	5.2	5.4	3.00	58	6.28	3.49	6.18	3.43
		200.3	93.5	7.0	6.8	3.78	58	8.09	4.49	8.03	4.46
120	36.6	127.5	53.1	4.0	1.8	1.00	59	1.75	0.97	1.74	0.96
		124.8	51.6	5.2	2.1	1.17	59	2.06	1.14	2.05	1.13
		119.6	48.7	7.0	2.8	1.56	59	2.79	1.55	2.80	1.56
		148.2	64.6	4.0	2.5	1.39	60	2.32	1.29	2.32	1.29
		145.7	63.2	5.2	3.1	1.72	60	3.15	1.75	3.17	1.77
		144.9	62.7	7.0	3.3	1.83	60	3.21	1.78	3.35	1.86
		164.8	73.8	4.0	3.1	1.72	61	2.95	1.64	2.96	1.65
		165.7	74.3	5.2	3.5	1.94	61	4.21	2.34	4.19	2.32
		161.8	72.1	7.0	4.2	2.33	61	4.23	2.33	4.32	2.40
		183.4	84.1	4.0	3.4	1.89	62	3.41	1.89	3.41	1.89
		184.2	84.6	5.2	4.6	2.56	62	4.52	2.51	4.52	2.51
		183.3	84.0	7.0	5.2	2.89	62	5.14	2.86	5.14	2.86
		199.8	93.2	4.0	4.5	2.50	63	4.00	2.22	4.01	2.23
		201.7	94.3	5.2	6.2	3.44	63	6.10	3.39	6.09	3.38
		200.4	93.6	7.0	7.5	4.17	63	7.32	4.07	7.31	4.06

*Figure number for ΔT versus X/L plot.

Table 6 - Tabulation of ΔT_{max} Data (Cont.)

MODEL: Zero-Caliber Ogive
DIAMETER: 0.635 cm (0.25 inch)
FLUID: Water

Velocity		Temperature			ΔT_{max} Experimental		Figure*	ΔT_{max} 1st Corr.		2nd Corr.	
fps	mps	°F	°C	L/D	°F	°C	Number	°F	°C	°F	°C
64	19.5	146.1	63.4	2.0	0.15	0.08	64	0.09	0.05	0.09	0.05
		147.3	64.1	3.5	0.20	0.11	64	0.15	0.08	0.16	0.09
		148.9	64.9	5.0	0.50	0.28	64	0.45	0.25	0.45	0.25
		197.0	91.7	2.0	0.30	0.17	65	0.24	0.13	0.24	0.13
		198.9	92.7	3.5	0.40	0.22	65	0.40	0.22	0.39	0.22
		199.7	93.2	5.0	0.60	0.33	65	0.52	0.29	0.51	0.28
		245.6	118.7	2.0	0.60	0.33	66	0.52	0.29	0.53	0.29
		248.2	120.1	3.5	0.70	0.39	66	0.65	0.36	0.64	0.36
		250.7	121.5	5.0	1.20	0.67	66	1.10	0.61	1.11	0.62
120	36.6	192.2	89.0	3.5	0.09	0.05	67	0.09	0.05	0.09	0.05
		192.7	89.3	5.0	0.40	0.22	67	0.42	0.23	0.42	0.23
		239.3	115.2	2.0	0.40	0.22	68	0.40	0.22	0.39	0.22
		240.6	115.9	3.5	0.50	0.28	68	0.60	0.33	0.65	0.36
		241.9	116.6	5.0	1.04	0.58	68	0.91	0.51	0.91	0.51

*Figure number for ΔT versus X/L plot.

Table 7 - Fluid Property Equations for Freon 113

[1] General form of equations for ρ_L, μ_L, ρ_v, λ, Cp_L, K_L, and S

$f(T) = a_0 + a_1T + a_2T^2 + \ldots + a_nT^n$

where T is the temperature in degrees Fahrenheit

[2] Coefficients for liquid mass density (ρ_L); units of $\rho_L = \dfrac{LB_f\text{-sec}^2}{\text{inch}^4}$

$a_0 = 0.0599$

$a_1 = -0.4124 \times 10^{-4}$

$a_2 = -0.3681 \times 10^{-7}$

[3] Coefficients for liquid dynamic viscosity (μ_L); units of $\mu_L = \dfrac{LB_f\text{-sec}}{\text{inch}^2}$

$a_0 = 0.8132 \times 10^{-4}$

$a_1 = -0.1029 \times 10^{-5}$

$a_2 = 0.7669 \times 10^{-8}$

$a_3 = -0.9971 \times 10^{-11}$

$a_4 = -0.2809 \times 10^{-12}$

$a_5 = 0.1830 \times 10^{-14}$

$a_6 = -0.3452 \times 10^{-17}$

[4] Coefficients for vapor mass density (ρ_v); units of $\rho_v = \dfrac{LB_f\text{-sec}^2}{\text{inch}^4}$

$a_0 = -0.2824 \times 10^{-4}$

$a_1 = 0.3725 \times 10^{-5}$

$a_2 = -0.8074 \times 10^{-7}$

$a_3 = 0.1306 \times 10^{-8}$

$a_4 = -0.1027 \times 10^{-10}$

$a_5 = 0.4868 \times 10^{-13}$

$a_6 = -0.1208 \times 10^{-15}$

$a_7 = 0.1231 \times 10^{-18}$

[5] Coefficients for latent heat of vaporization (λ); units of $\lambda = \dfrac{\text{BTU-inch}}{LB_f\text{-sec}^2}$

$a_0 = 72.5755$

$a_1 = -0.1524$

$a_2 = 0.2079 \times 10^{-2}$

$a_3 = -0.2460 \times 10^{-4}$

$a_4 = 0.1521 \times 10^{-6}$

$a_5 = -0.4919 \times 10^{-9}$

$a_6 = 0.6440 \times 10^{-12}$

Table 7 - Fluid Property Equations for Freon 113 (Cont.)

[6] Coefficients for liquid specific heat (Cp_L); units of $Cp_L = \frac{\text{BTU-inch}}{\text{LB}_f\text{-sec}^2\text{-°F}}$

$a_0 = 0.22714$

$a_1 = -0.4513 \times 10^{-3}$

$a_2 = 0.1147 \times 10^{-4}$

$a_3 = -0.7254 \times 10^{-7}$

$a_4 = -0.9724 \times 10^{-10}$

$a_5 = 0.2412 \times 10^{-11}$

$a_6 = -0.5995 \times 10^{-14}$

[7] Coefficients for liquid thermal conductivity (K_L); units of $K_L = \frac{\text{BTU}}{\text{inch-sec-°F}}$

$a_0 = 0.11199 \times 10^{-5}$

$a_1 = -0.15277 \times 10^{-8}$

[8] Coefficients for surface tension (S); units of $S = \frac{\text{LB}_f}{\text{inch}}$

$a_0 = 0.1359 \times 10^{-3}$

$a_1 = -0.3804 \times 10^{-6}$

$a_2 = -0.1700 \times 10^{-10}$

$a_3 = 0.9873 \times 10^{-12}$

$a_4 = -0.4178 \times 10^{-14}$

[9] Equation for vapor pressure (P_v); units of $P_v = \frac{\text{LB}_f}{\text{inch}^2}$ absolute

$P_v = 10^{g(T)}$

where $g(T) = 33.0655 - \frac{4330.98}{T} - 9.2635 \log_{10}T + 0.0020539\ T$

and where T is the temperature in degrees Rankine.

Table 8 - Fluid Property Equations for Water

[1] General form of equations for ρ_L, ν_L, ρ_v, λ, α_L, K_L, S, and P_v

$$f(T) = a_0 + a_1T + a_2T^2 + \ldots + a_nT^n$$

where T is the temperature in degrees Fahrenheit

[2] Coefficients for liquid mass density (ρ_L); units of $\rho_L = \frac{LB_f\text{-sec}^2}{\text{inch}^4}$

$a_0 = 0.9345 \times 10^{-4}$ $a_3 = 0.4036 \times 10^{-12}$

$a_1 = 0.1294 \times 10^{-7}$ $a_4 = -0.4056 \times 10^{-15}$

$a_2 = -0.2104 \times 10^{-9}$

[3] Coefficients for liquid kinematic viscosity (ν_L); units of $\nu_L = \frac{\text{inch}^2}{\text{sec}}$

$a_0 = 0.4504 \times 10^{-2}$ $a_4 = -0.5370 \times 10^{-11}$

$a_1 = -0.7123 \times 10^{-4}$ $a_5 = 0.4123 \times 10^{-13}$

$a_2 = 0.5078 \times 10^{-6}$ $a_6 = -0.9724 \times 10^{-16}$

$a_3 = -0.1188 \times 10^{-8}$ $a_7 = 0.8112 \times 10^{-19}$

[4] Coefficients for vapor mass density (ρ_v); units of $\rho_v = \frac{LB_f\text{-sec}^2}{\text{inch}^4}$

$a_0 = 0.2548 \times 10^{-10}$ $a_3 = -0.1730 \times 10^{-16}$

$a_1 = 0.5652 \times 10^{-11}$ $a_4 = 0.1514 \times 10^{-16}$

$a_2 = 0.1819 \times 10^{-12}$ $a_5 = 0.3768 \times 10^{-19}$

[5] Coefficients for latent heat of vaporization (λ); units of $\lambda = \frac{\text{BTU-inch}}{LB_f\text{-sec}^2}$

$a_0 = 0.4201 \times 10^{6}$ $a_3 = -0.1991 \times 10^{-3}$

$a_1 = -0.2187 \times 10^{3}$ $a_4 = -0.2981 \times 10^{-6}$

$a_2 = 0.3115 \times 10^{-1}$

Table 8 - Fluid Property Equations for Water (Cont.)

[6] Coefficients for liquid thermal diffusivity (α_L); units of $\alpha_L = \frac{inch^2}{sec}$

$a_0 = 0.1795 \times 10^{-3}$	$a_3 = 0.2448 \times 10^{-10}$
$a_1 = 0.8871 \times 10^{-6}$	$a_4 = 0.6256 \times 10^{-13}$
$a_2 = -0.5335 \times 10^{-8}$	$a_5 = 0.6104 \times 10^{-16}$

[7] Coefficients for liquid thermal conductivity (K_L); units of $K_L = \frac{BTU}{inch\text{-}sec\text{-}°F}$

$a_0 = 0.6579 \times 10^{-5}$	$a_3 = 0.7771 \times 10^{-12}$
$a_1 = 0.3003 \times 10^{-7}$	$a_4 = -0.1922 \times 10^{-14}$
$a_2 = -0.1818 \times 10^{-9}$	$a_5 = 0.1854 \times 10^{-17}$

[8] Coefficients for surface tension (S); units of $S = \frac{LB_f}{inch}$

$a_0 = 4.4269 \times 10^{-4}$	$a_4 = -1.7329 \times 10^{-13}$
$a_1 = -2.2418 \times 10^{-7}$	$a_5 = 3.4789 \times 10^{-16}$
$a_2 = -4.8683 \times 10^{-9}$	$a_6 = -2.6182 \times 10^{-19}$
$a_3 = 4.0331 \times 10^{-11}$	

[9] Coefficients for vapor pressure (P_v); units of $P_v = \frac{LB_f}{inch^2}$ absolute

$a_0 = -0.7533 \times 10^{-1}$	$a_4 = -0.7887 \times 10^{-8}$
$a_1 = 0.6523 \times 10^{-2}$	$a_5 = 0.4794 \times 10^{-10}$
$a_2 = -0.1024 \times 10^{-3}$	$a_6 = -0.3561 \times 10^{-13}$
$a_3 = 0.1736 \times 10^{-5}$	$a_7 = 0.5746 \times 10^{-17}$

Table 9 - Tabulation of the Fluid Properties of Freon 113

TEMP.		P_v	ρ_v	ρ_L	C_{P_L}	K_L	α_L	λ	μ_L	ν_L	S
°F	°C	$\frac{LB_f}{inch^2}$ abs.	$\frac{LB_f\text{-}sec^2}{inch^4}$	$\frac{LB_f\text{-}sec^2}{inch^4}$	$\frac{BTU\text{-}inch}{LB_f\text{-}sec^2\text{-}°F}$	$\frac{BTU}{inch\text{-}sec\text{-}°F}$	$\frac{inch^2}{sec}$	$\frac{BTU\text{-}inch}{LB_f\text{-}sec}$	$\frac{LB_f\text{-}sec}{inch^2}$	$\frac{inch^2}{sec}$	$\frac{LB_f}{inch}$
60	15.6	4.374	0.2233×10^{-6}	148.5×10^{-6}	87.26	1.03×10^{-6}	0.795×10^{-4}	2.595×10^{4}	1.102×10^{-7}	0.742×10^{-3}	1.130×10^{-4}
80	26.7	6.902	0.3413×10^{-6}	146.1×10^{-6}	88.80	0.995×10^{-6}	0.767×10^{-4}	2.544×10^{4}	0.949×10^{-7}	0.650×10^{-3}	1.057×10^{-4}
100	37.8	10.480	0.5036×10^{-6}	143.6×10^{-6}	89.65	0.972×10^{-6}	0.755×10^{-4}	2.489×10^{4}	0.819×10^{-7}	0.570×10^{-3}	0.983×10^{-4}
120	48.9	15.400	0.7214×10^{-6}	141.0×10^{-6}	90.54	0.937×10^{-6}	0.734×10^{-4}	2.430×10^{4}	0.725×10^{-7}	0.514×10^{-3}	0.908×10^{-4}
140	60.0	21.93	1.005×10^{-6}	138.4×10^{-6}	91.50	0.905×10^{-6}	0.715×10^{-4}	2.367×10^{4}	0.640×10^{-7}	0.462×10^{-3}	0.834×10^{-4}
160	71.1	30.44	1.370×10^{-6}	135.7×10^{-6}	92.66	0.880×10^{-6}	0.699×10^{-4}	2.299×10^{4}	0.579×10^{-7}	0.427×10^{-3}	0.765×10^{-4}
180	82.2	41.22	1.830×10^{-6}	132.9×10^{-6}	94.21	0.847×10^{-6}	0.676×10^{-4}	2.226×10^{4}	0.515×10^{-7}	0.388×10^{-3}	0.692×10^{-4}
200	93.3	54.66	2.401×10^{-6}	130.0×10^{-6}	95.75	0.812×10^{-6}	0.653×10^{-4}	2.147×10^{4}	0.464×10^{-7}	0.357×10^{-3}	0.622×10^{-4}
220	104.4	71.07	3.106×10^{-6}	127.1×10^{-6}		0.787×10^{-6}		2.063×10^{4}			0.554×10^{-4}

NOTE: P_v, λ, ρ_L, ρ_v and μ_L at 220°F were obtained from Dupont Report T-113A, 1938 (Reference [17])
K_L, C_{P_L} and μ_L were obtained from Dupont Report C-30, 1973 (Reference [18])
S was obtained from Dupont Report D-27, 1967 (Reference [19])

Table 10 - Tabulation of the Fluid Properties of Water

TEMP.		P_v	ρ_v	ρ_L	Cp_L	K_L	α_L	λ	μ_L	ν_L	S
°F	°C	$\frac{LB_f}{inch^2}$ abs.	$\frac{LB_f-sec^2}{inch^4}$	$\frac{LB_f-sec^2}{inch^4}$	$\frac{BTU-inch}{LB_f-sec^2-°F}$	$\frac{BTU}{inch-sec-°F}$	$\frac{inch^2}{sec}$	$\frac{BTU-inch}{LB_f-sec}$	$\frac{LB_f-sec}{inch^2}$	$\frac{inch^2}{sec}$	$\frac{LB_f}{inch}$
60	15.6	0.256	0.1242×10^{-8}	93.447×10^{-6}	385.9	0.789×10^{-5}	2.188×10^{-4}	4.092×10^{5}	16.31×10^{-8}	1.745×10^{-3}	0.420×10^{-3}
80	26.7	0.507	0.2368×10^{-8}	93.215×10^{-6}	385.4	0.817×10^{-5}	2.274×10^{-4}	4.049×10^{5}	12.47×10^{-8}	1.338×10^{-3}	0.410×10^{-3}
100	37.8	0.949	0.4278×10^{-8}	92.926×10^{-6}	385.3	0.840×10^{-5}	2.346×10^{-4}	4.005×10^{5}	9.89×10^{-8}	1.064×10^{-3}	0.399×10^{-3}
120	48.9	1.692	0.7374×10^{-8}	92.524×10^{-6}	385.5	0.859×10^{-5}	2.408×10^{-4}	3.960×10^{5}	8.09×10^{-8}	0.874×10^{-3}	0.388×10^{-3}
140	60.0	2.889	1.216×10^{-8}	92.013×10^{-6}	385.9	0.875×10^{-5}	2.464×10^{-4}	3.915×10^{5}	6.78×10^{-8}	0.737×10^{-3}	0.377×10^{-3}
160	71.1	4.741	1.939×10^{-8}	91.452×10^{-6}	386.4	0.889×10^{-5}	2.516×10^{-4}	3.870×10^{5}	5.80×10^{-8}	0.634×10^{-3}	0.367×10^{-3}
180	82.2	7.510	2.984×10^{-8}	90.787×10^{-6}	387.1	0.898×10^{-5}	2.555×10^{-4}	3.823×10^{5}	5.03×10^{-8}	0.554×10^{-3}	0.356×10^{-3}
200	93.3	11.526	4.456×10^{-8}	90.132×10^{-6}	388.1	0.907×10^{-5}	2.593×10^{-4}	3.776×10^{5}	4.42×10^{-8}	0.490×10^{-3}	0.344×10^{-3}
220	104.4	17.186	5.475×10^{-8}	89.379×10^{-6}	389.3	0.912×10^{-5}	2.621×10^{-4}	3.727×10^{5}	3.93×10^{-8}	0.440×10^{-3}	0.332×10^{-3}
240	115.6	24.969	9.183×10^{-8}	88.588×10^{-6}	390.9	0.917×10^{-5}	2.648×10^{-4}	3.676×10^{5}	3.53×10^{-8}	0.398×10^{-3}	0.319×10^{-3}
260	126.7	35.429	12.74×10^{-8}	87.707×10^{-6}	392.8	0.919×10^{-5}	2.668×10^{-4}	3.624×10^{5}	3.20×10^{-8}	0.365×10^{-3}	0.306×10^{-3}
280	137.8	49.203	17.34×10^{-8}	86.842×10^{-6}	395.0	0.919×10^{-5}	2.679×10^{-4}	3.570×10^{5}	2.92×10^{-8}	0.336×10^{-3}	0.293×10^{-3}
300	148.9	67.013	23.18×10^{-8}	85.900×10^{-6}	397.6	0.917×10^{-5}	2.685×10^{-4}	3.514×10^{5}	2.69×10^{-8}	0.313×10^{-3}	0.279×10^{-3}
320	160.0	89.660	30.50×10^{-8}	84.923×10^{-6}	400.3	0.914×10^{-5}	2.689×10^{-4}	3.455×10^{5}	2.51×10^{-8}	0.296×10^{-3}	0.266×10^{-3}
340	171.1	118.010	39.57×10^{-8}	83.878×10^{-6}	403.5	0.910×10^{-5}	2.689×10^{-4}	3.394×10^{5}	2.36×10^{-8}	0.281×10^{-3}	0.252×10^{-3}

Table 10 - Tabulation of the Fluid Properties of Water (Cont.)

NOTE: P_v, λ, ρ_L and ρ_v were obtained from Keenan and Keyes, 1936 (Reference [20])

K_L, C_{P_L}, and μ_L were obtained from Table A-5 page 431 of Gebhart, 1961 (Reference [21])

S was obtained from page 53 of Vargaftik, 1975 (Reference [22])

Table 11 - ΔT_{max} Correlations for Constant Fluid Properties

SHAPE	FLUIDS	CORRELATION METHOD	EQUATIONS FOR ΔT_{max}
Zero-Caliber Ogive	Water Freon 113	Entrainment Method First Correlation	$\Delta T_{max} = C(L/D)^{0.83} V^{-0.25} D^{-0.22}$
Zero-Caliber Ogive		Entrainment Method Second Correlation	$\Delta T_{max} = C(L/D)^{0.87} V^{-0.28} D^{-0.14}$
Quarter-Caliber Ogive		Entrainment Method First Correlation	$\Delta T_{max} = C(L/D)^{0.26} V^{0.39} D^{0.45}$
Quarter-Caliber Ogive		Entrainment Method Second Correlation	$\Delta T_{max} = C(L/D)^{0.26} V^{0.39} D^{0.46}$

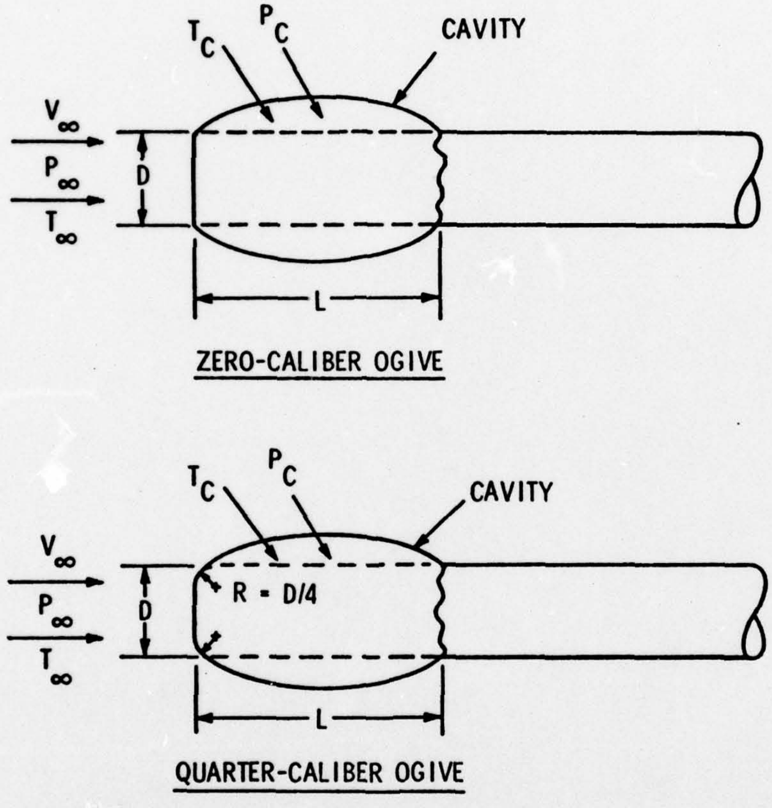

Figure 1 - Description of the Nose Contour of Ogive Test Models

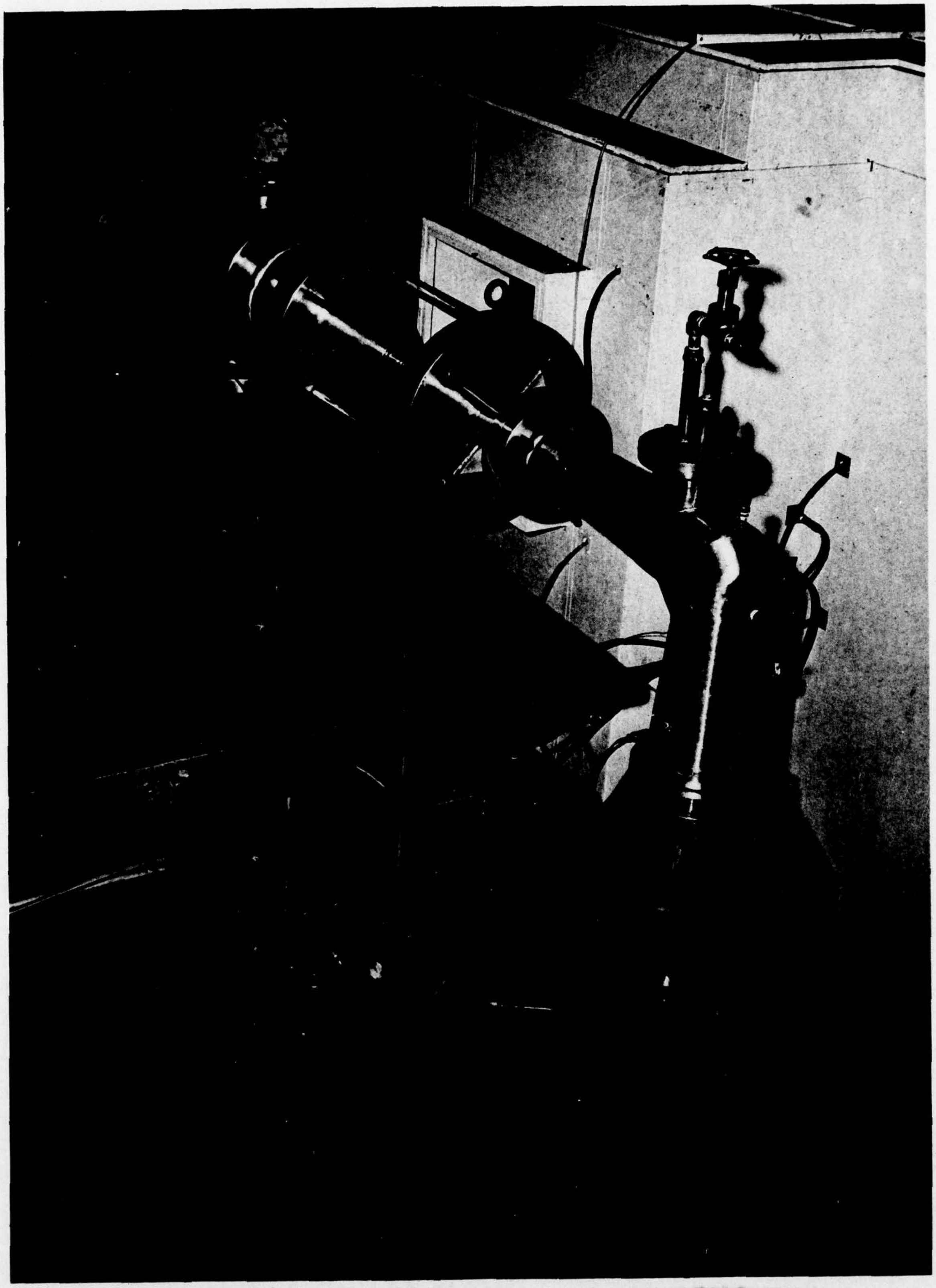

Figure 2 - Photograph of 3.8 cm Ultra-High-Speed Cavitation Tunnel

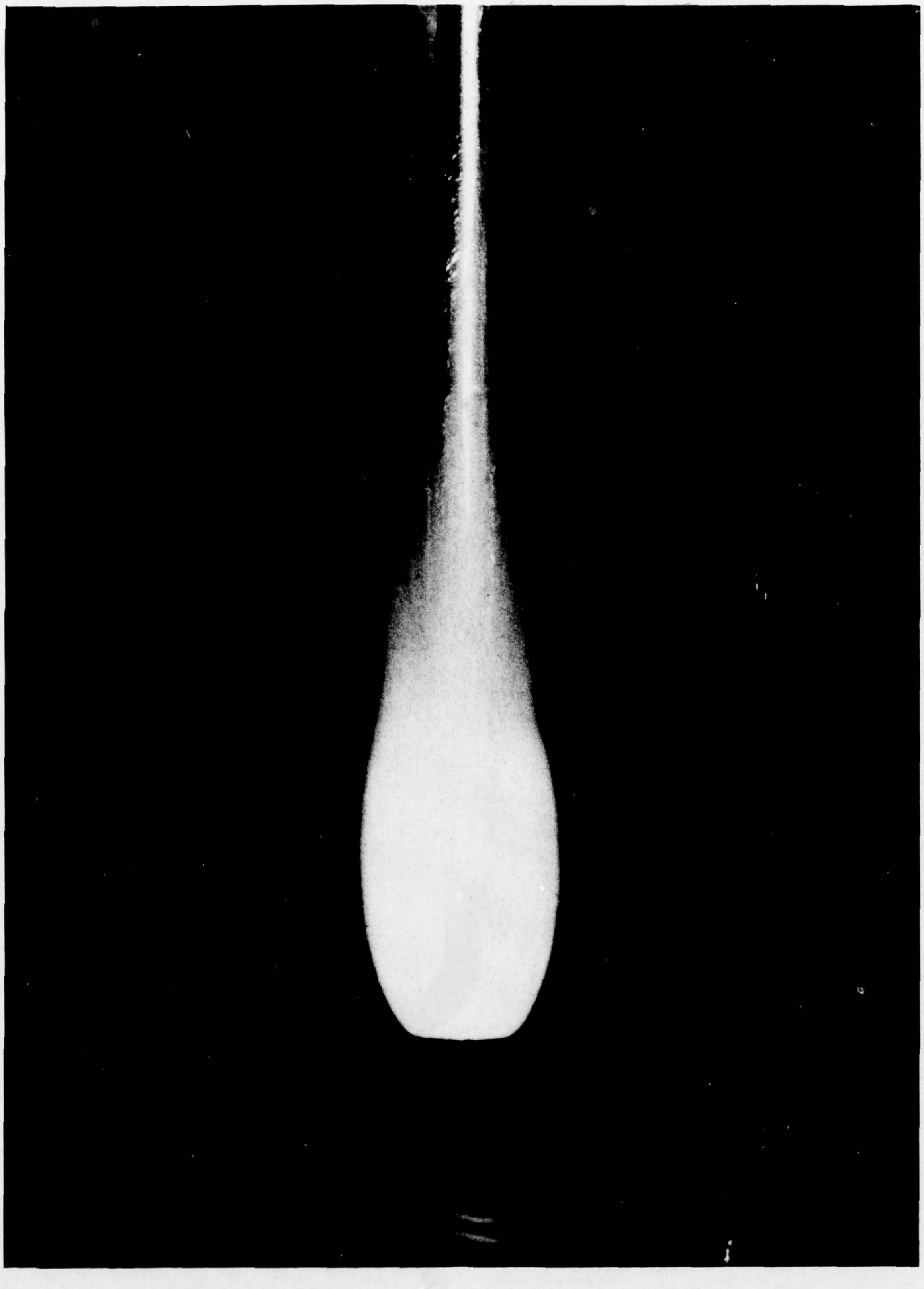

Figure 3A - Photograph of Natural Cavities on a Zero-Caliber Ogive in Freon 113 (D=0.635 cm, V_∞=19.5 m/sec, L/D=5.0, T_∞=26°C)

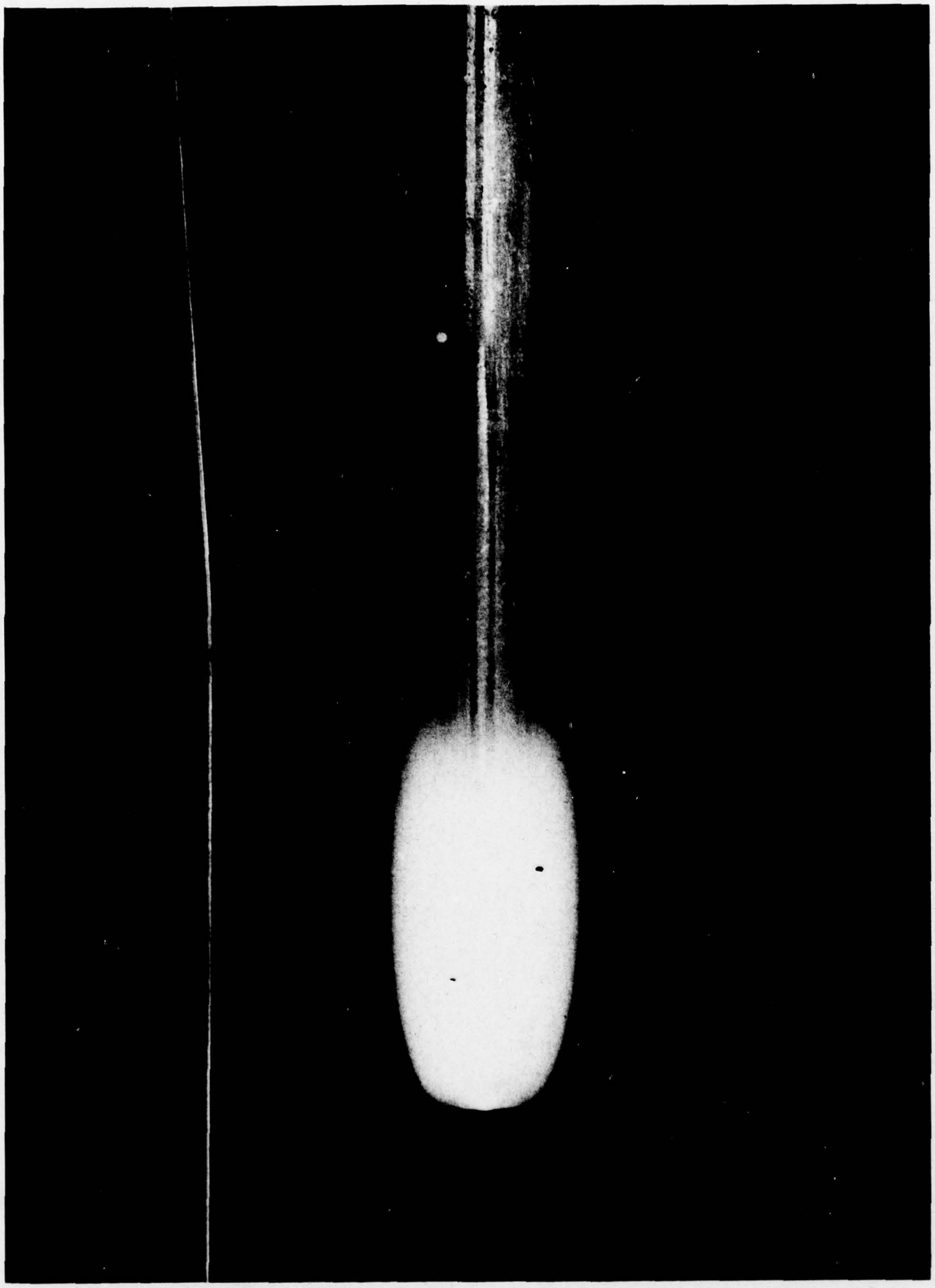

Figure 3B - Photograph of Natural Cavities on a Zero-Caliber Ogive in Water (D=0.635 cm, V_∞=19.5 m/sec, L/D=5.0, T_∞=26°C)

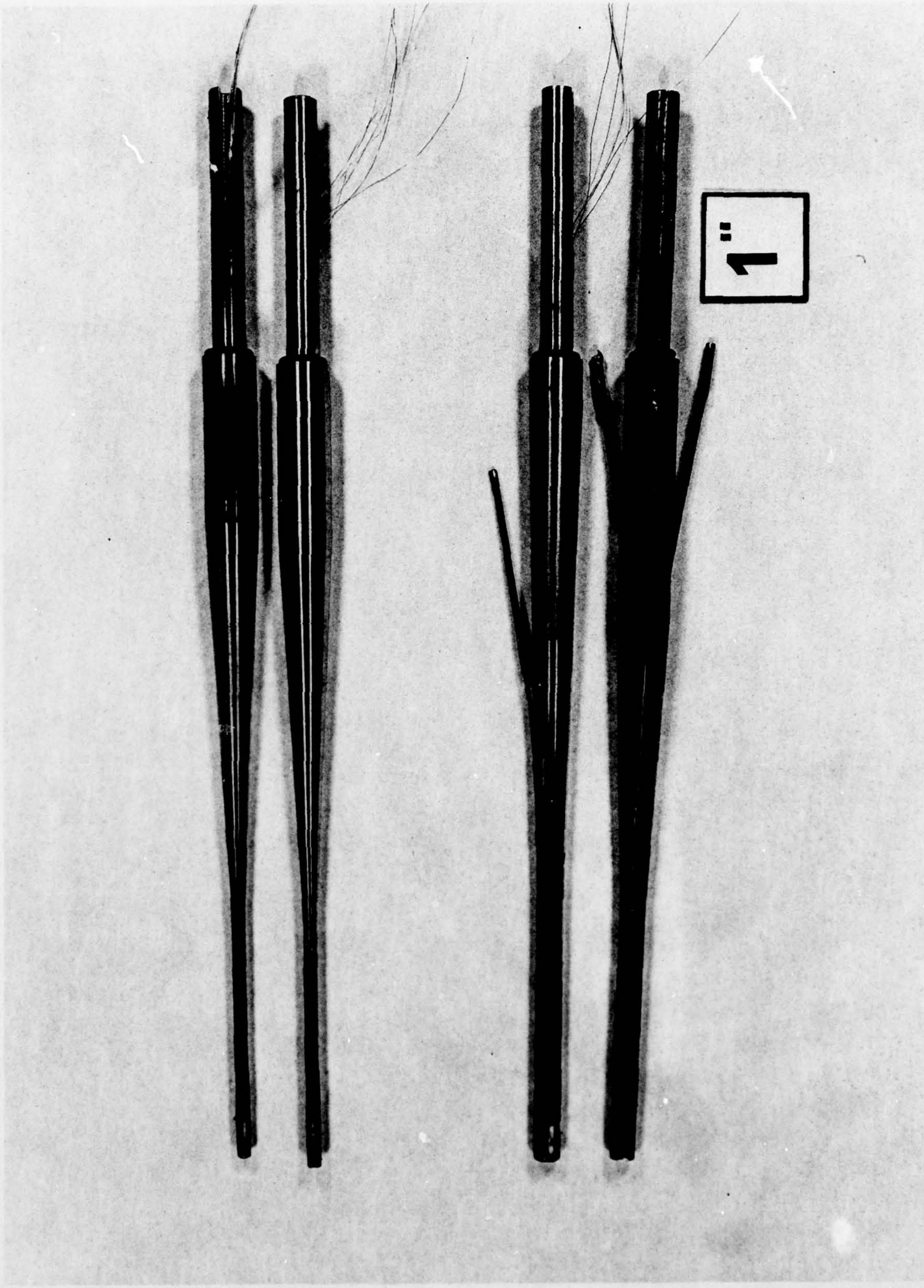

Figure 4 - Photograph of Test Models for Cavity Temperature Measurements

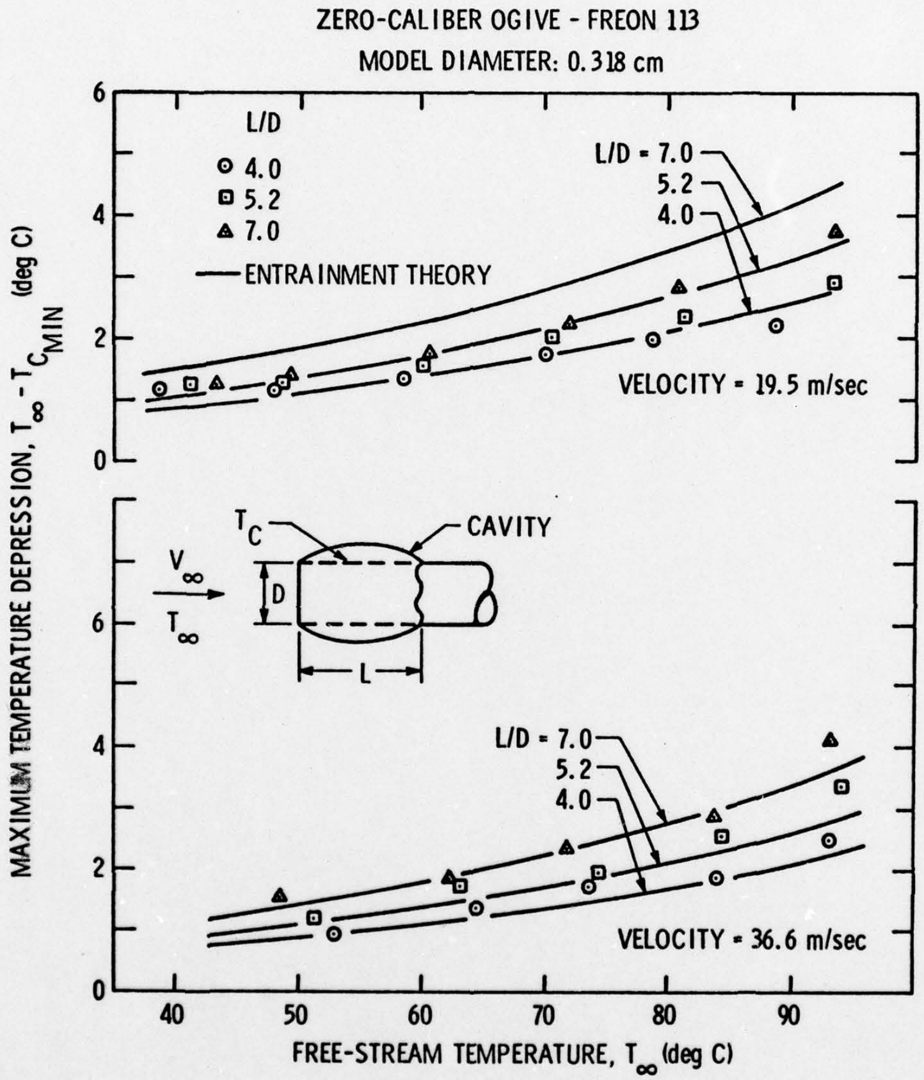

Figure 5 - Maximum Temperature Depression Versus Free Stream Temperature for the 0.318 cm Diameter Zero-Caliber Ogive in Freon 113

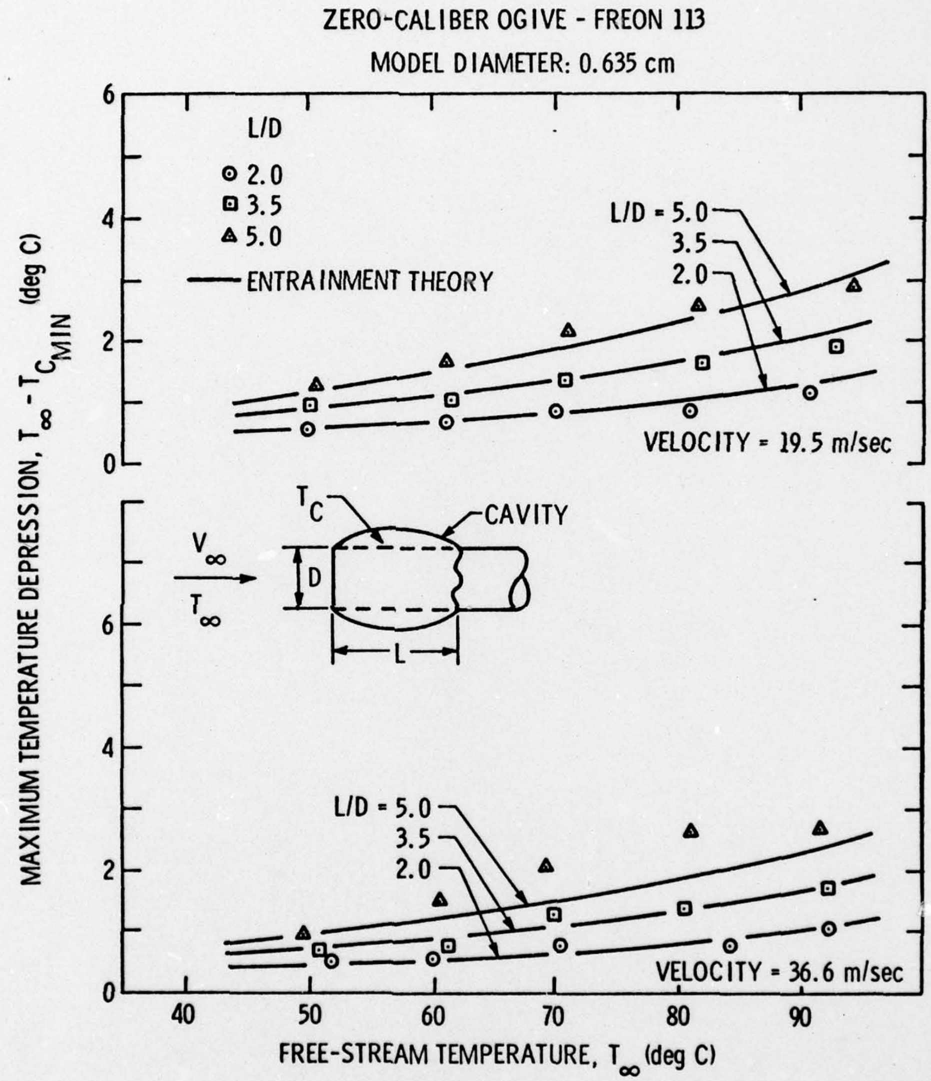

Figure 6 - Maximum Temperature Depression Versus Free Stream Temperature for the 0.635 cm Diameter Zero-Caliber Ogive in Freon 113

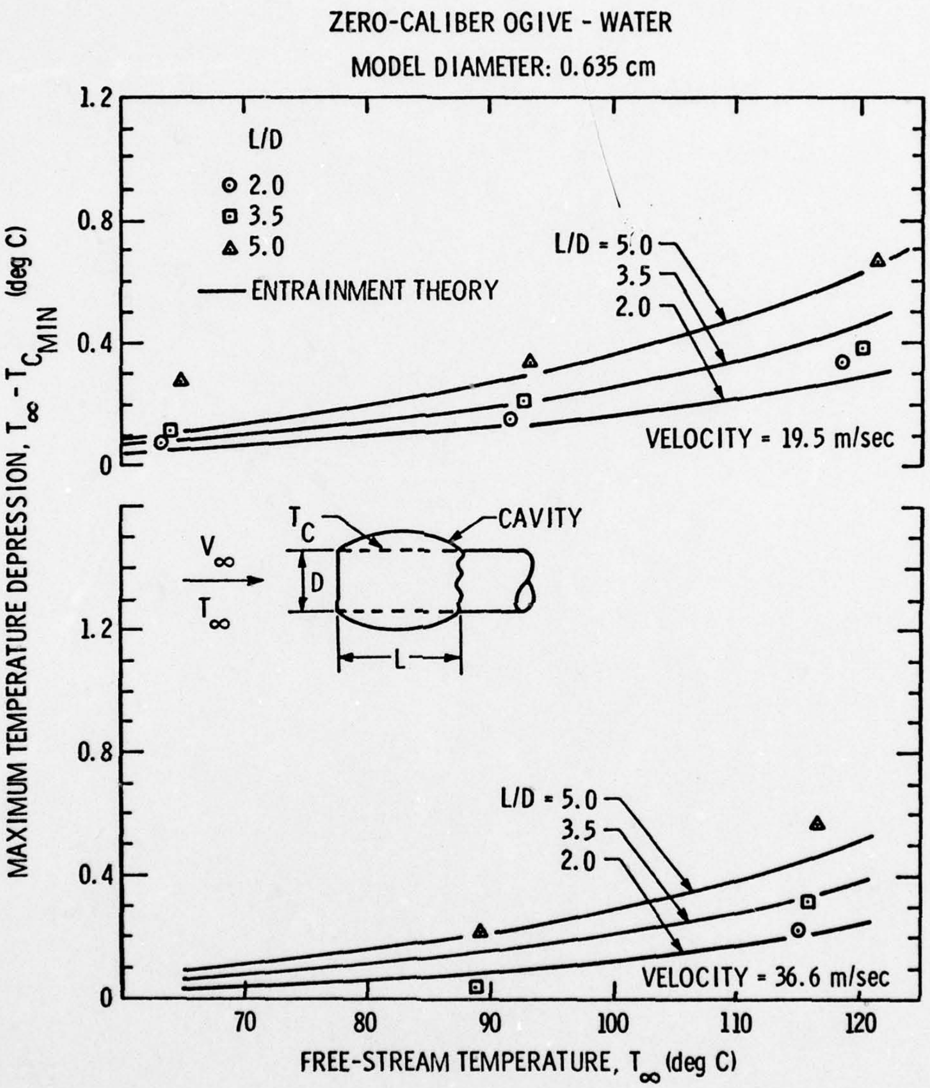

Figure 7 - Maximum Temperature Depression Versus Free Stream Temperature for the 0.635 cm Diameter Zero-Caliber Ogive in Water

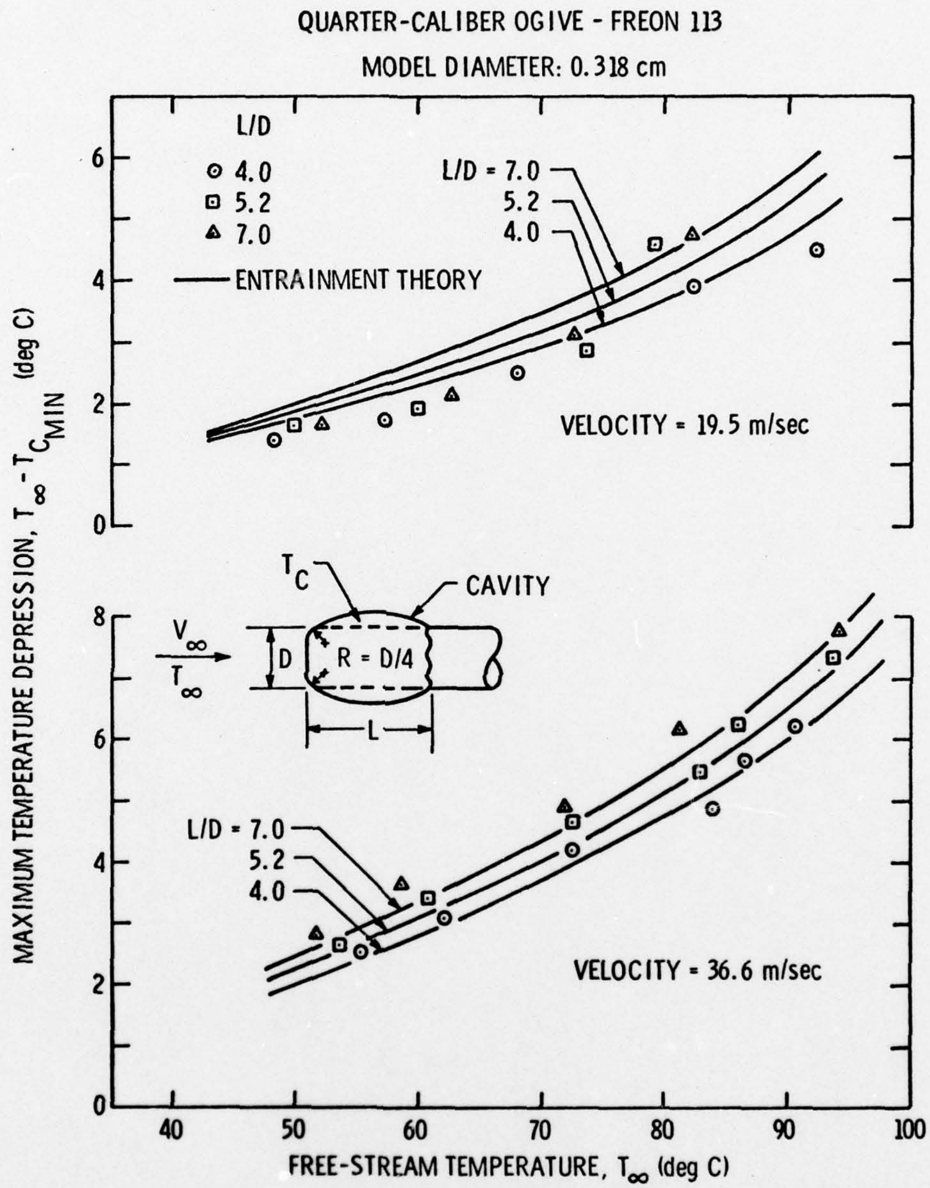

Figure 8 - Maximum Temperature Depression Versus Free Stream Temperature for the 0.318 cm Diameter Quarter-Caliber Ogive in Freon 113

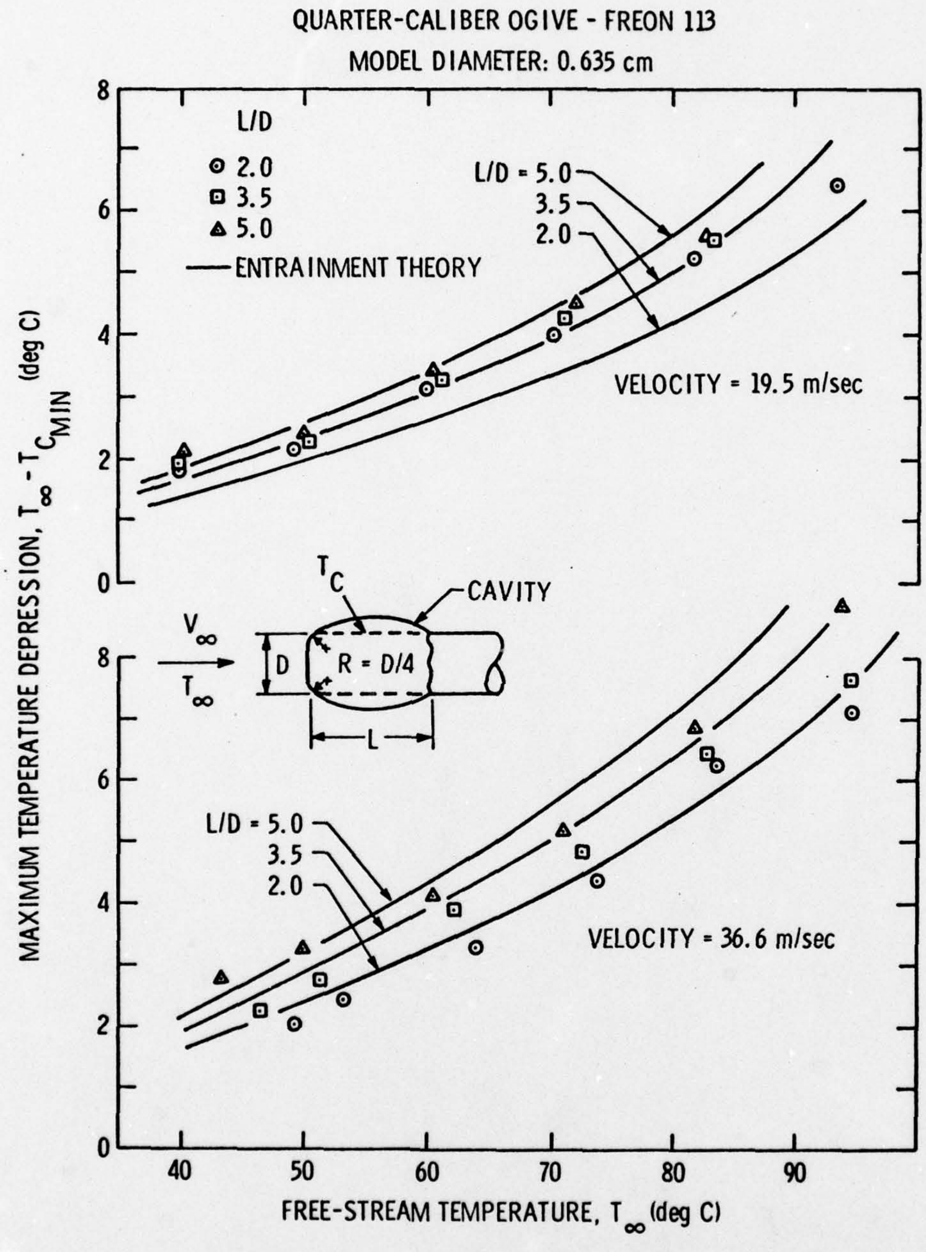

Figure 9 - Maximum Temperature Depression Versus Free Stream Temperature for the 0.635 cm Diameter Quarter-Caliber Ogive in Freon 113

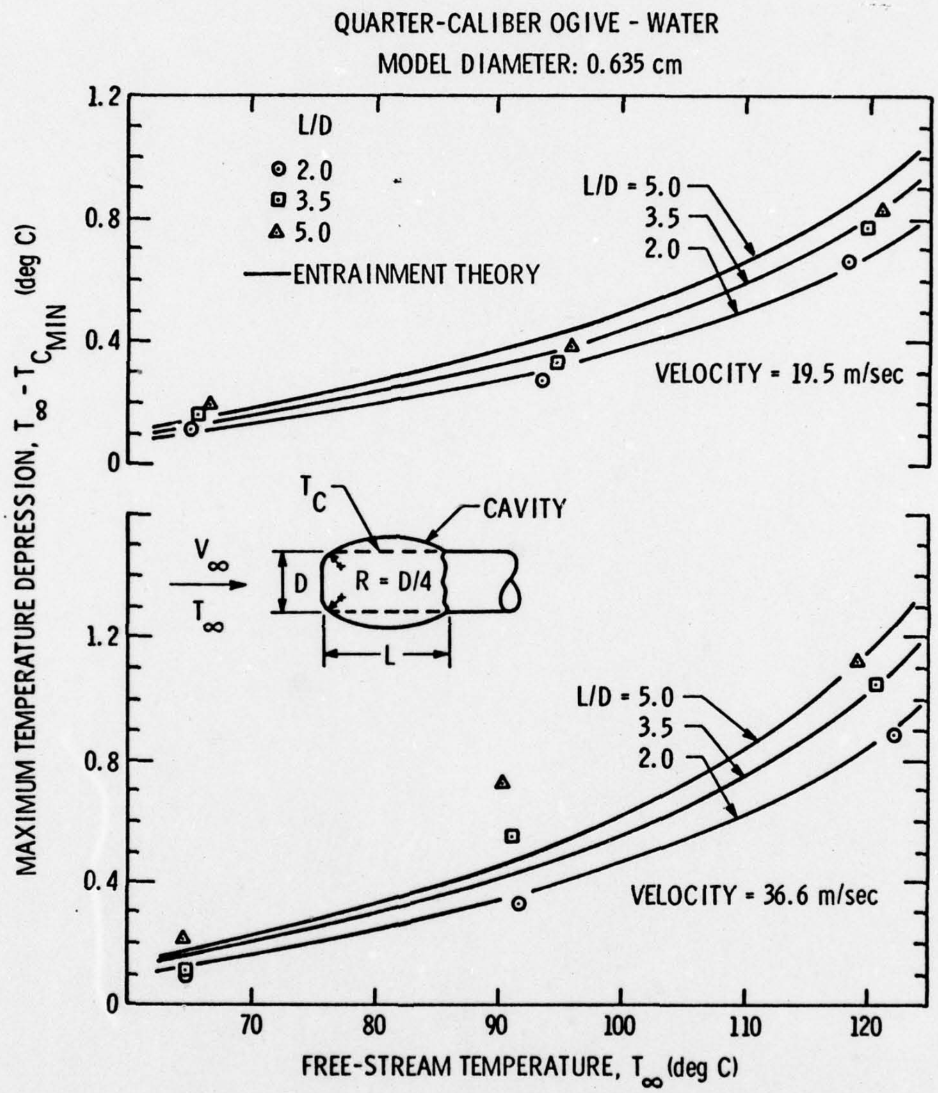

Figure 10 - Maximum Temperature Depression Versus Free Stream Temperature for the 0.635 cm Diameter Quarter-Caliber Ogive in Water

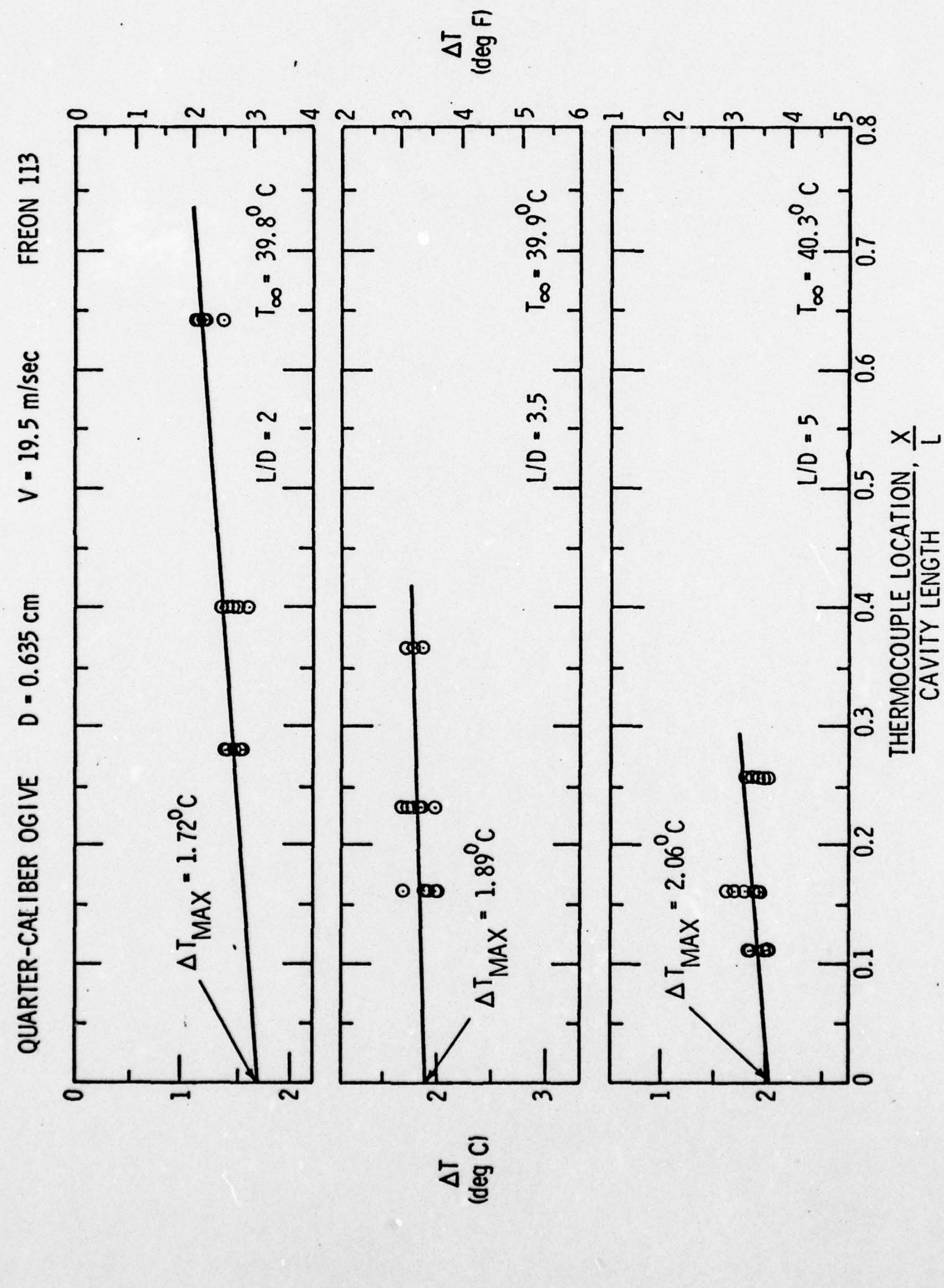

Figure 11 - ΔT vs X/L for T_∞ = 39.8, 39.9, and 40.3°C: QCO, D=0.635 cm, V=19.5 m/sec, Freon 113

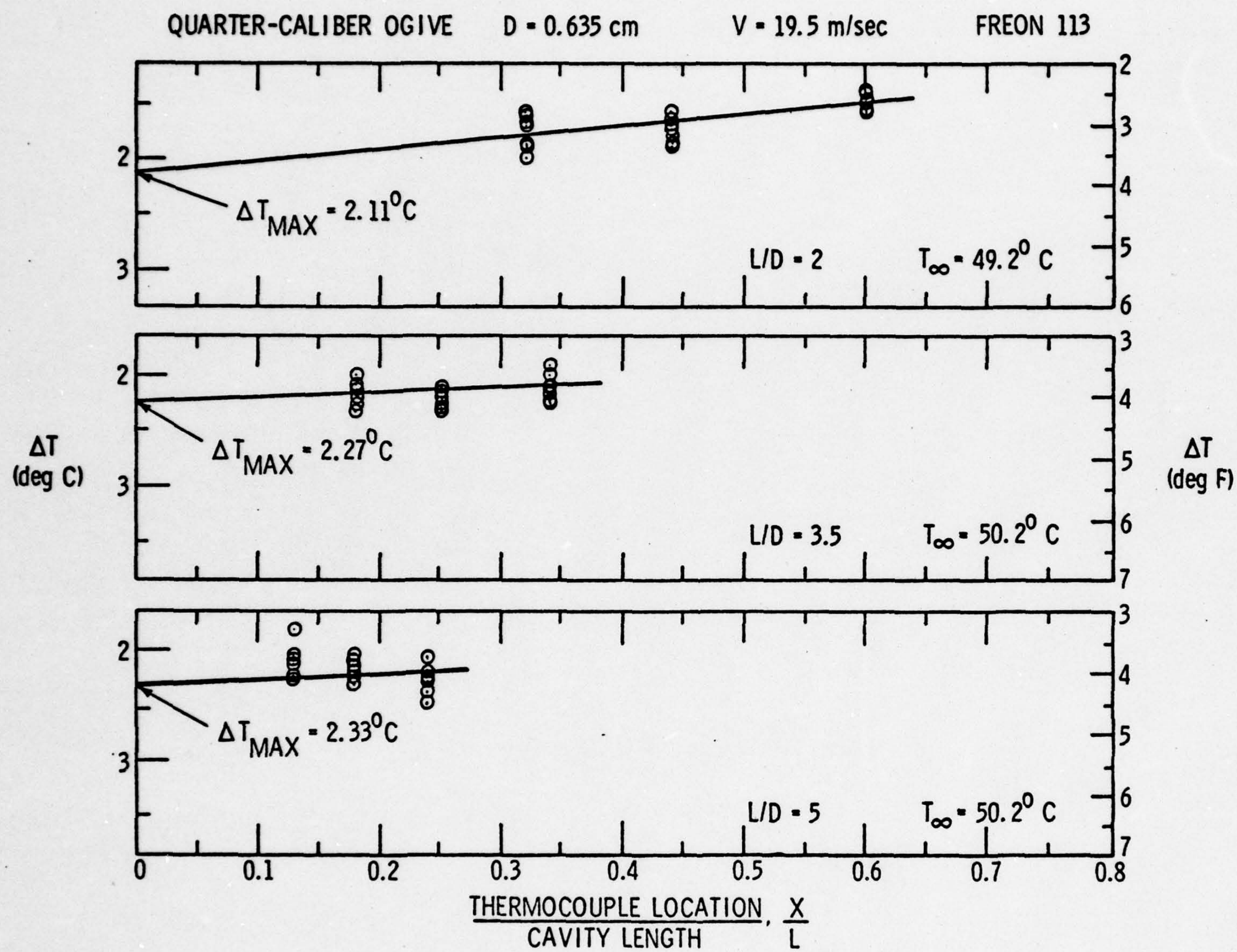

Figure 12 - ΔT vs X/L for T_∞ = 49.2, 50.2, and 50.2°C: QCO, D=0.635 cm, V=19.5 m/sec, Freon 113

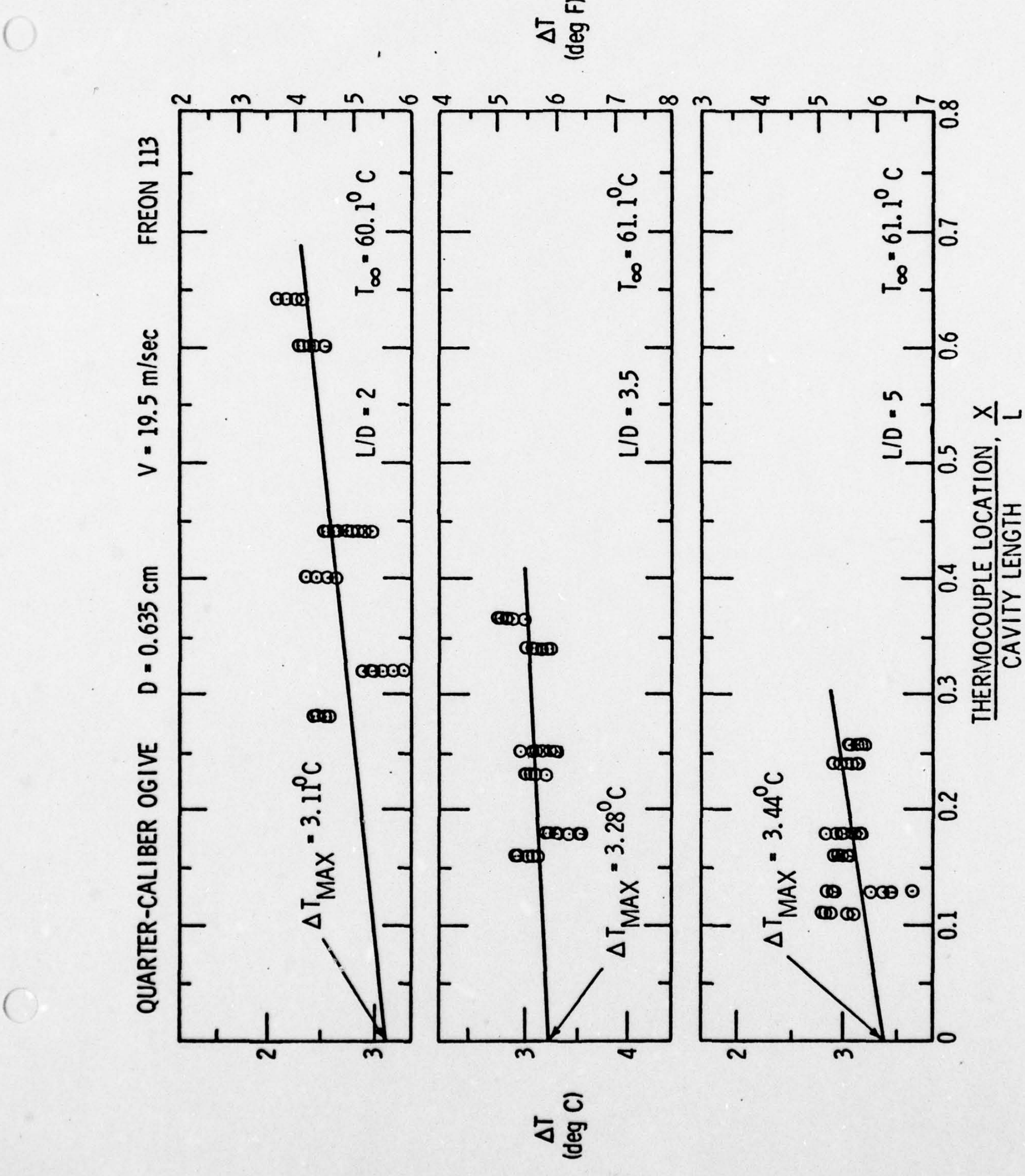

Figure 13 - ΔT vs X/L for T_∞ = 60.1, 61.1, and 61.1°C: QCO, D=0.635 cm, V=19.5 m/sec, Freon 113

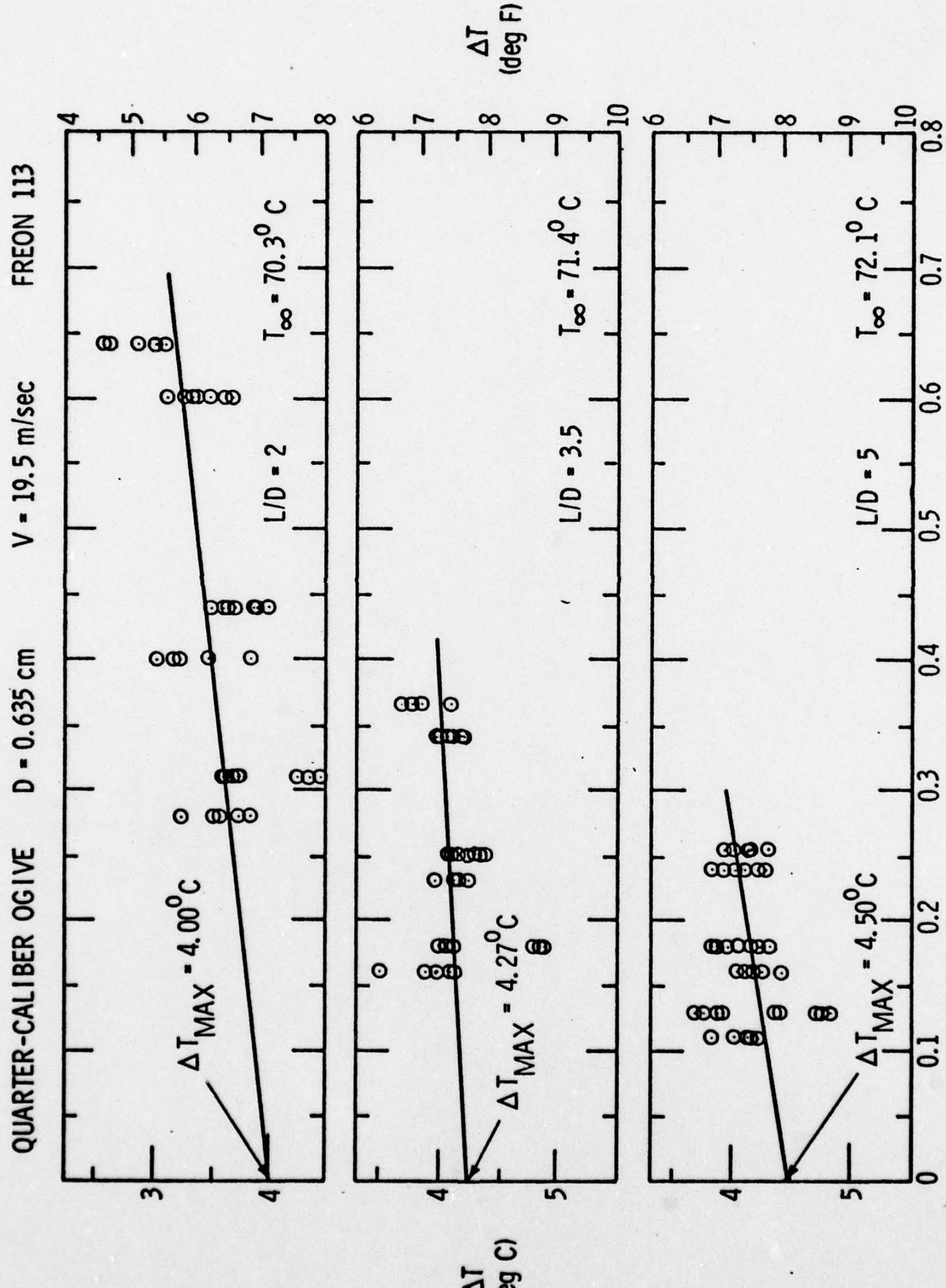

Figure 14 - ΔT vs X/L for T_∞ = 70.3, 71.4, and 72.1°C: QCO, D=0.635 cm, V=19.5 m/sec, Freon 113

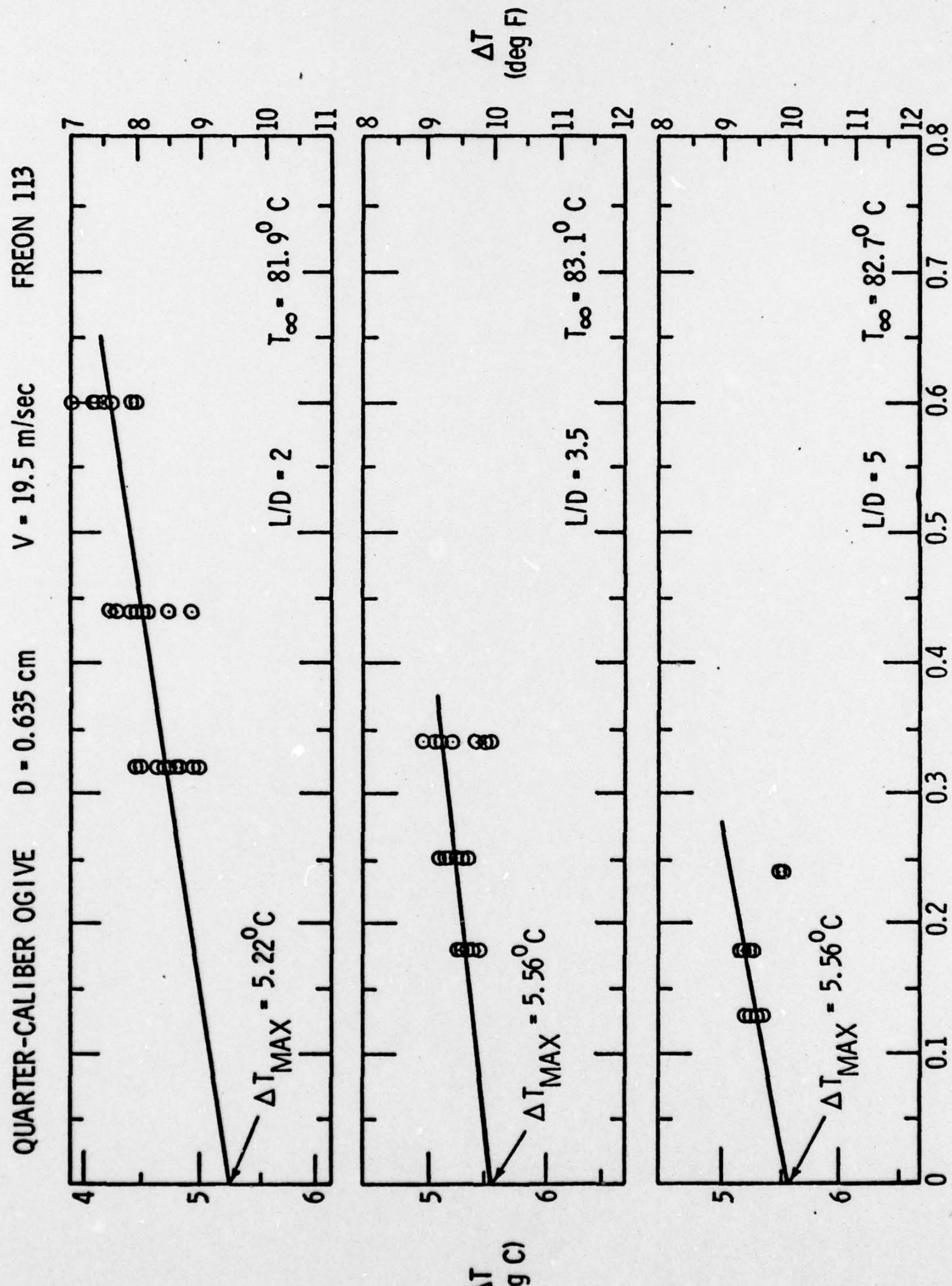

Figure 15 - ΔT vs X/L for T_∞ = 81.9, 83.1, and 82.7°C: QCO, D=0.635 cm, V=19.5 m/sec, Freon 113

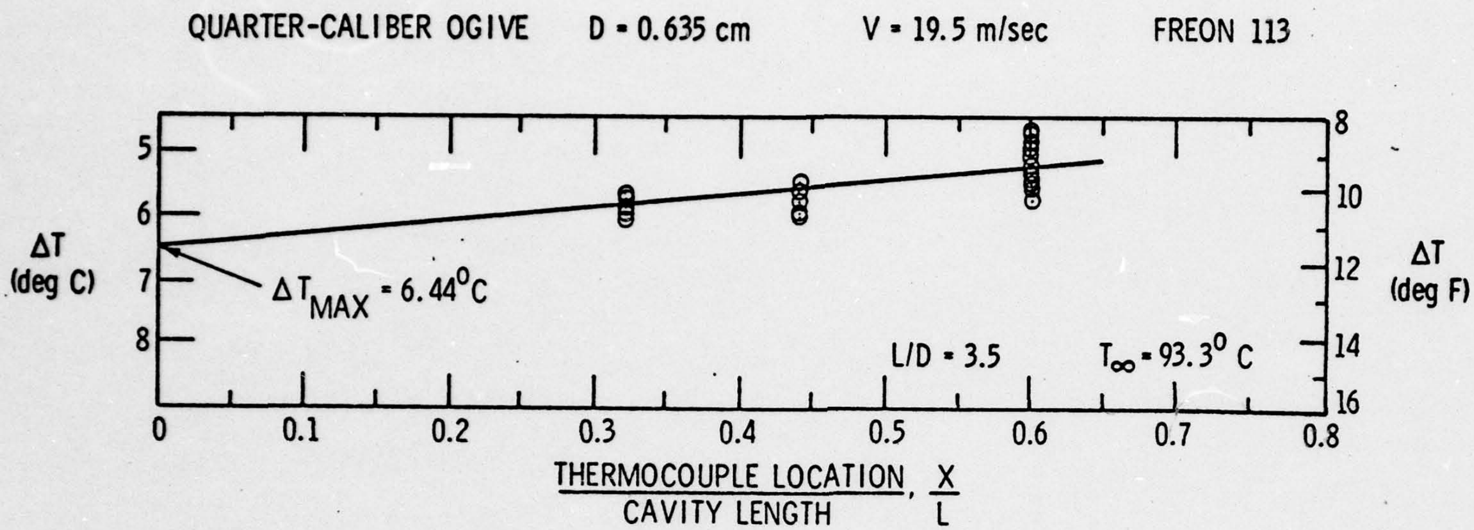

Figure 16 - ΔT vs X/L for T_{∞} = 93.3°C: QCO, D=0.635 cm, V=19.5 m/sec, Freon 113

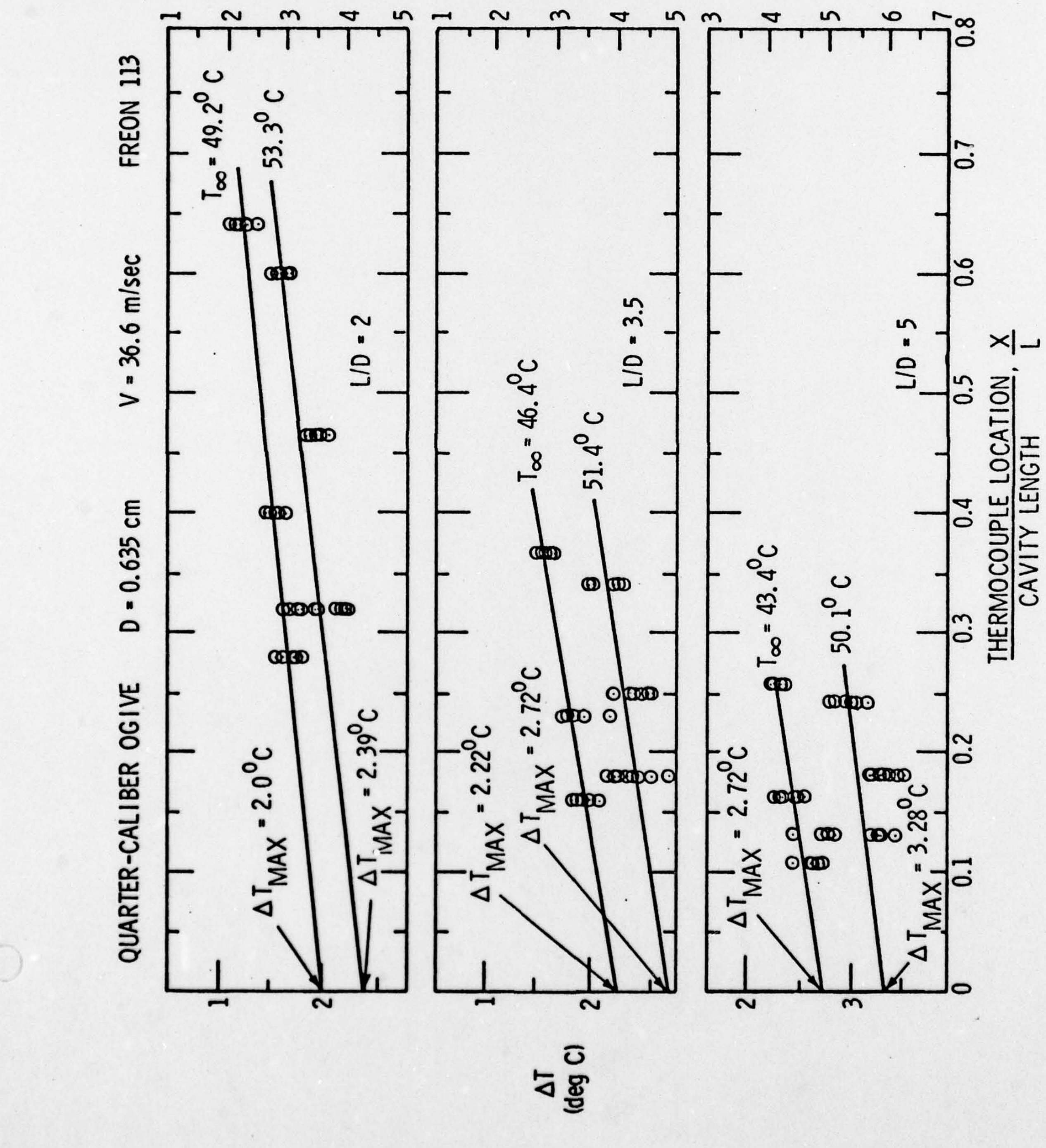

Figure 17 - ΔT vs X/L for T_∞ = 49.2, 53.3, 46.4, 51.4, 43.4 and 50.1°C: QCO, D=0.635 cm, V=36.6 m/sec, Freon 113

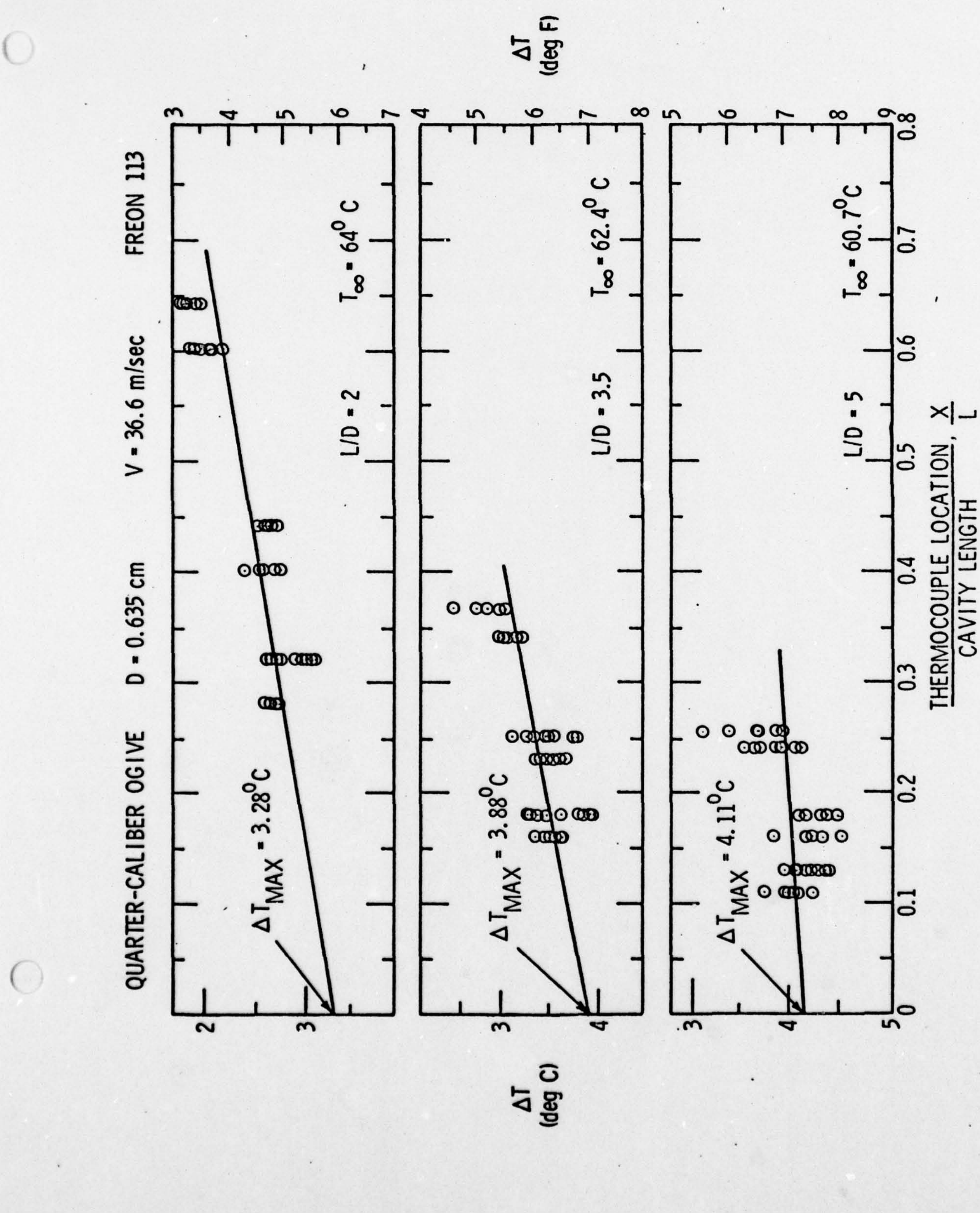

Figure 18 - ΔT vs X/L for T_∞ = 64.0, 62.4, and 60.7°C: QCO, D=0.635 cm, V=36.6 m/sec, Freon 113

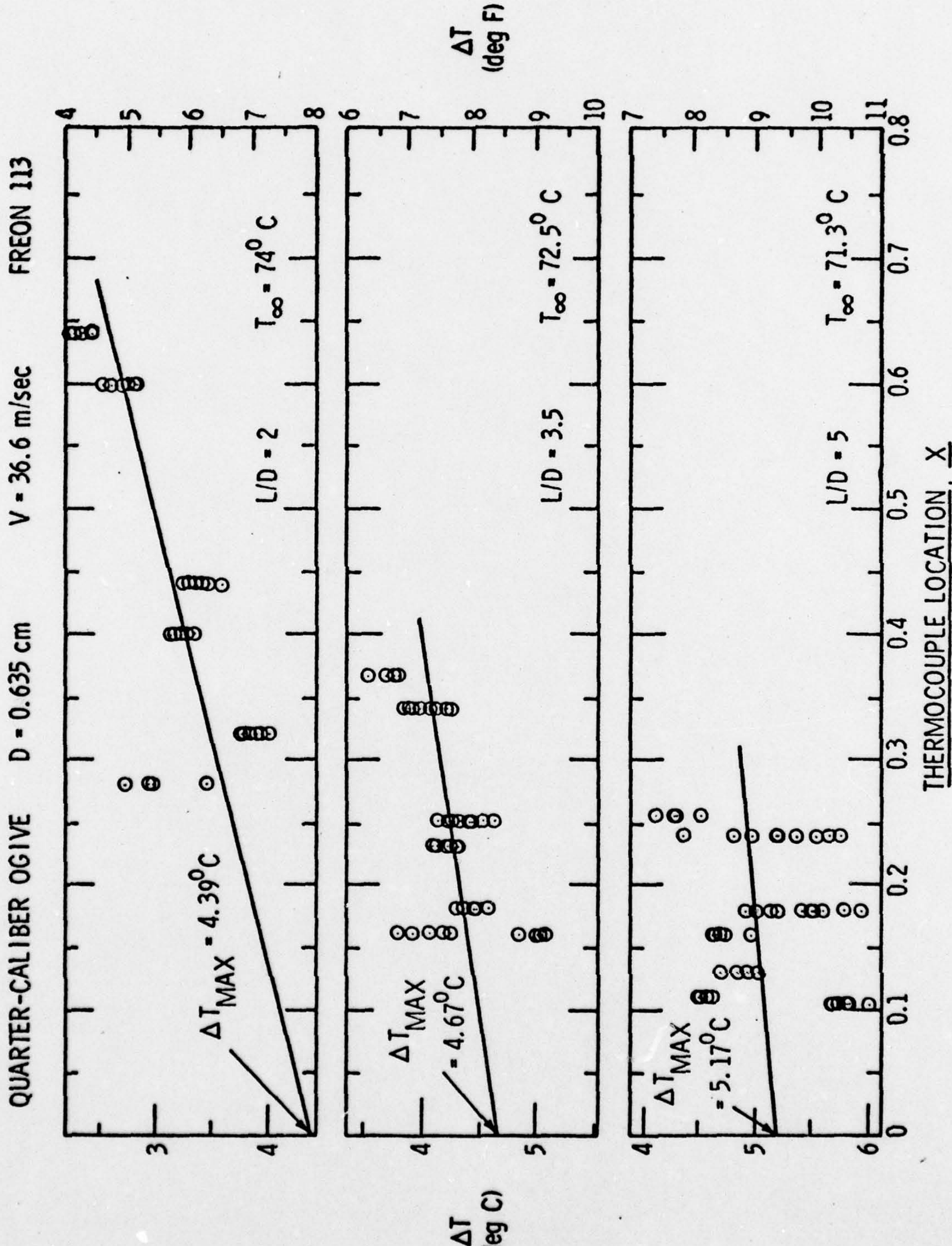

Figure 19 - ΔT vs X/L for T_∞ = 74.0, 72.5, and 71.3°C: QCO, D=0.635 cm, V=36.6 m/sec, Freon 113

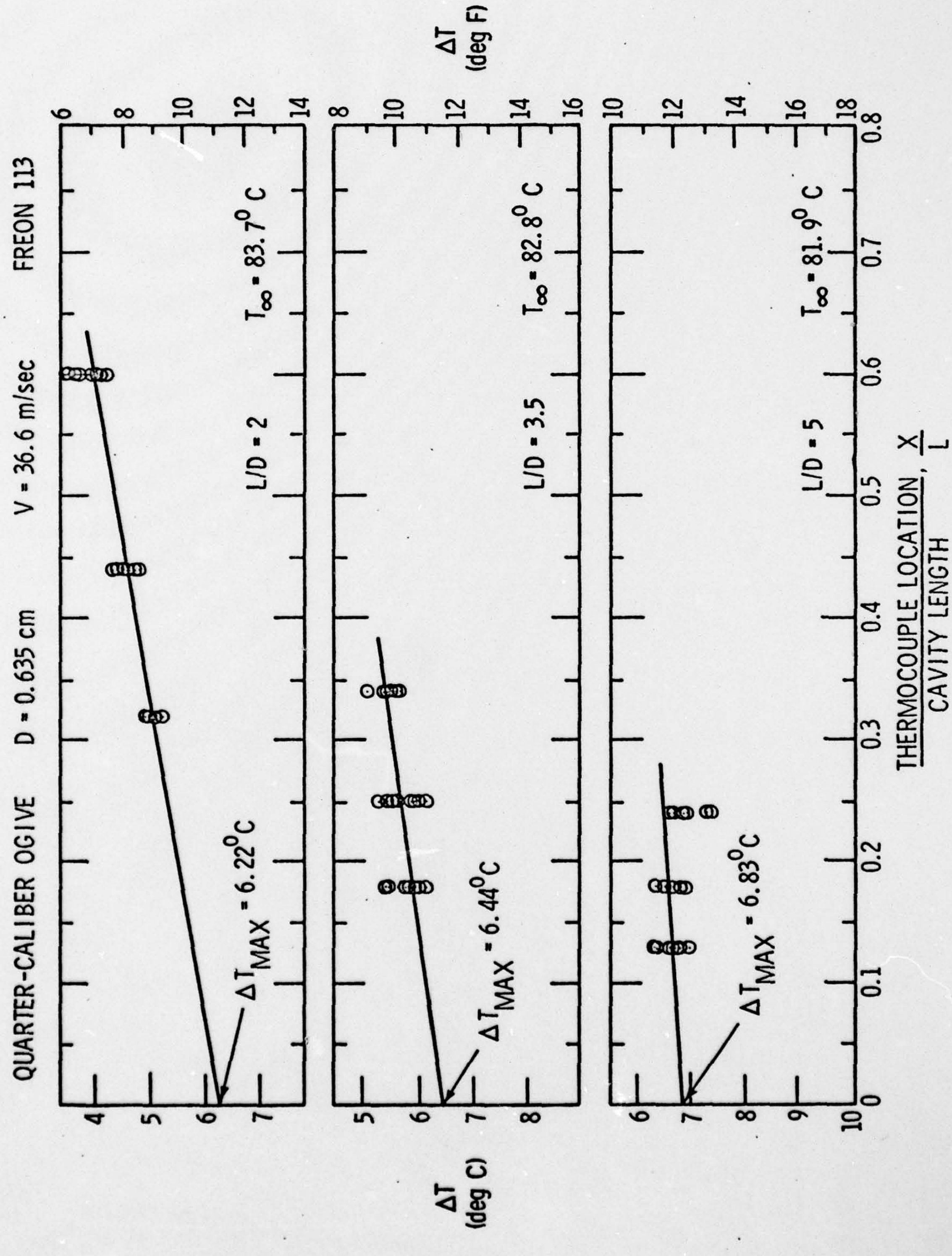

Figure 20 - ΔT vs X/L for T_∞ = 83.7, 82.8, and 81.9°C: QCO, D=0.635 cm, V=36.6 m/sec, Freon 113

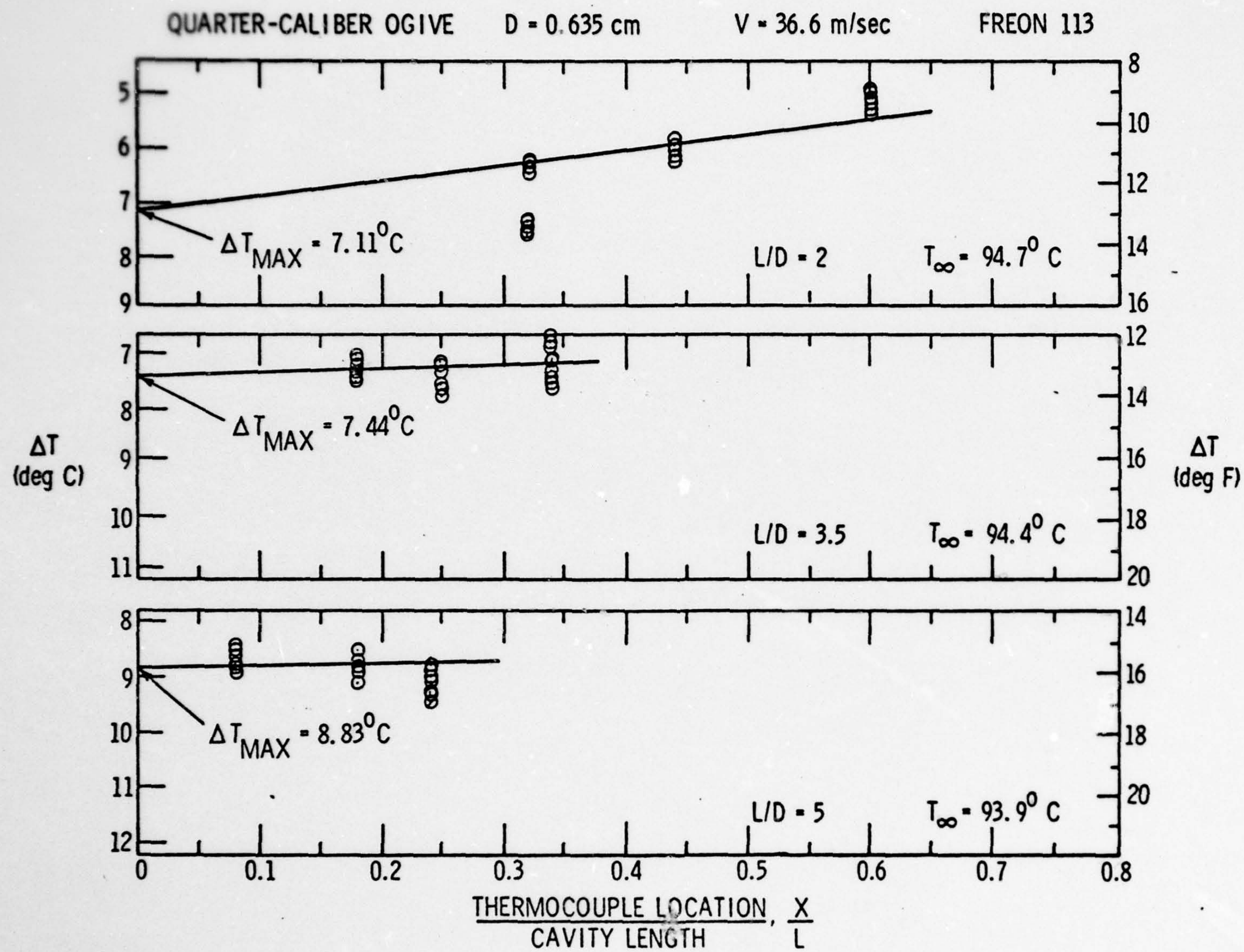

Figure 21 - ΔT vs X/L for T_∞ = 94.7, 94.4, and 93.9°C: QCO, D=0.635 cm, V=36.6 m/sec, Freon 113

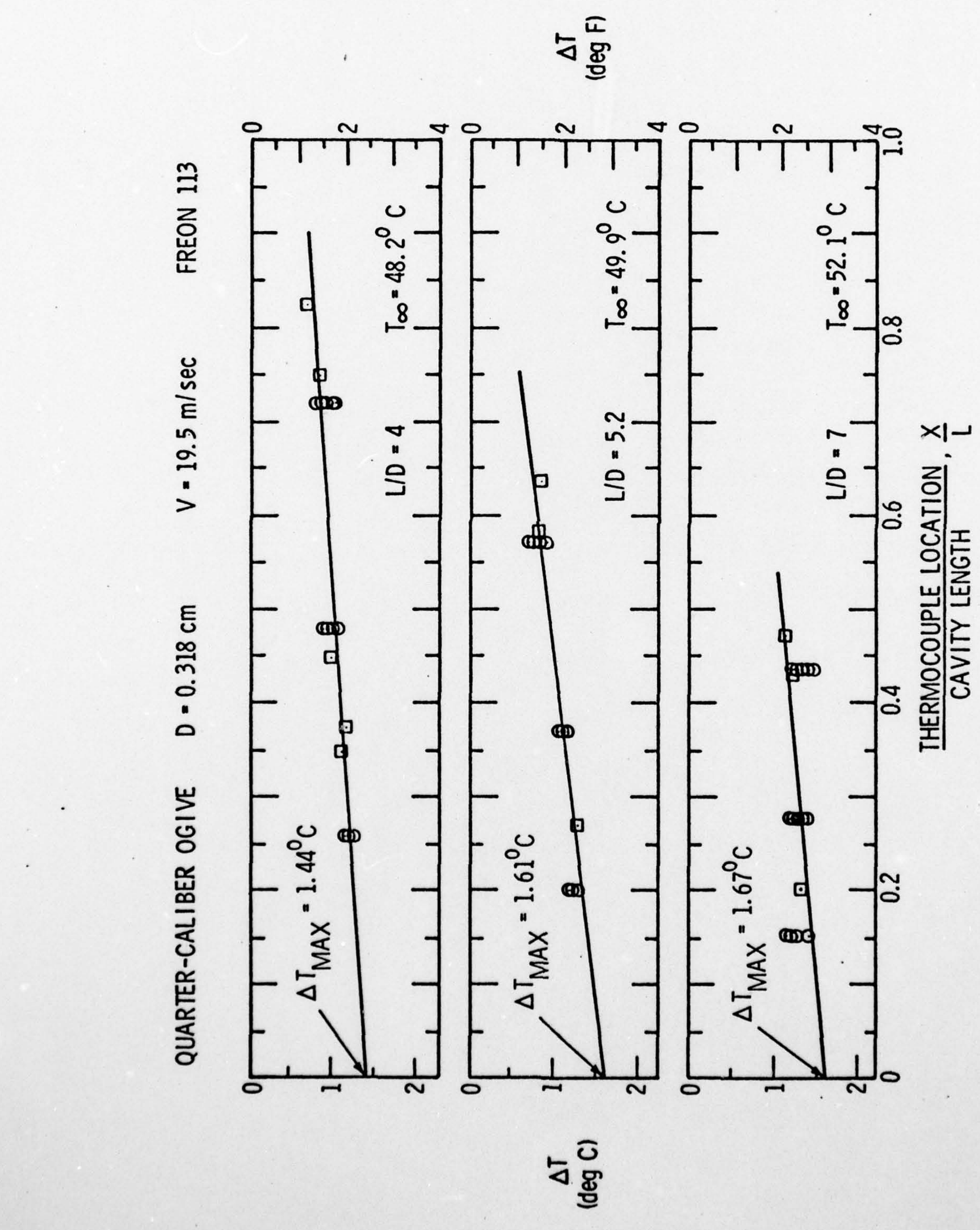

Figure 22 - ΔT vs X/L for T_∞ = 48.2, 49.9, and 52.1°C: QCO, D=0.318 cm, V=19.5 m/sec, Freon 113

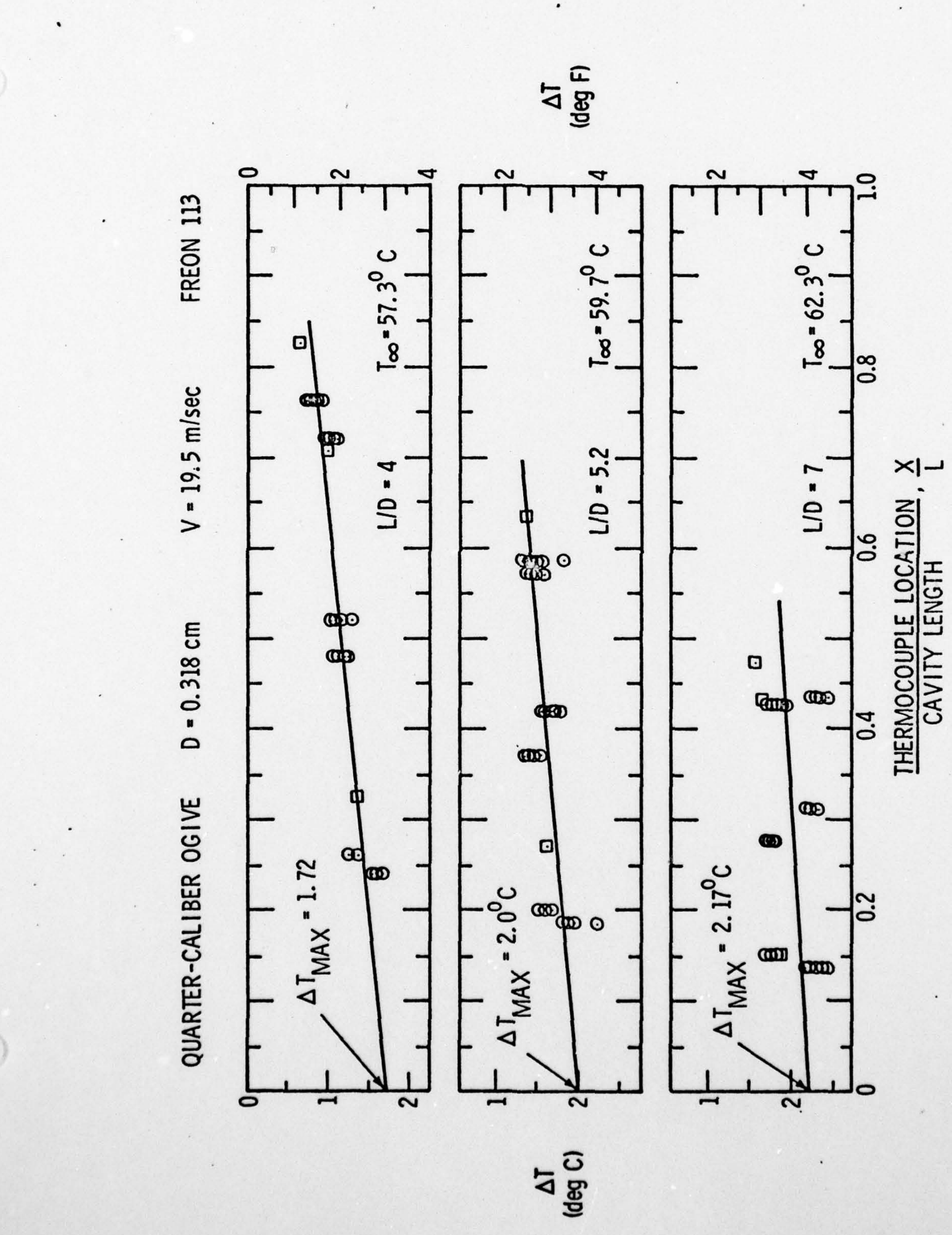

Figure 23 - ΔT vs X/L for T_∞ = 57.3, 59.7, and 62.3°C: QCO, D=0.318 cm, V=19.5 m/sec, Freon 113

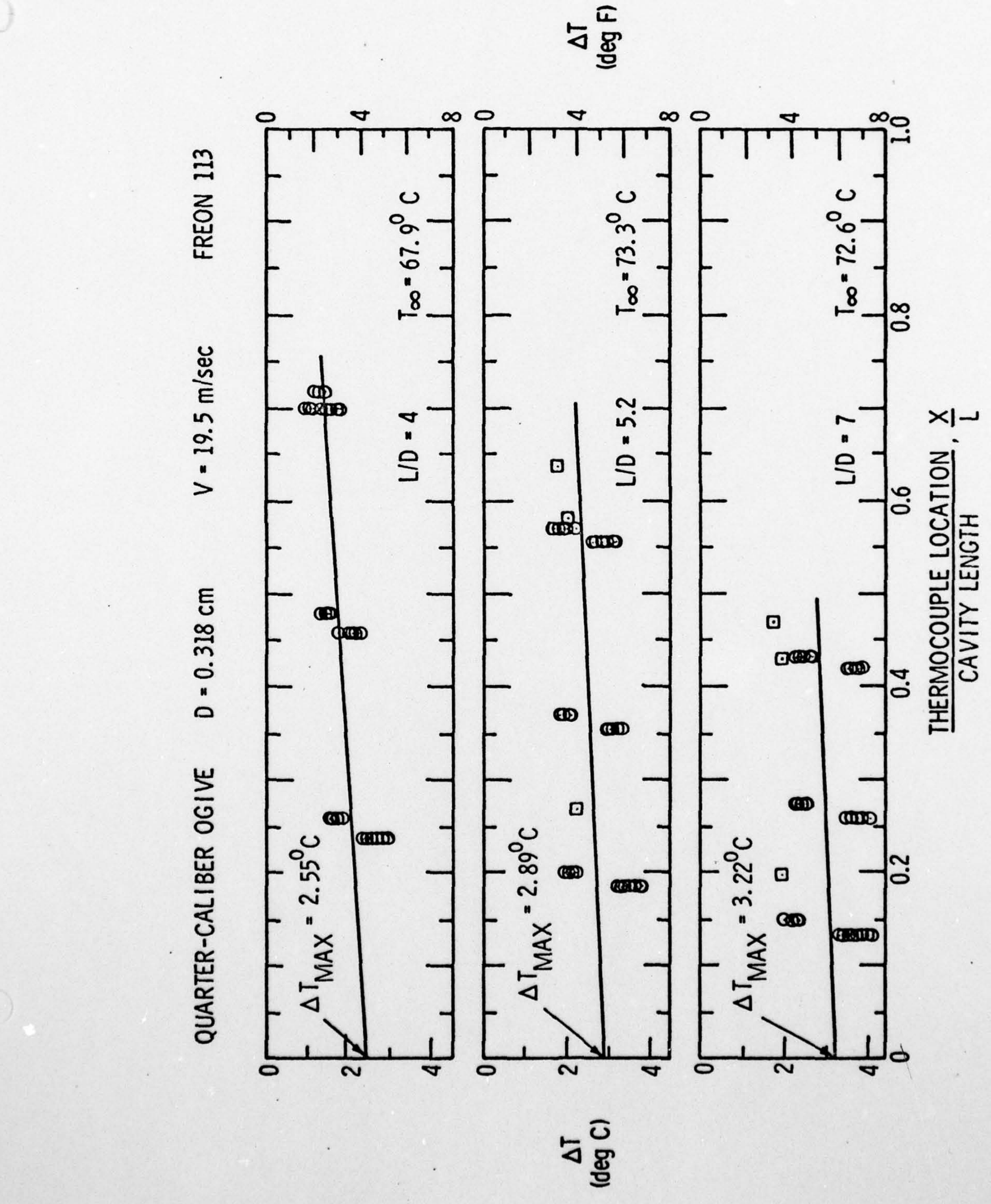

Figure 24 - ΔT vs X/L for T_∞ = 67.9, 73.3, and 72.6°C: QCO, D=0.318 cm, V=19.5 m/sec, Freon 113

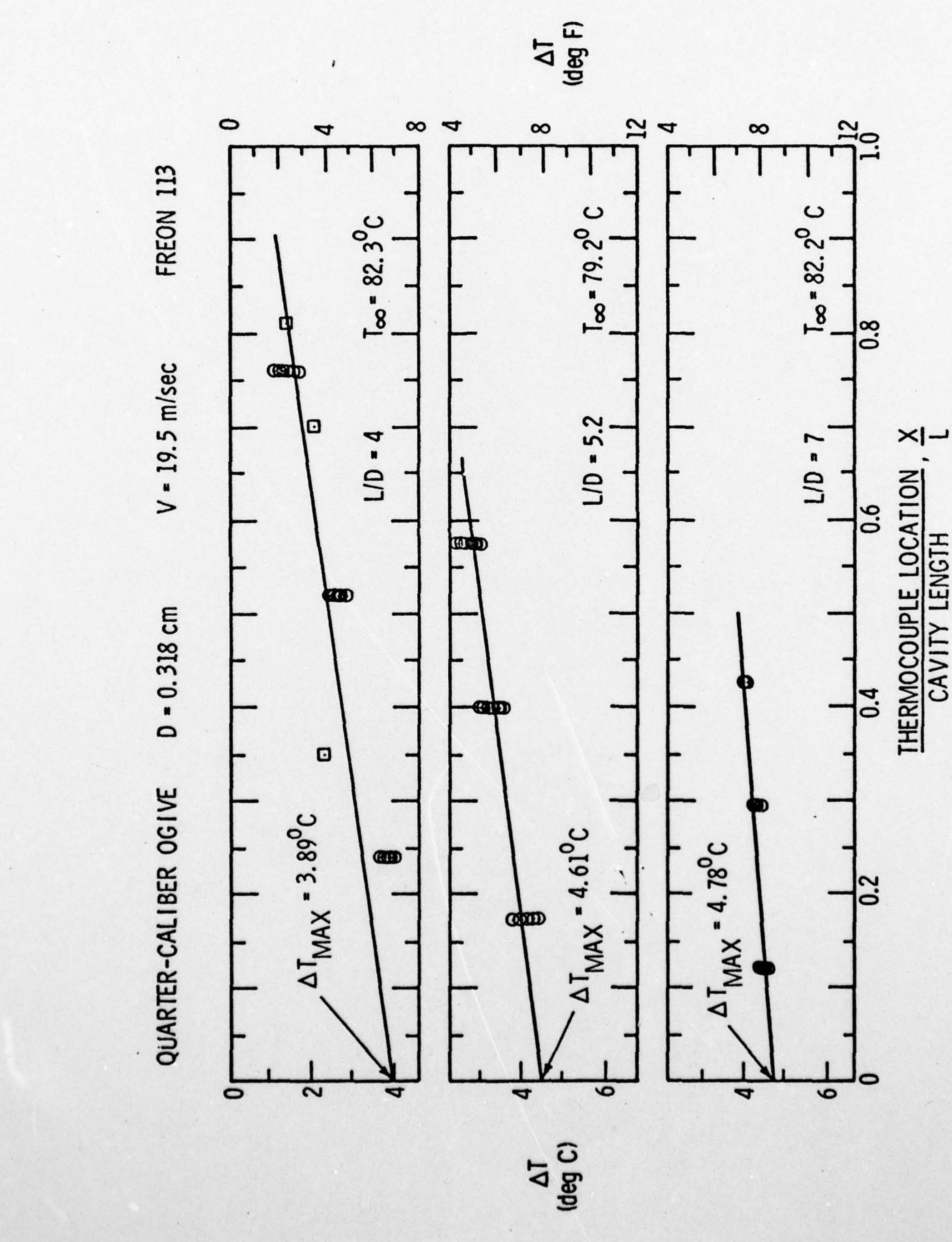

Figure 25 - ΔT vs X/L for T_∞ = 82.3, 79.2, and 82.2°C: QCO, D=0.318 cm, V=19.5 m/sec, Freon 113

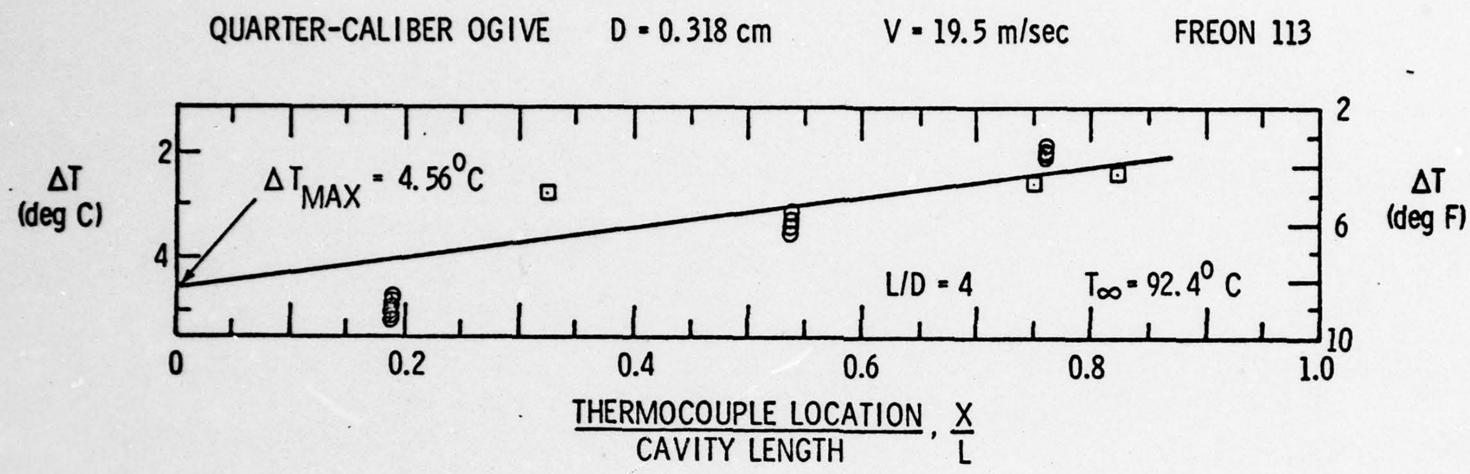

Figure 26 - ΔT vs X/L for T_∞ = 92.4°C: QCO, D=0.318 cm, V=19.5 m/sec, Freon 113

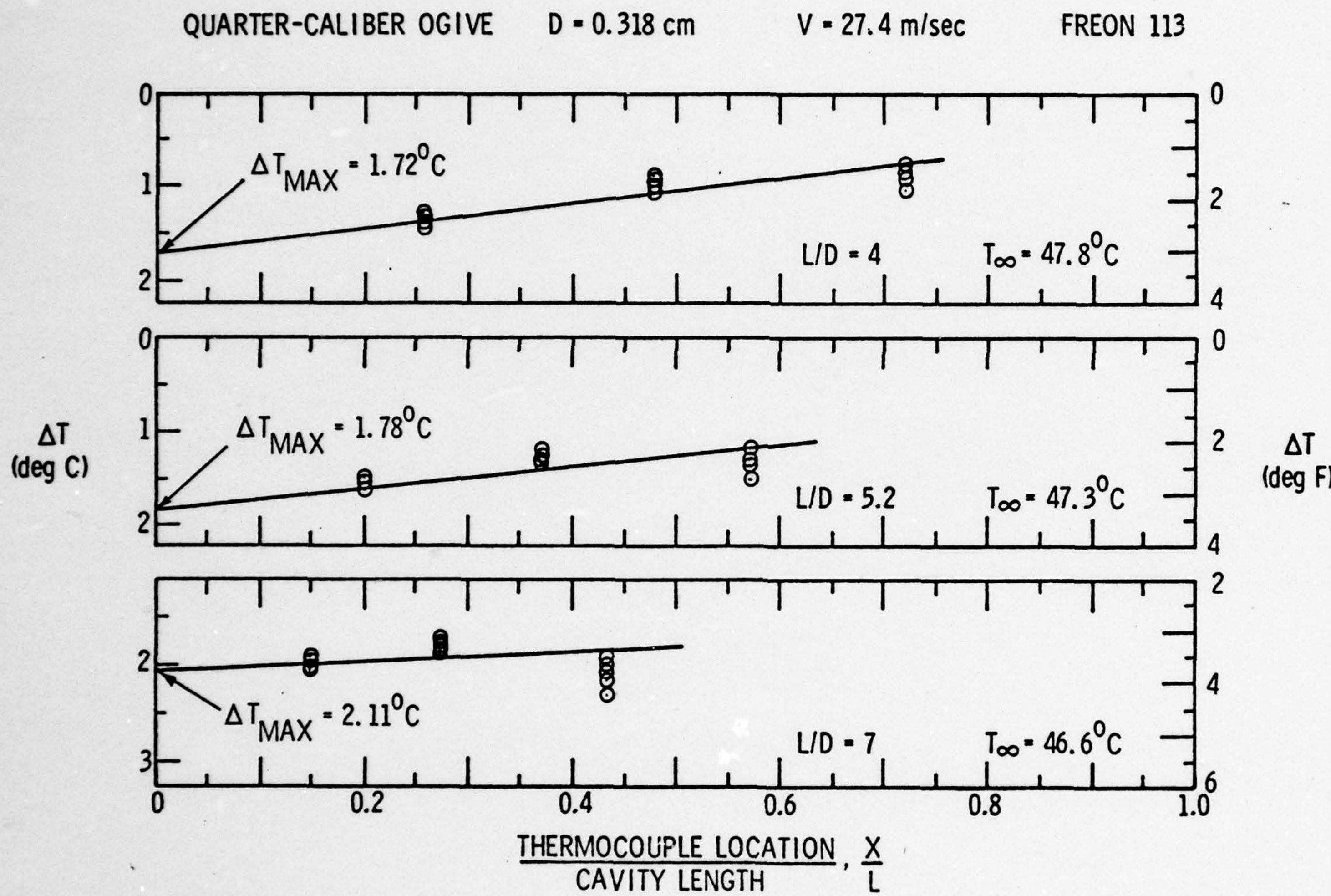

Figure 27 - ΔT vs X/L for T_∞ = 47.8, 47.3, and 46.6°C: QCO, D=0.318 cm, V=27.4 m/sec, Freon 113

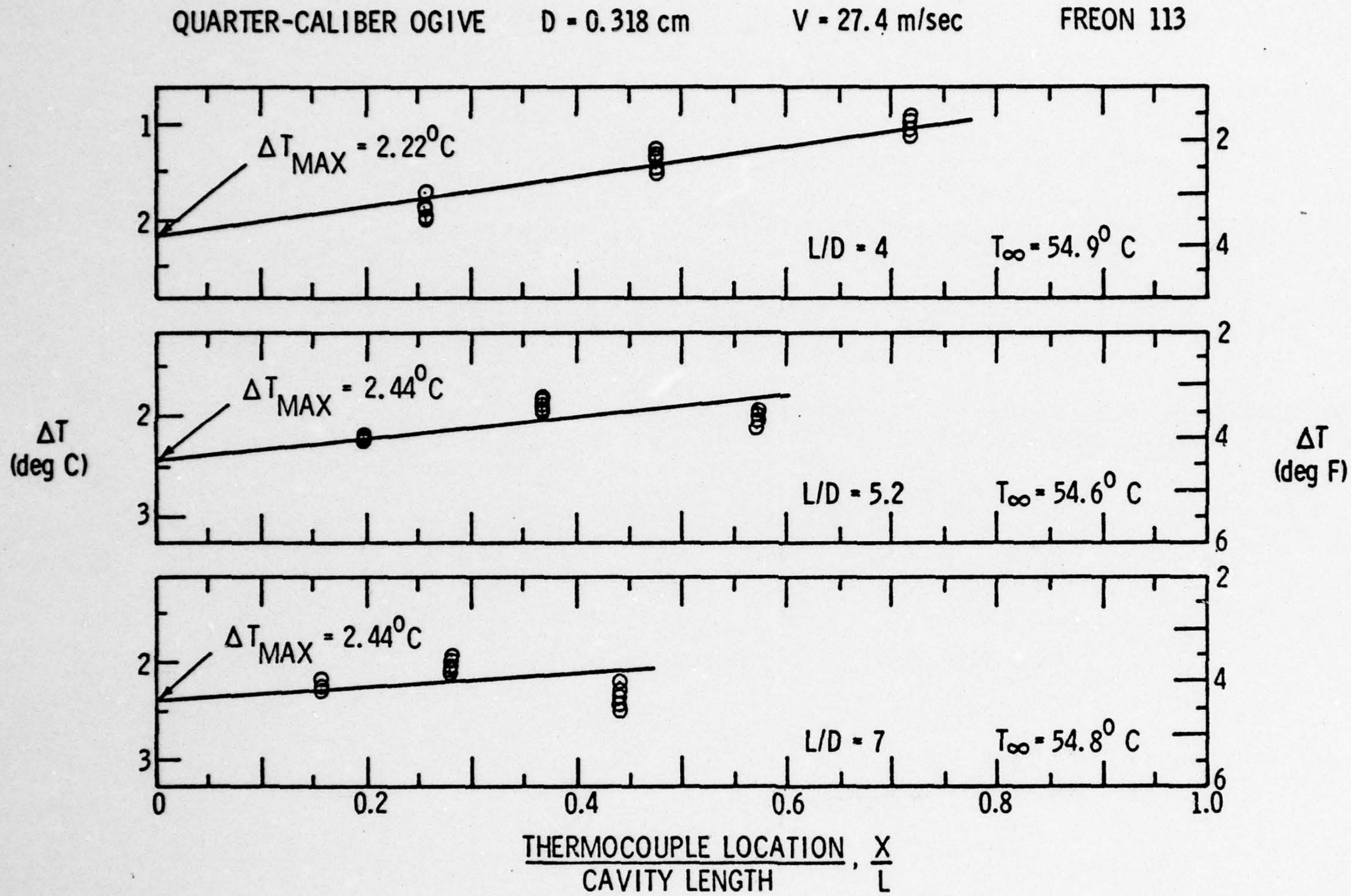

Figure 28 - ΔT vs X/L for T_∞ = 54.9, 54.6, and 54.8°C: QCO, D=0.318 cm, V=27.4 m/sec, Freon 113

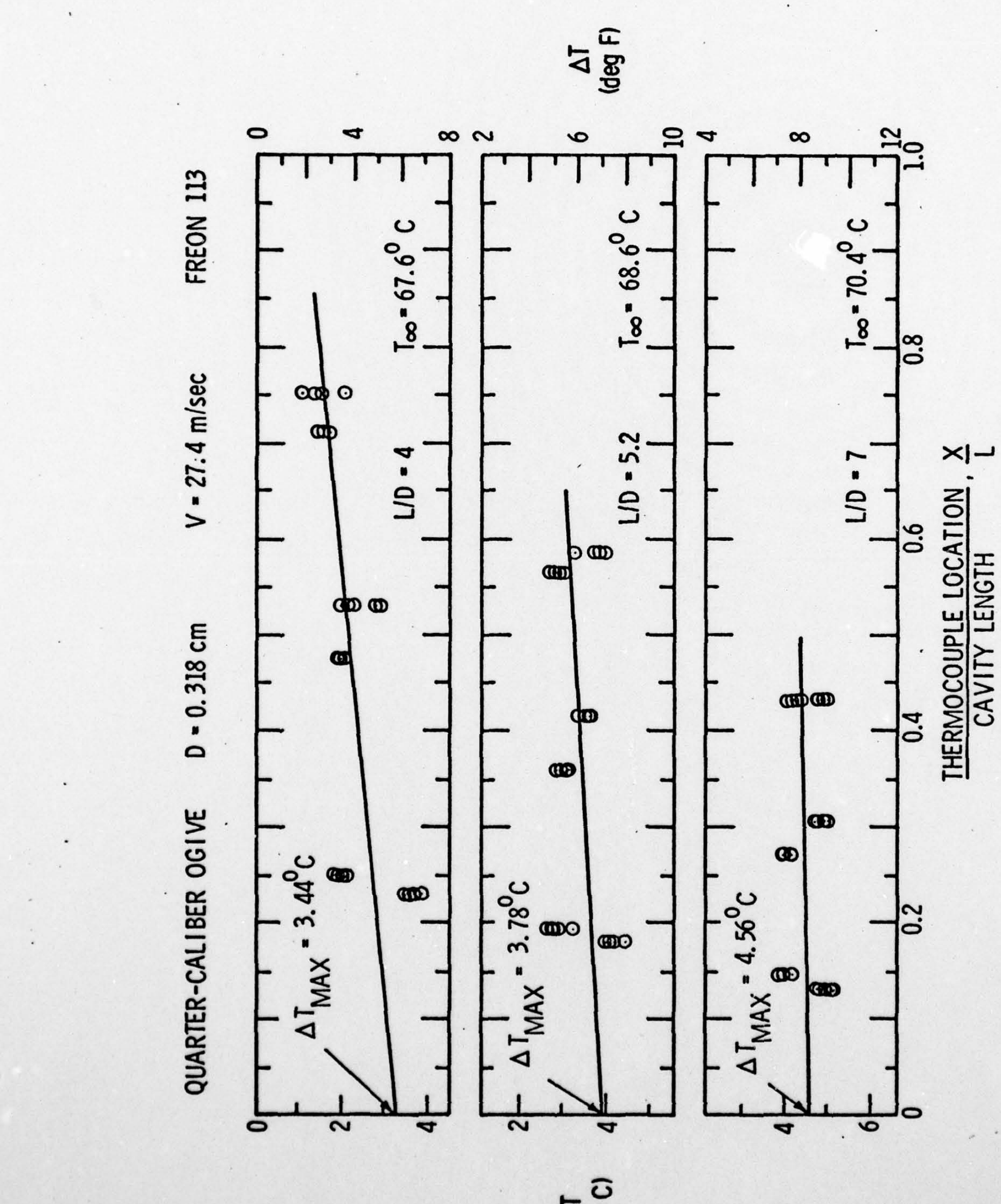

Figure 29 - ΔT vs X/L for T_∞ = 67.6, 68.6, and 70.4°C: QCO, D=0.318 cm, V=27.4 m/sec, Freon 113

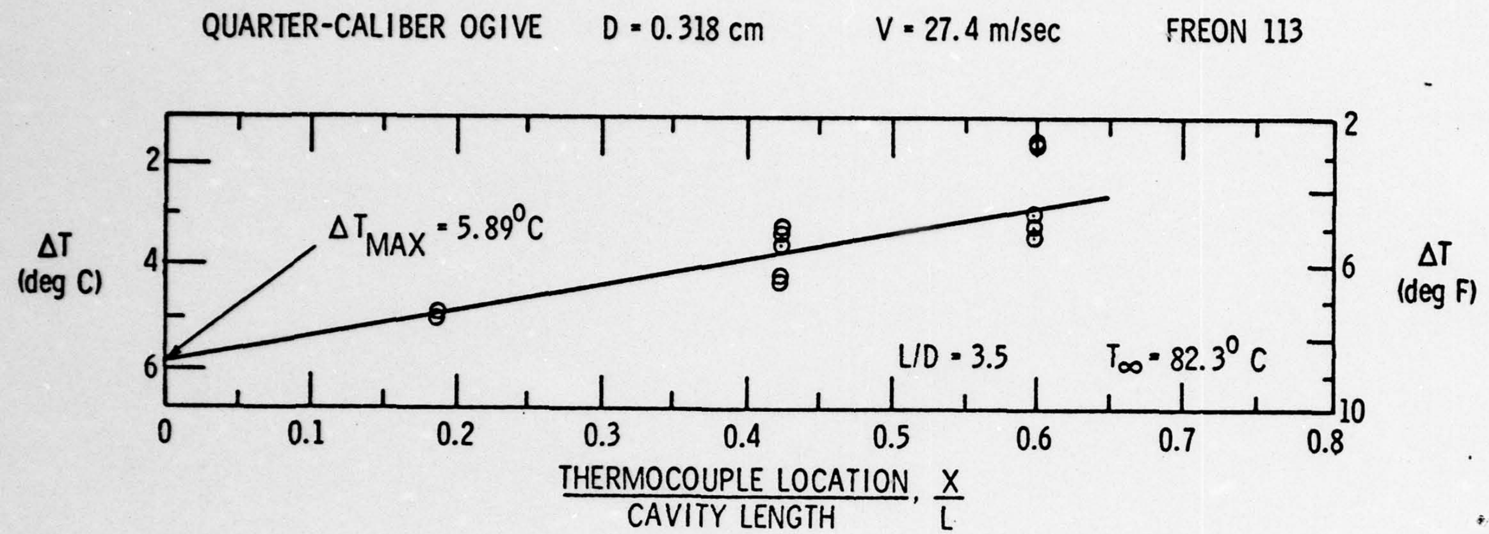

Figure 30 - ΔT vs X/L for T_∞ = 82.3°C: QCO, D=0.318, V=27.4 m/sec, Freon 113

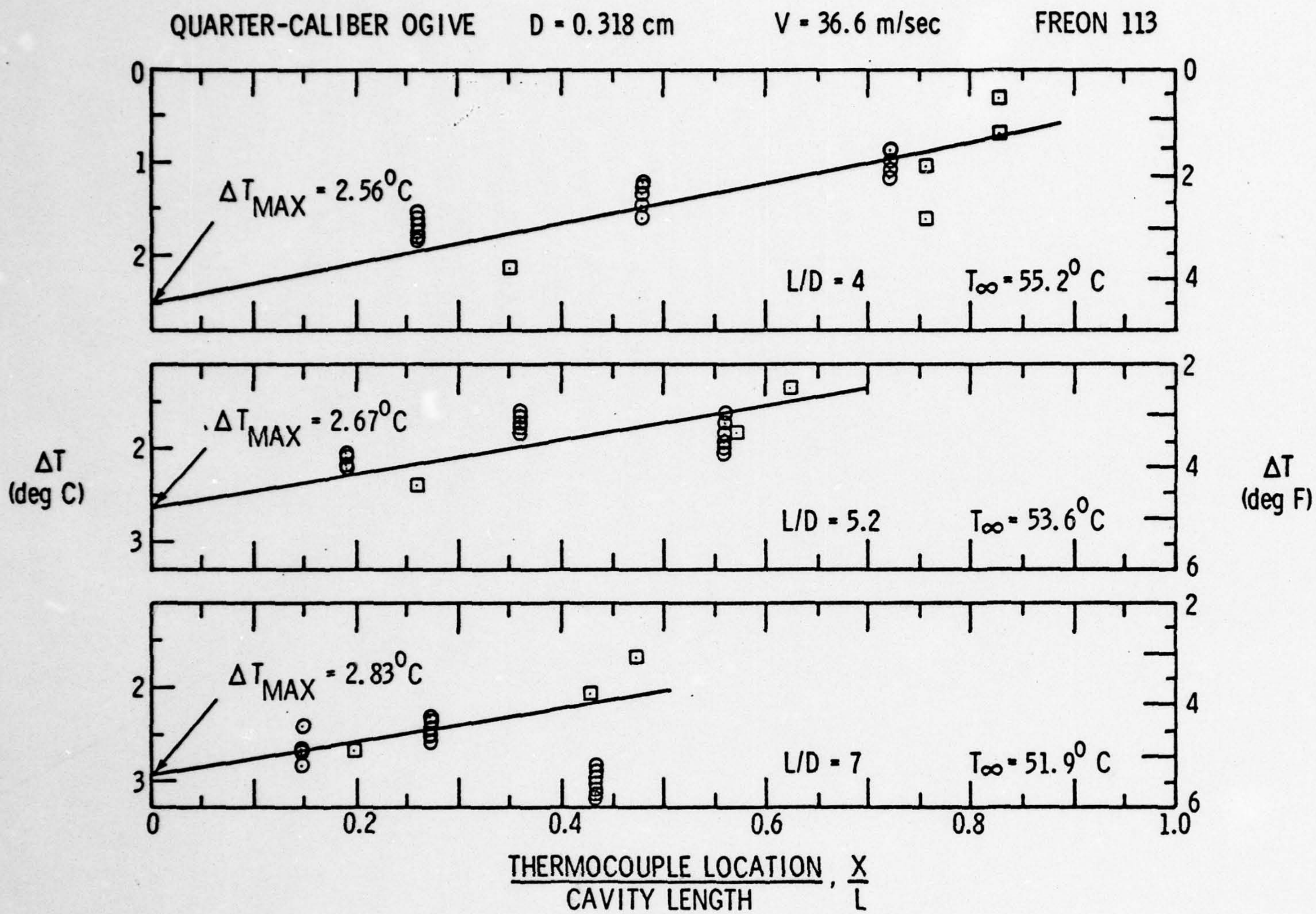

Figure 31 - ΔT vs X/L for T_∞ = 55.2, 53.6, and 51.9°C: QCO, D=0.318 cm, V=36.6 m/sec, Freon 113

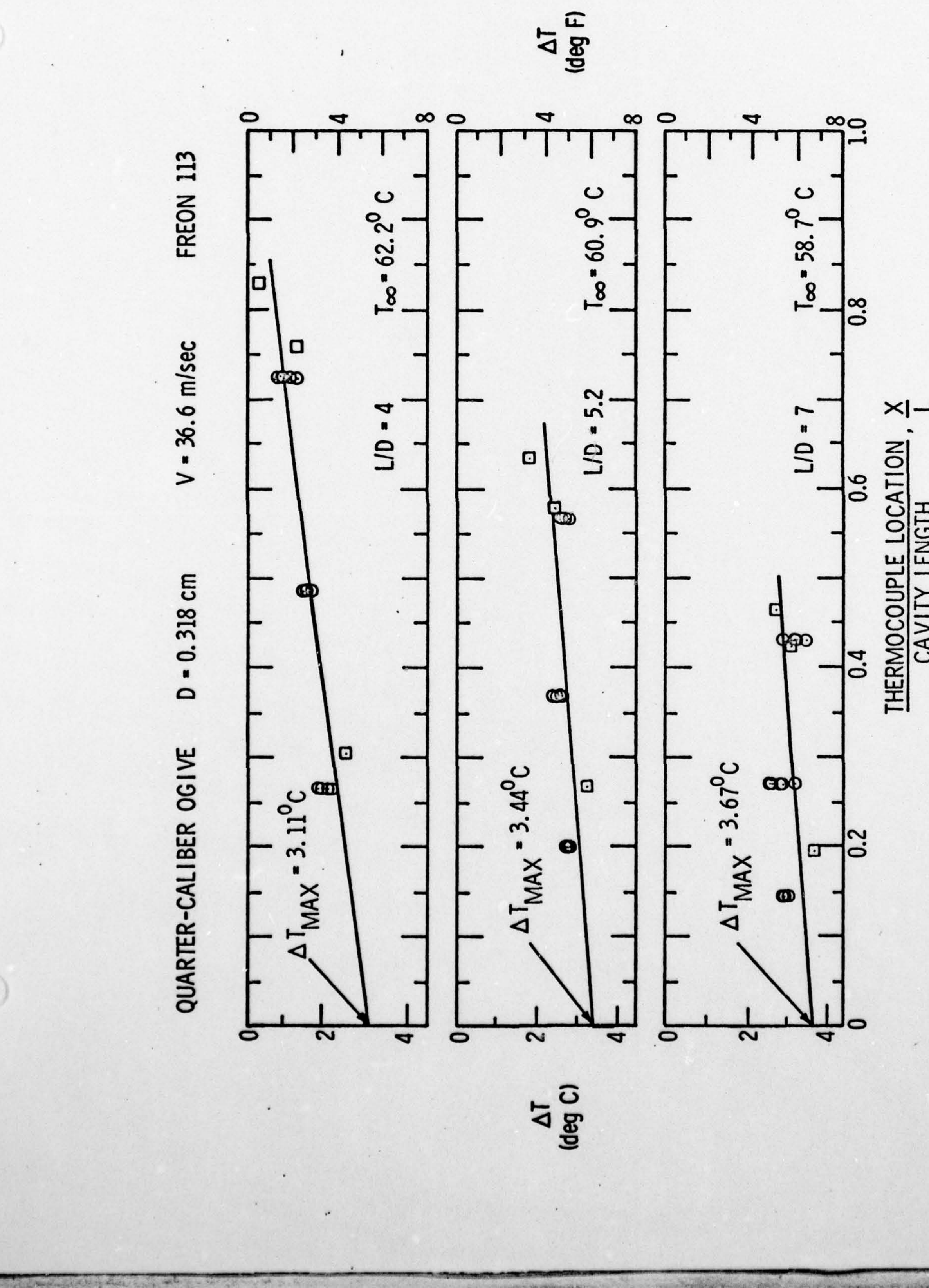

Figure 32 - ΔT vs X/L for T_∞ = 62.2, 60.9, and 58.7°C: QCO, D=0.318 cm, V=36.6 m/sec, Freon 113

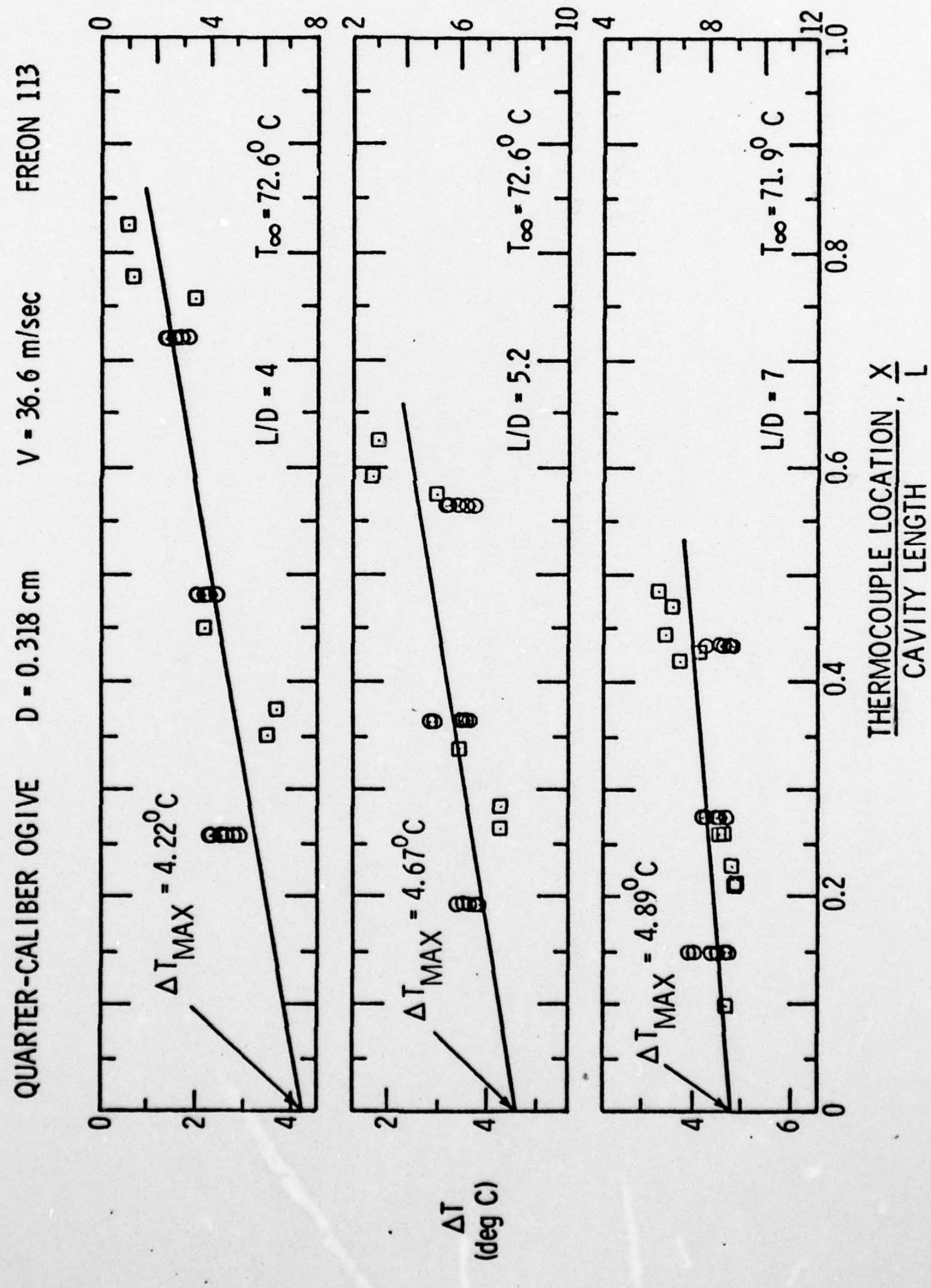

Figure 33 - ΔT vs X/L for T_∞ = 72.6, 72.6, and 71.9°C: QCO, D=0.318 cm, V=36.6 m/sec, Freon 113

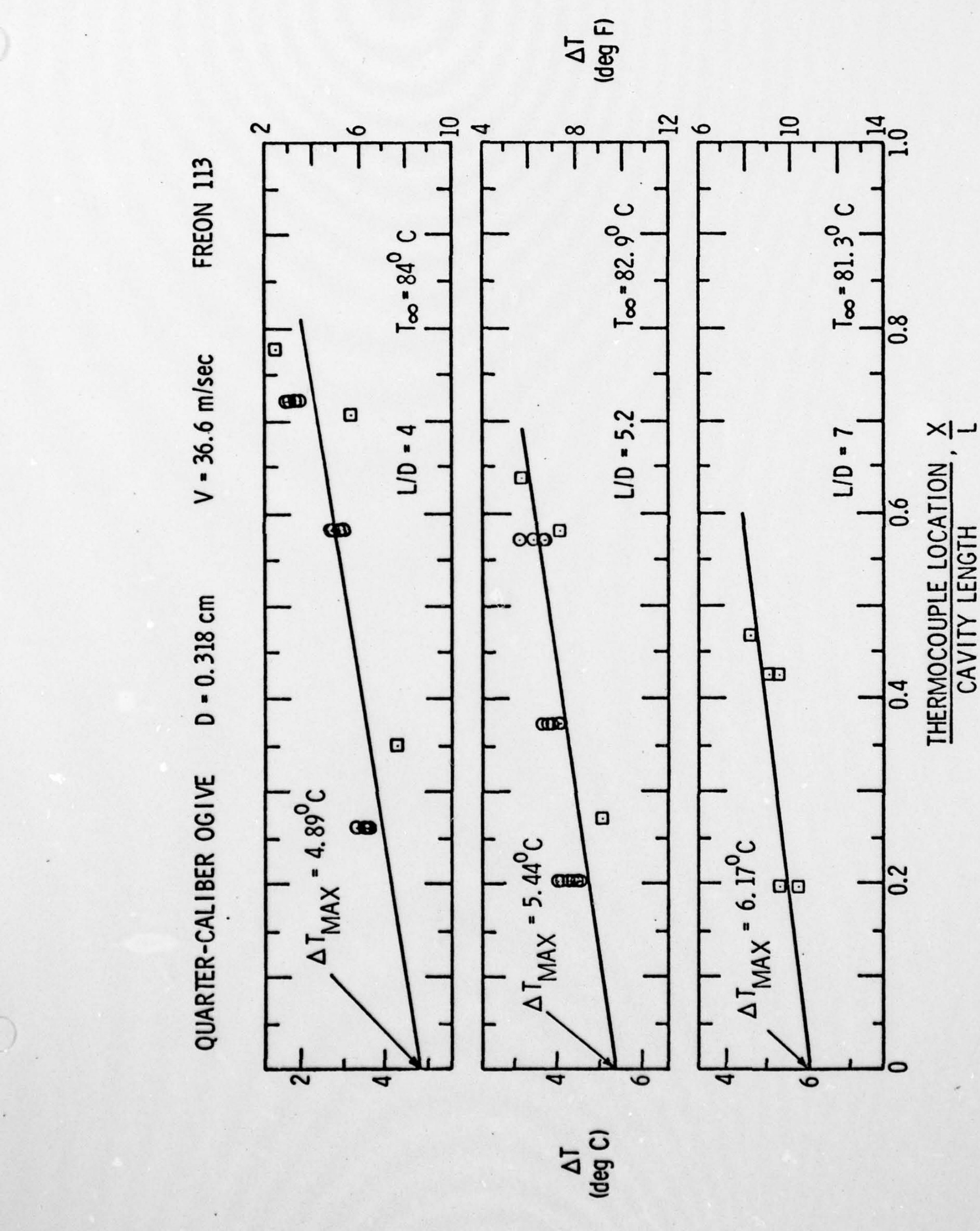

Figure 34 - ΔT vs X/L for T_∞ = 84.0 82.9, and 81.3°C: QCO, D=0.318 cm, V=36.6 m/sec, Freon 113

AD-A052 839 PENNSYLVANIA STATE UNIV UNIVERSITY PARK APPLIED RESE--ETC F/G 20/4
TABULATION AND SUMMARY OF THERMODYNAMIC EFFECTS DATA FOR DEVELO--ETC(U)
JAN 78 J W HOLL, M L BILLET, D S WEIR N00017-73-C-1418

UNCLASSIFIED TM-78-18 NL

2 OF 2
AD
A052839

END
DATE
FILMED
5-78
DDC

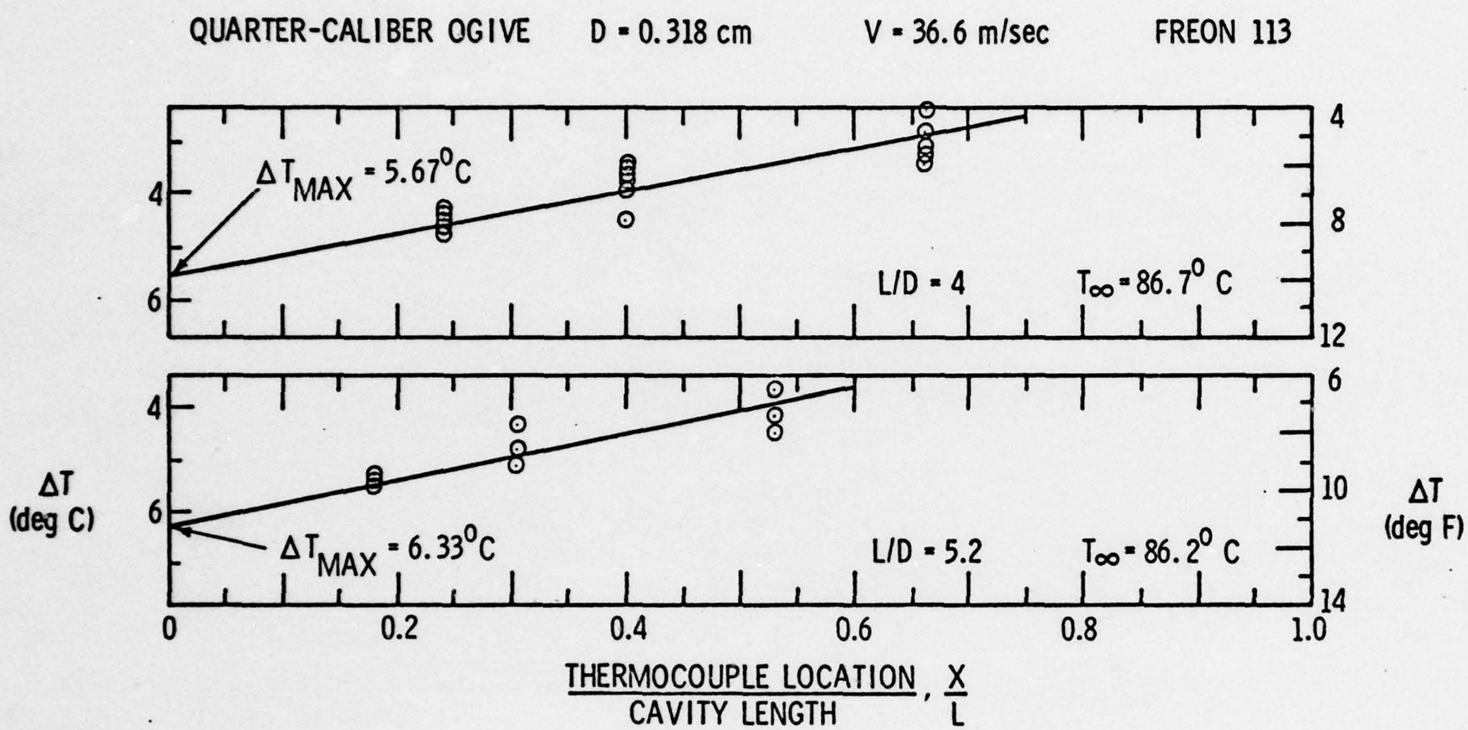

Figure 35 - ΔT vs X/L for T_∞ = 86.7 and 86.2°C: QCO, D=0.318 cm, V=36.6 m/sec, Freon 113

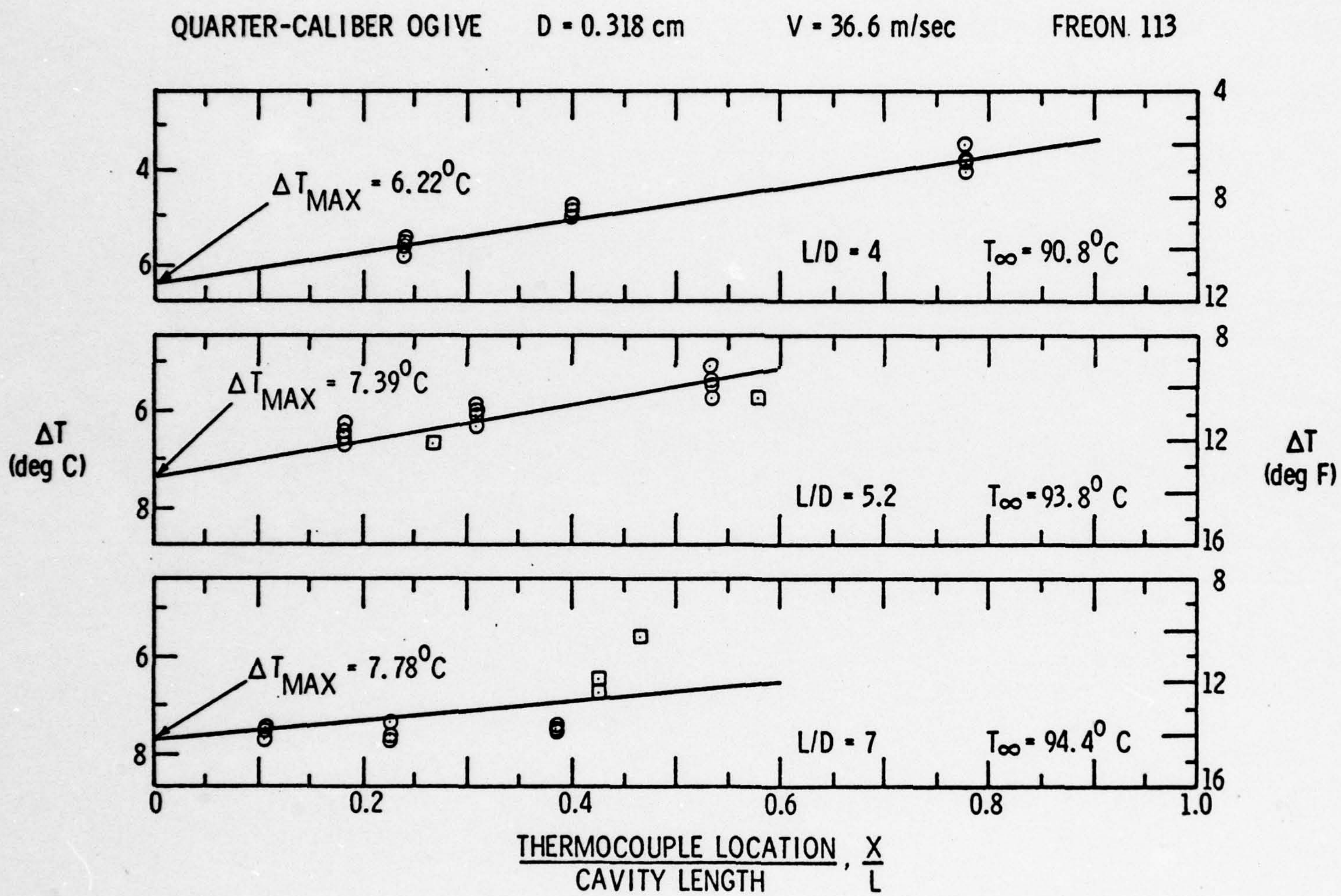

Figure 36 - ΔT vs X/L for T_∞ = 90.8, 93.8, and 94.4°C: QCO, D=0.318 cm, V=36.6 m/sec, Freon 113

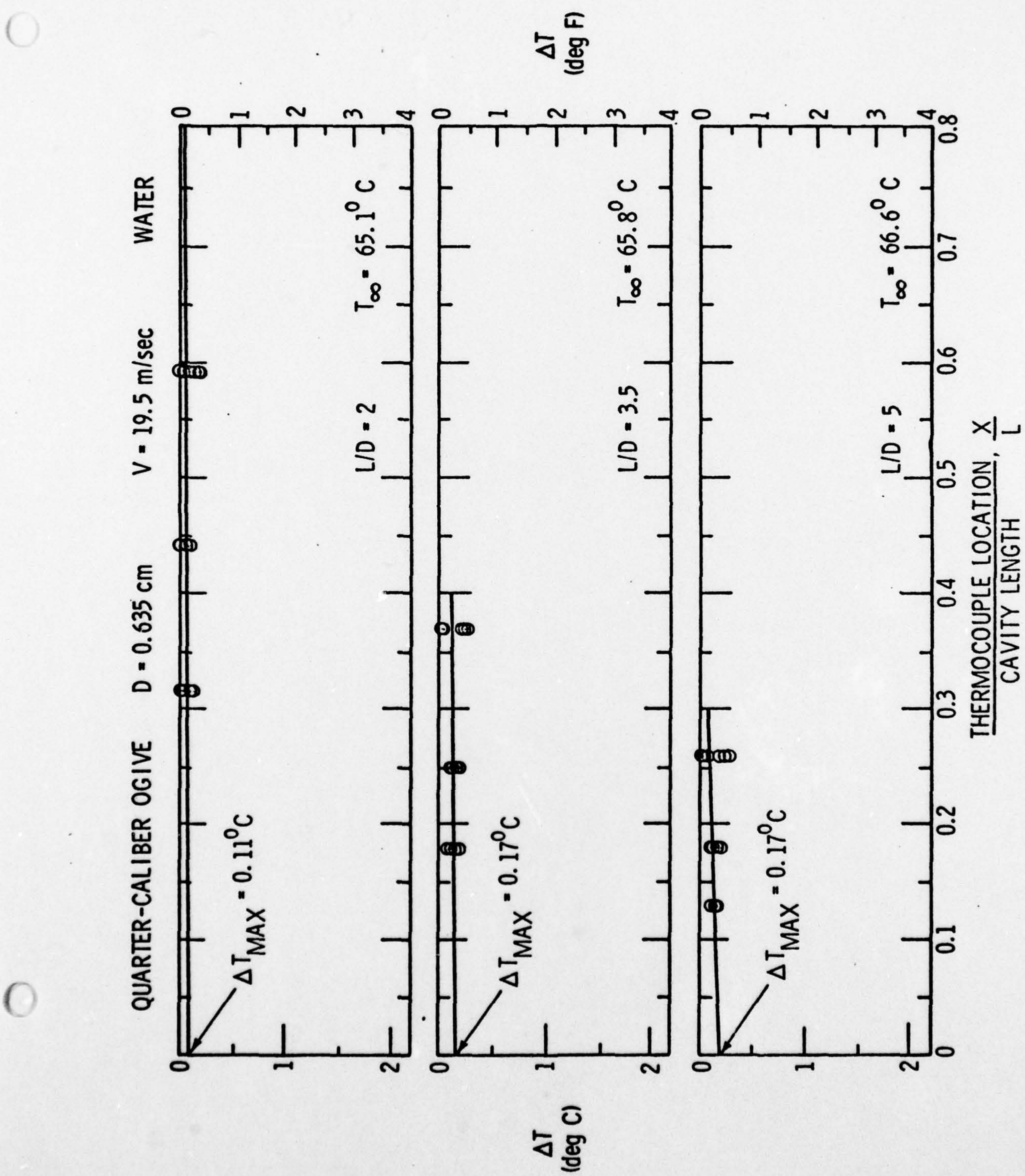

Figure 37 - ΔT vs X/L for T_∞ = 65.1, 65.8, and 66.6°C: QCO, D=0.635 cm, V=19.5 m/sec, Water

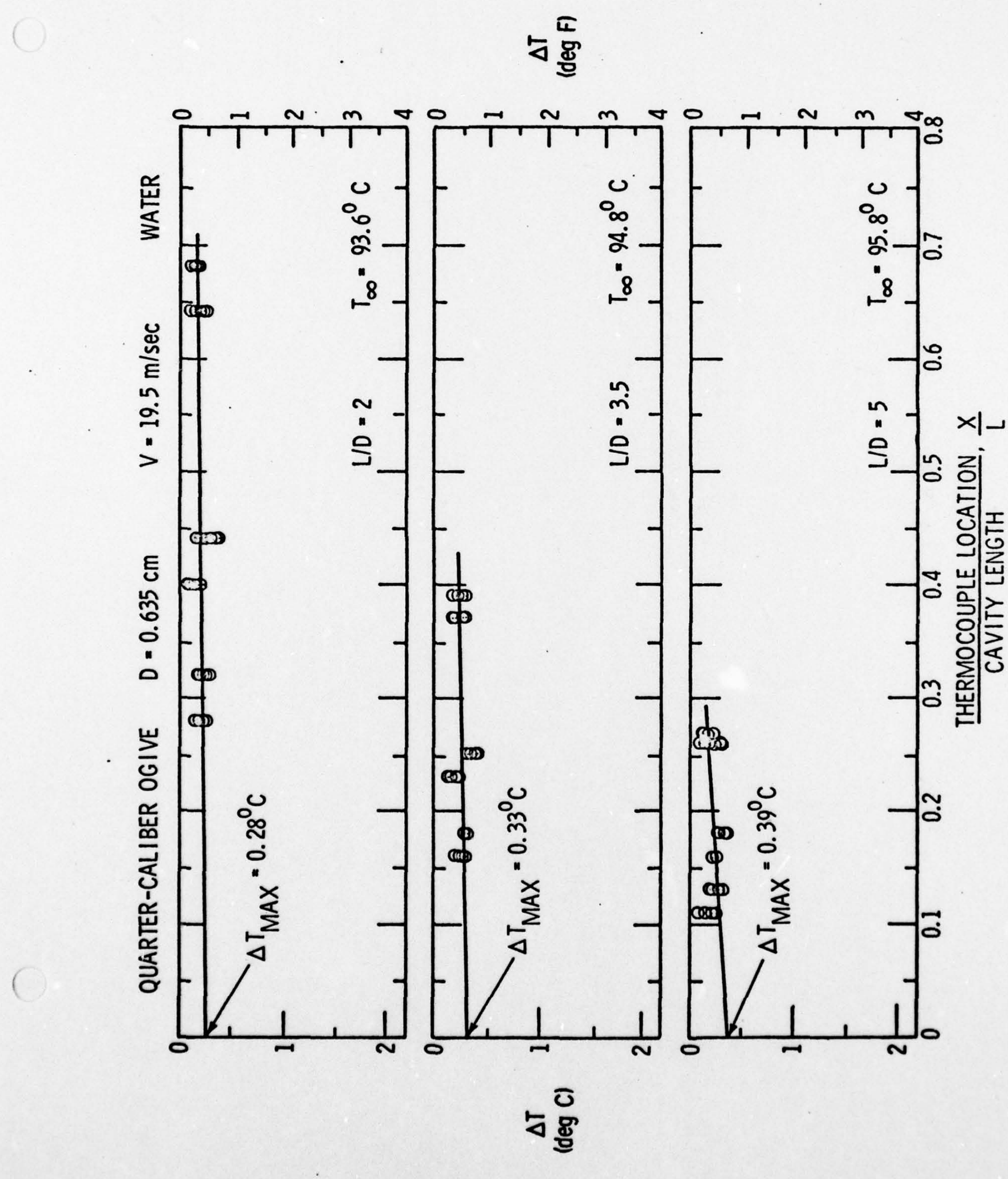

Figure 38 - ΔT vs X/L for T_∞ = 93.6, 94.8, and 95.8°C: QCO, D=0.635 cm, V=19.5 m/sec, Water

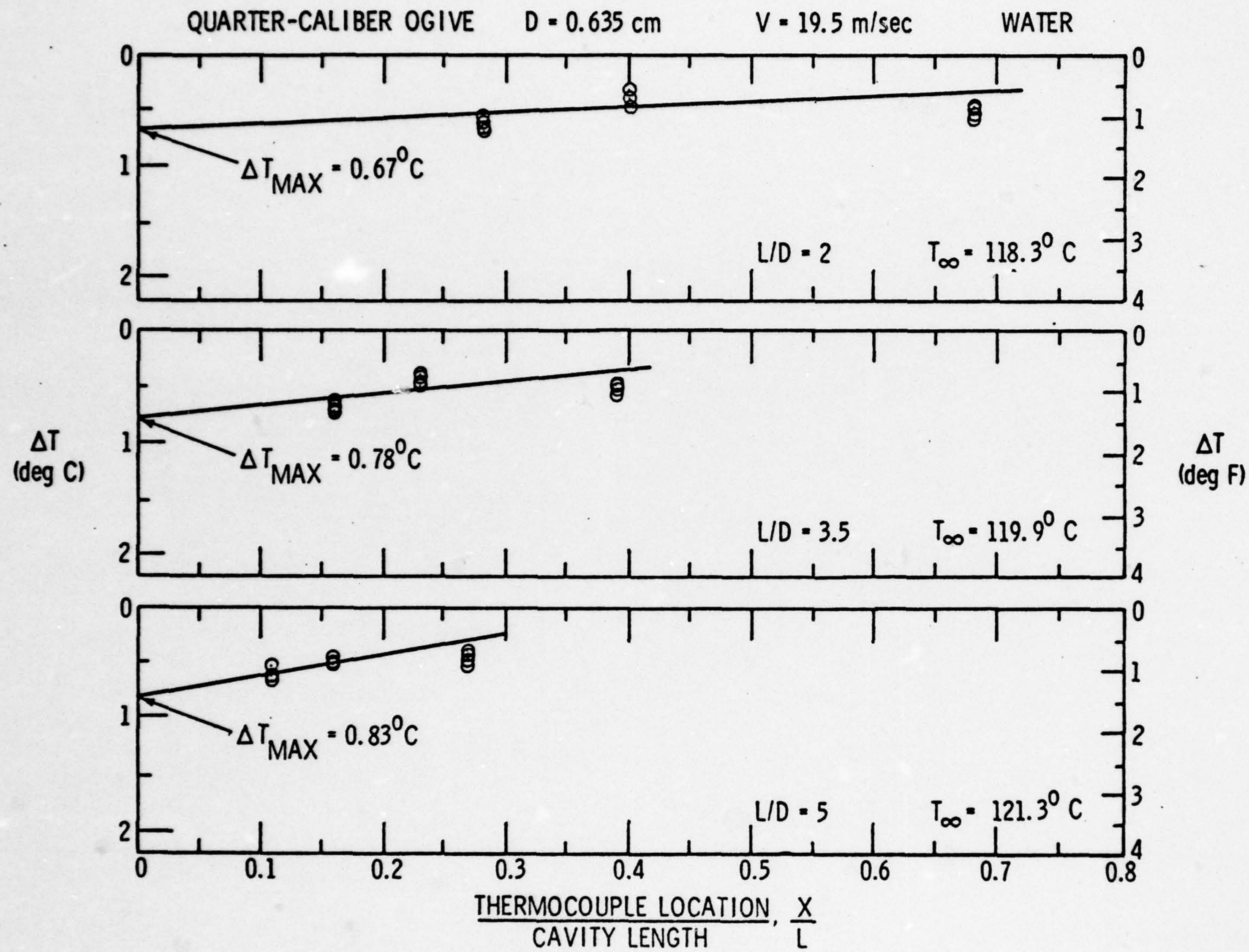

Figure 39 - ΔT vs X/L for T_∞ = 118.3, 119.9, and 121.3°C: QCO, D=0.635 cm, V=19.5 m/sec, Water

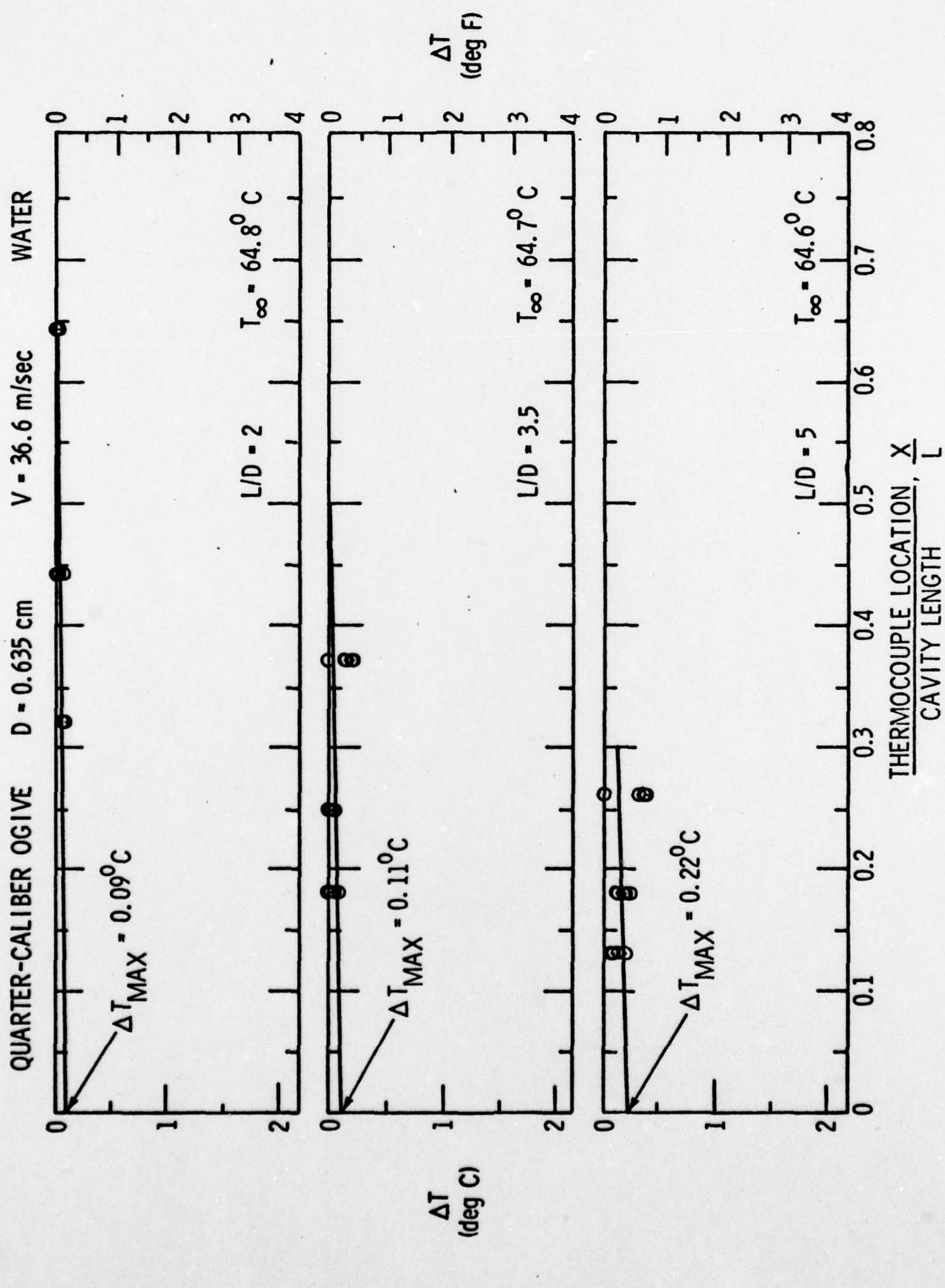

Figure 40 - ΔT vs X/L for T_∞ = 64.8, 64.7, and 64.6°C: QCO, D=0.635 cm, V=36.6 m/sec, Water

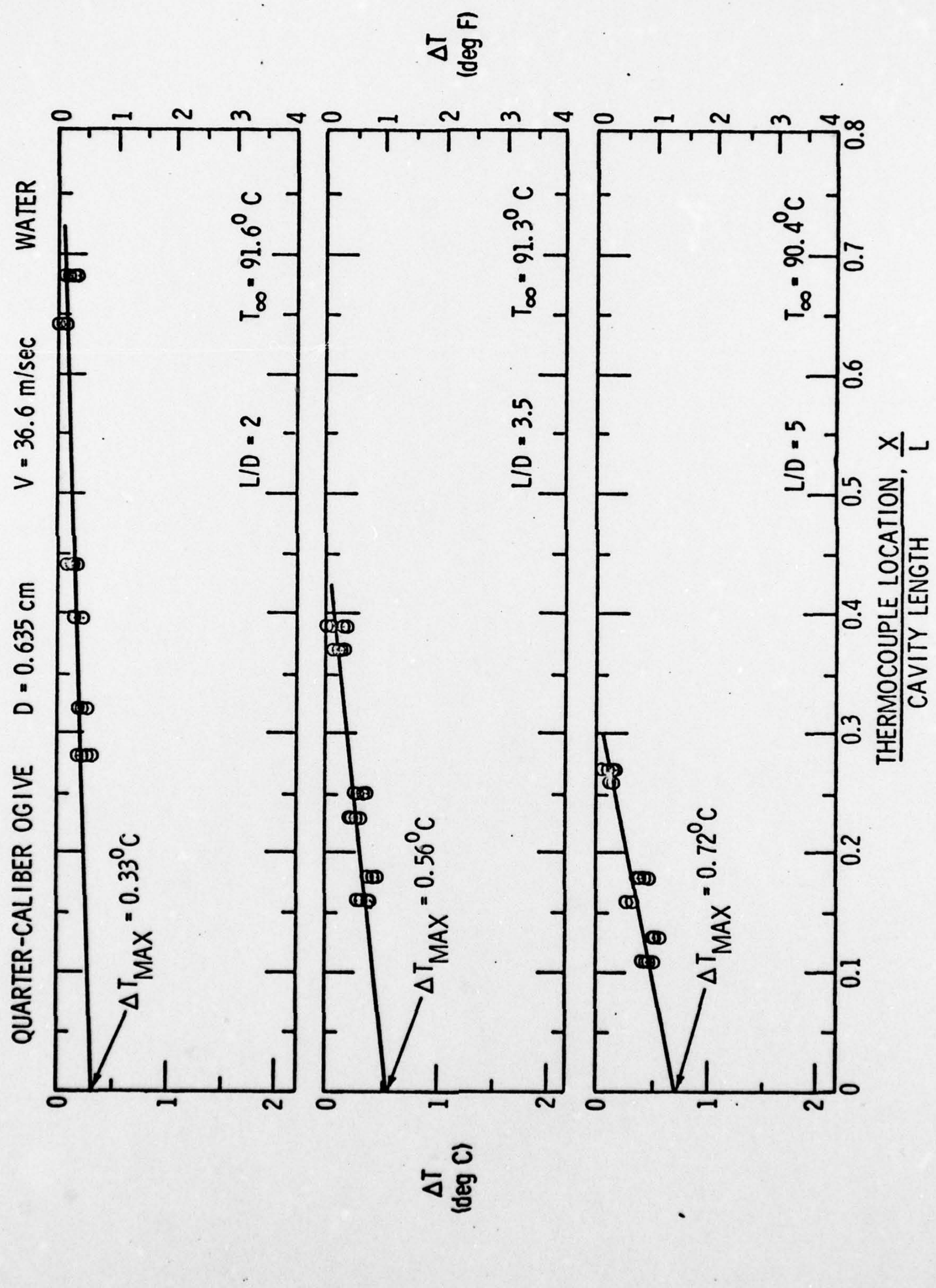

Figure 41 - ΔT vs X/L for T_∞ = 91.6, 91.3, and 90.4°C: QCO, D=0.635 cm, V=36.6 m/sec, Water

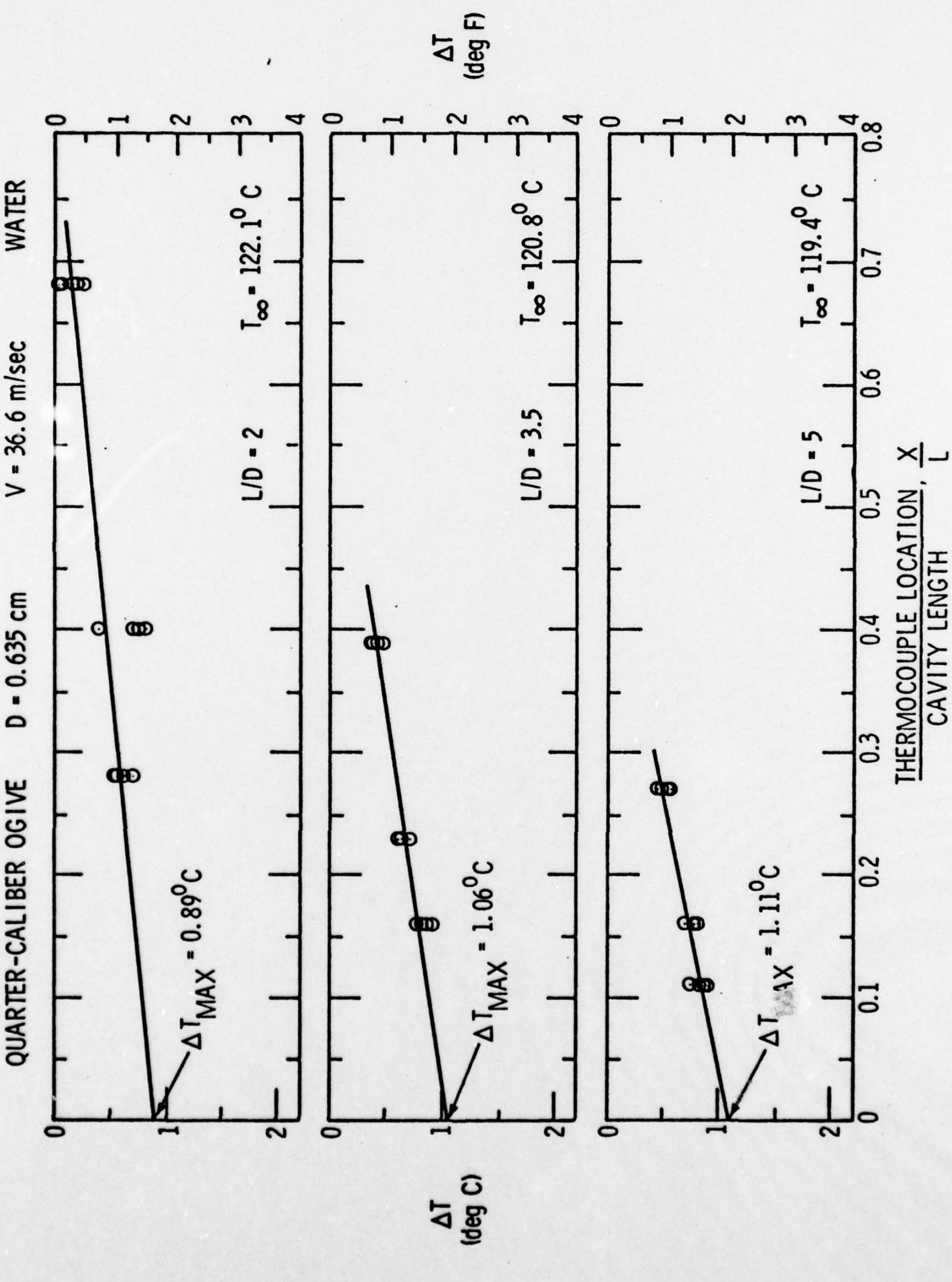

Figure 42 - ΔT vs X/L for T_∞ = 122.1, 120.8, and 119,4°C: QCO, D=0.635 cm, V=36.6 m/sec, Water

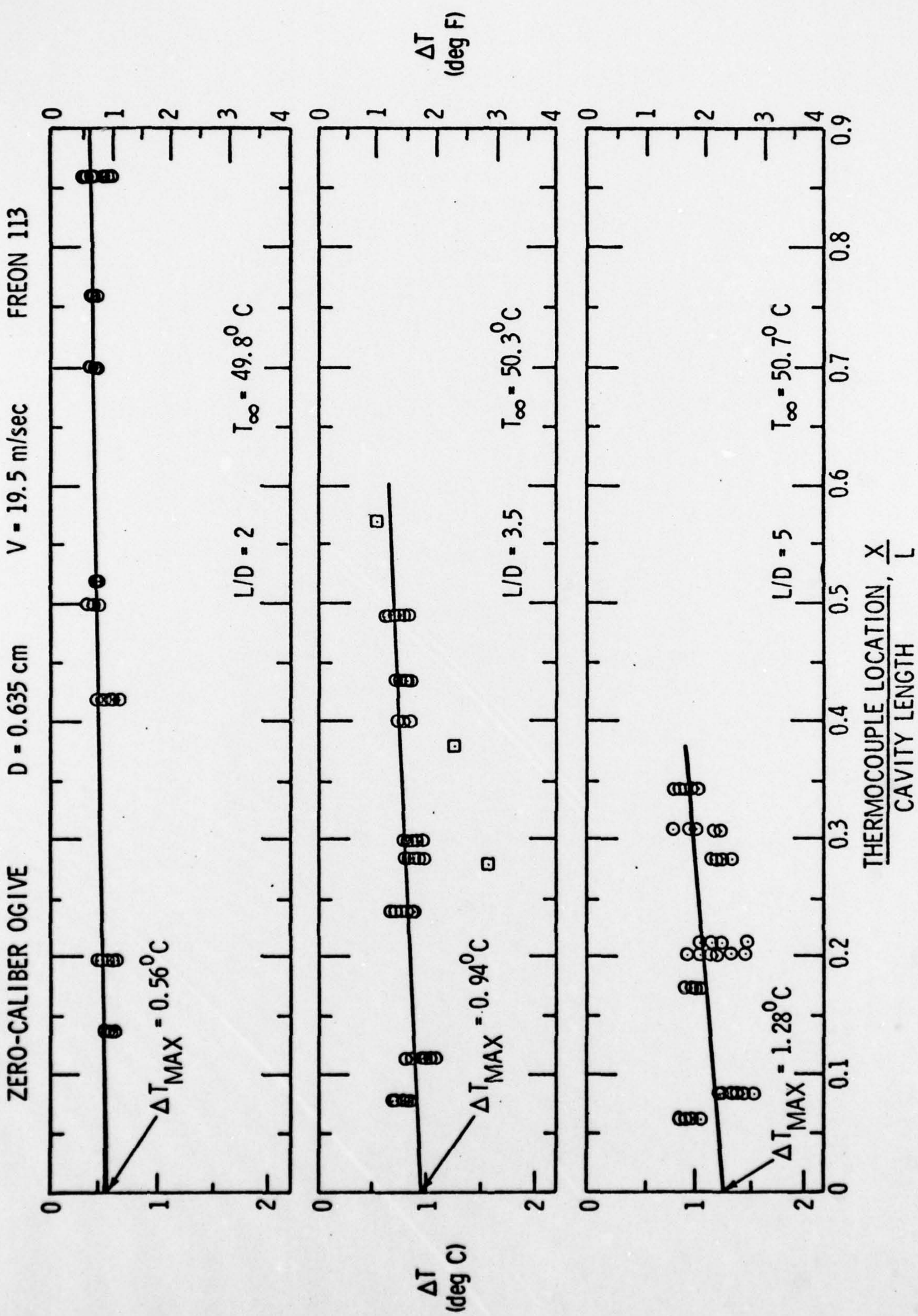

Figure 43 - ΔT vs X/L for T_∞ = 49.8, 50.3, and 50.7°C: ZCO, D=0.635 cm, V=19.5 m/sec, Freon 113

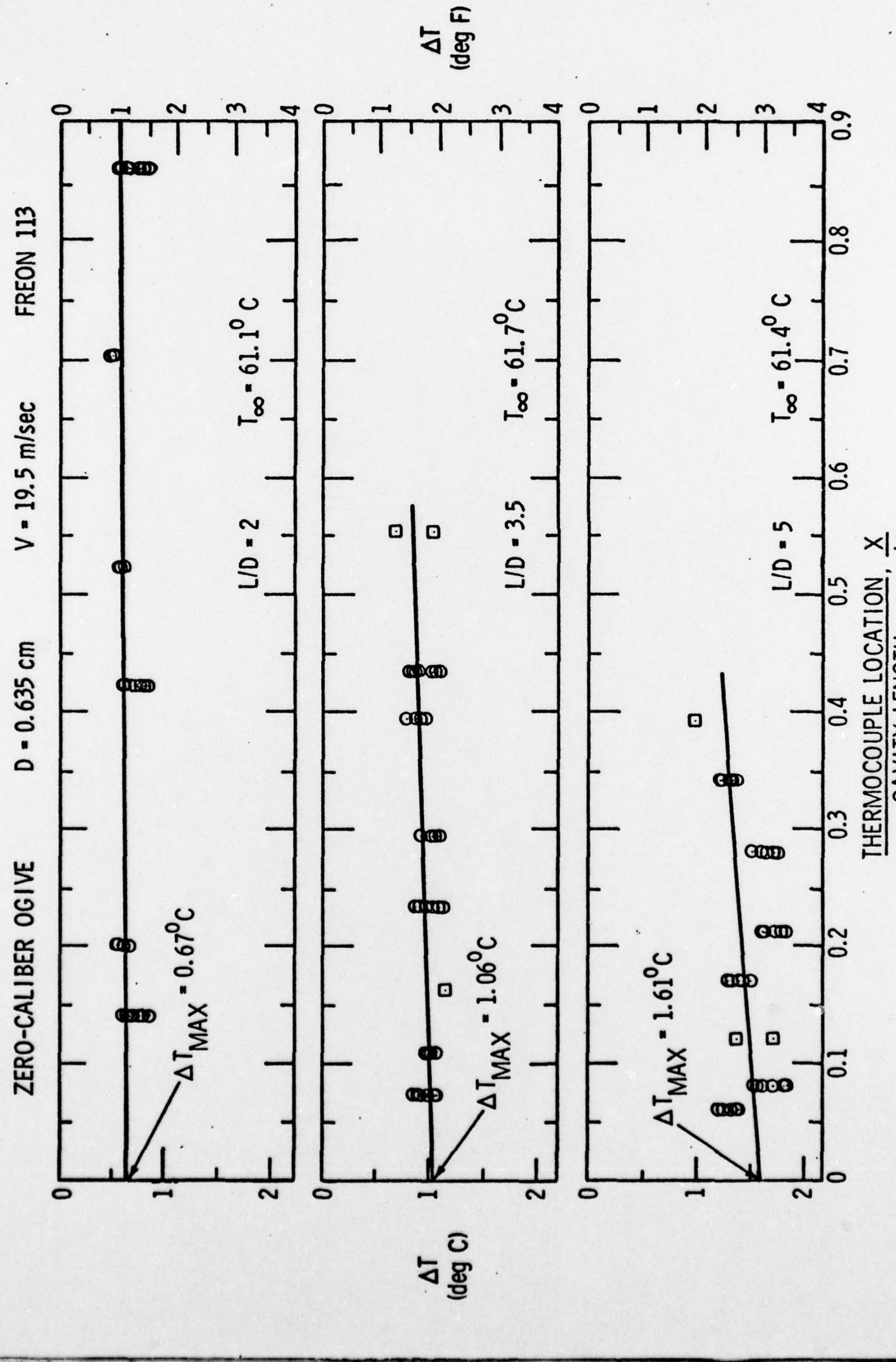

Figure 44 - ΔT vs X/L for T_∞ = 61.1, 61.7, and 61.4°C: ZCO, D=0.635 cm, V=19.5 m/sec, Freon 113

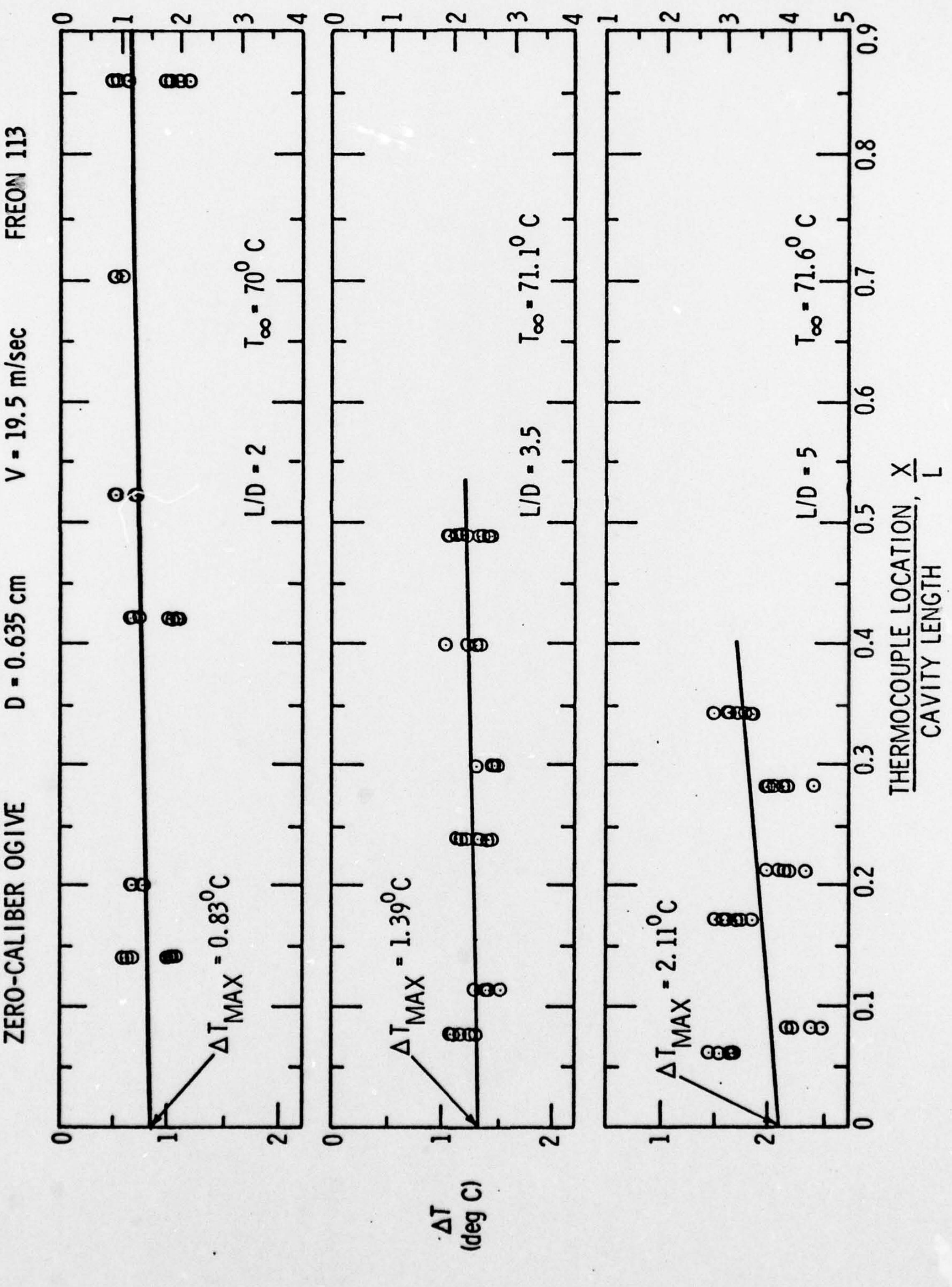

Figure 45 - ΔT vs X/L for T_∞ = 70.0, 71.1, and 71.6°C: ZCO, D=0.635 cm, V=19.5 m/sec, Freon 113

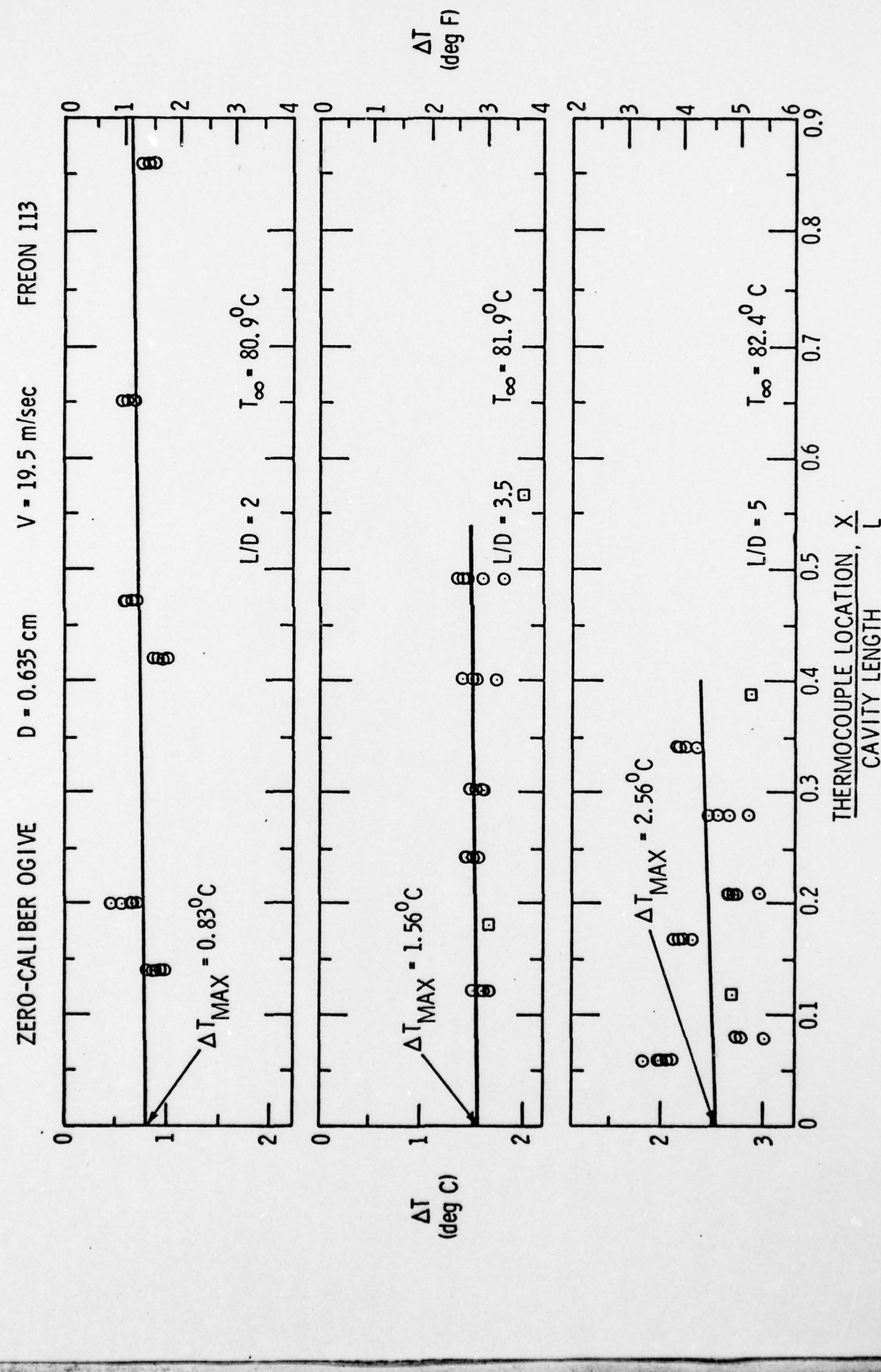

Figure 46 - ΔT vs X/L for T_∞ = 80.9, 81.9, and 82.4°C: ZCO, D=0.635 cm, V=19.5 m/sec, Freon 113

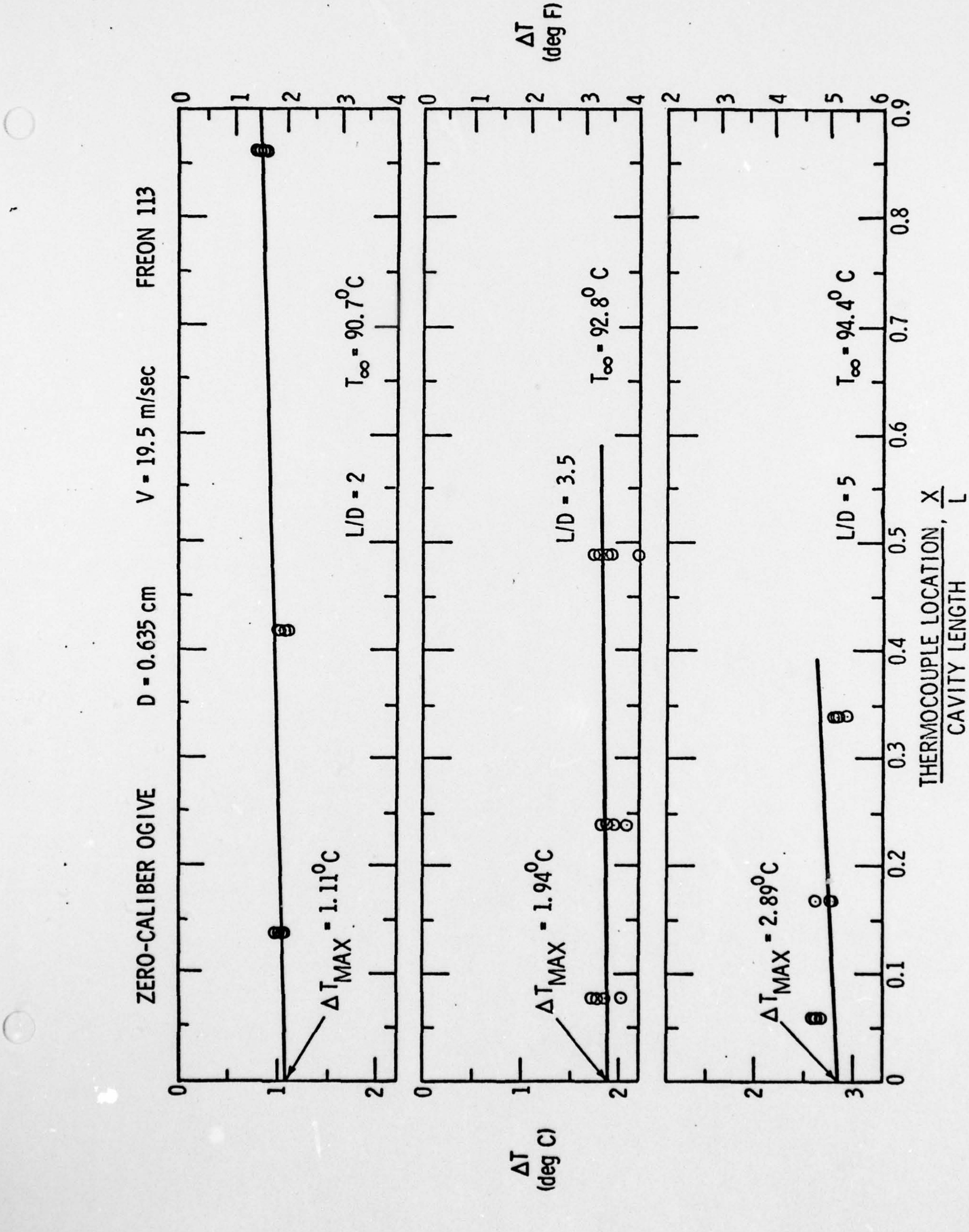

Figure 47 - ΔT vs X/L for T_∞ = 90.7, 92.8, and 94.4°C: ZCO, D=0.635 cm, V=19.5 m/sec, Freon 113

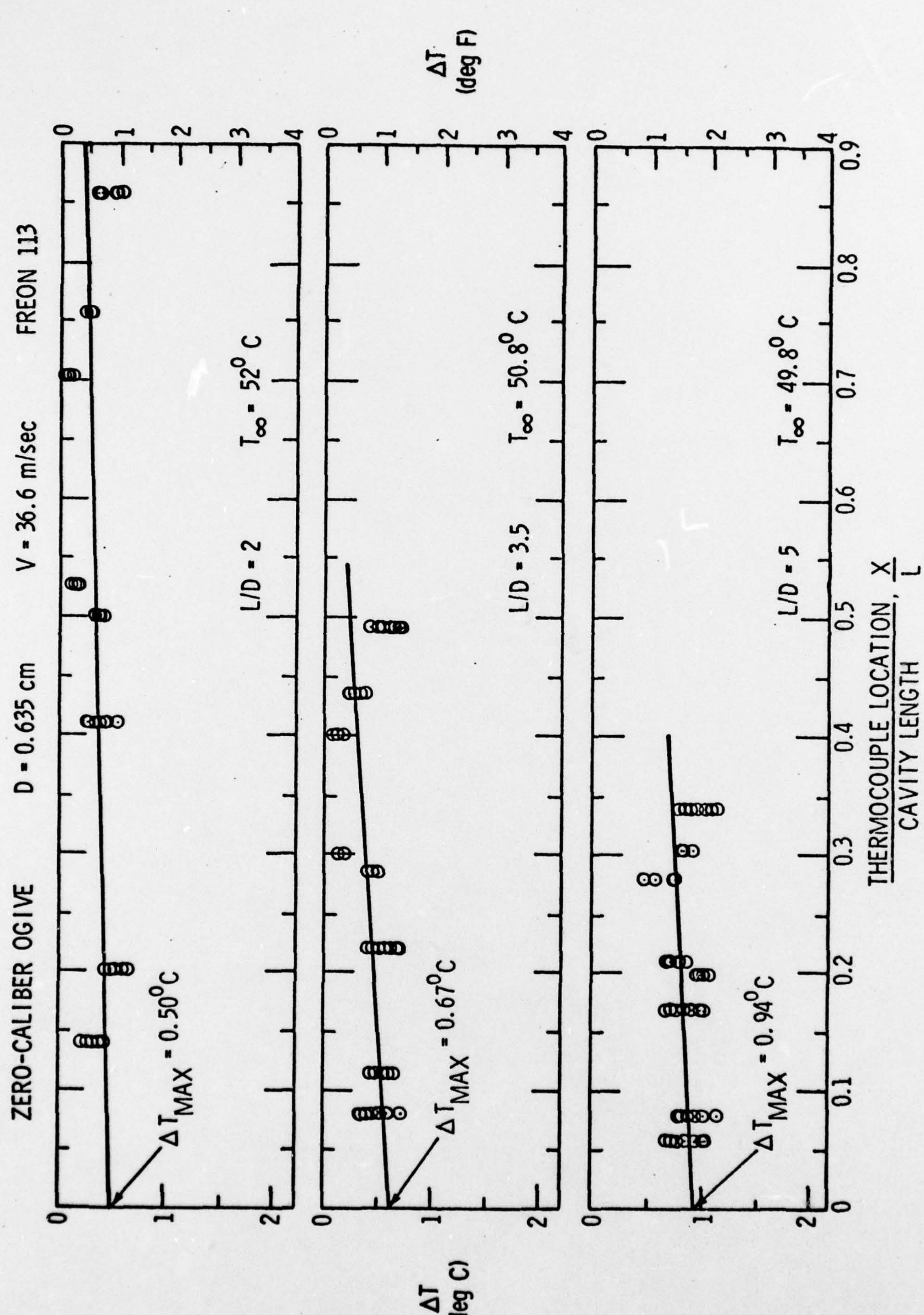

Figure 48 - ΔT vs X/L for T_∞ = 52.0, 50.8, and 49.8°C: ZCO, D=0.635 cm, V=36.6 m/sec, Freon 113

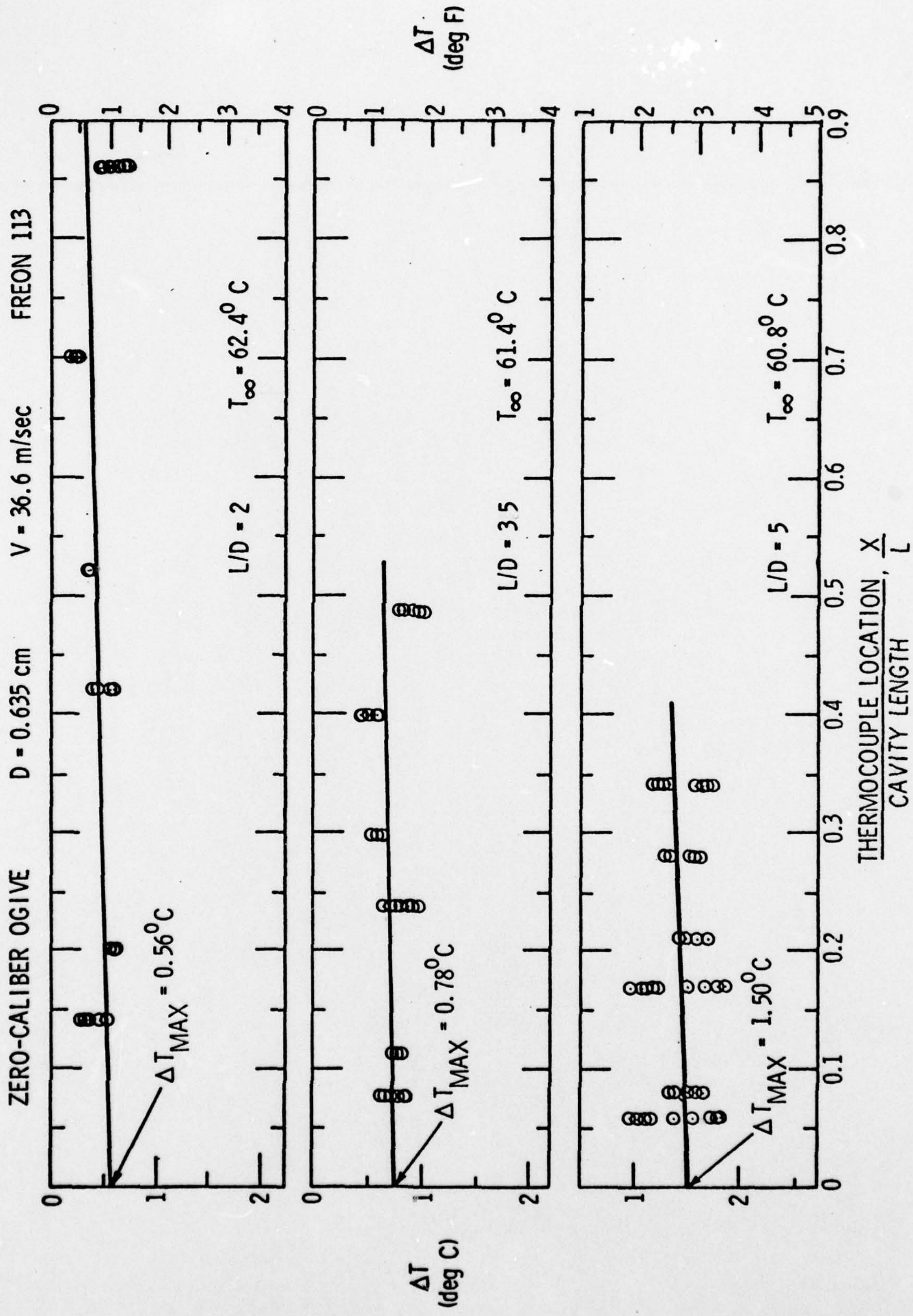

Figure 49 - ΔT vs X/L for T_∞ = 62.4, 61.4, and 60.8°C: ZCO, D=0.635 cm, V=36.6 m/sec, Freon 113

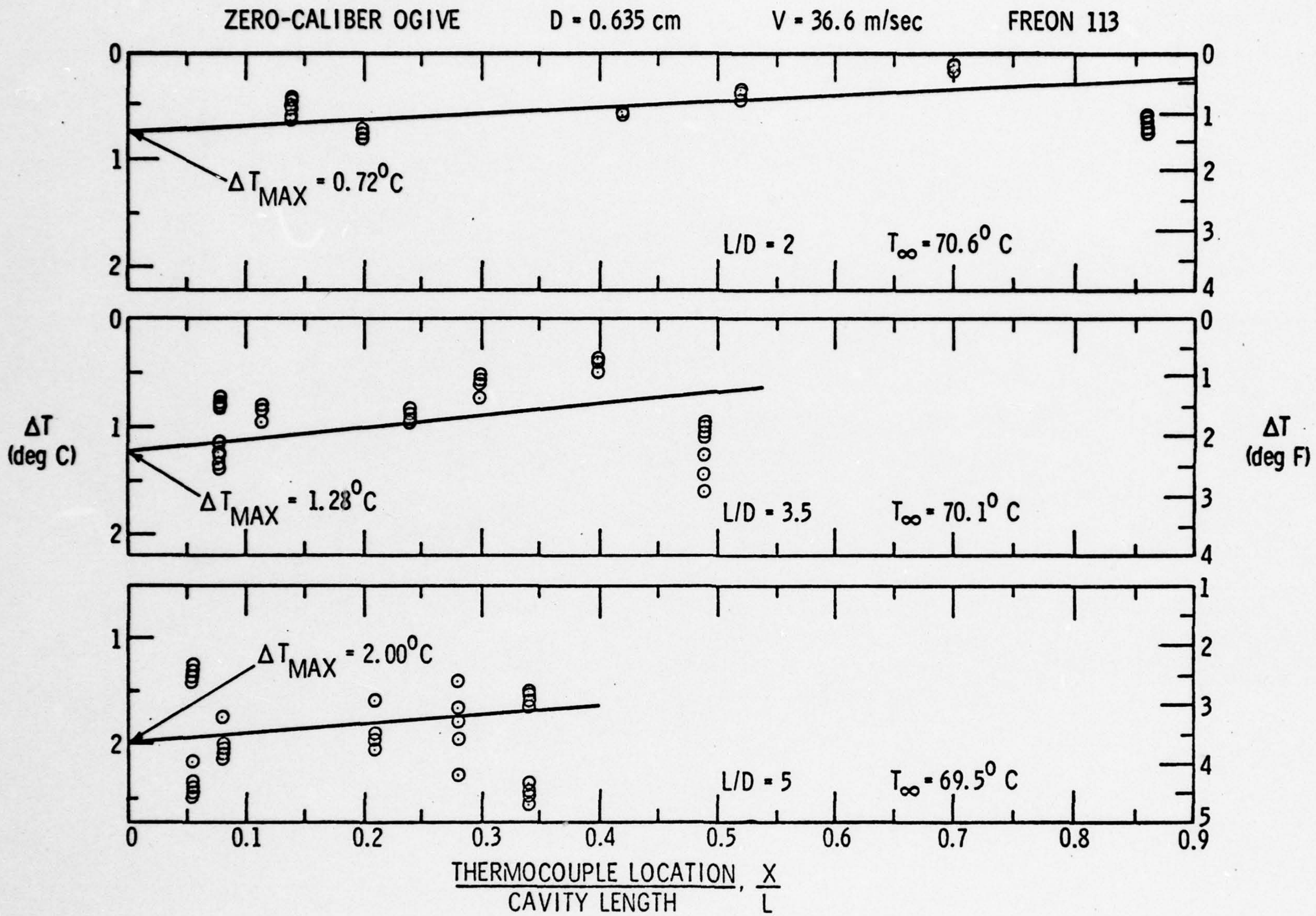

Figure 50 - ΔT vs X/L for T_∞ = 70.6, 70.1, and 69.5°C: ZCO, D=0.635 cm, V=36.6 m/sec, Freon 113

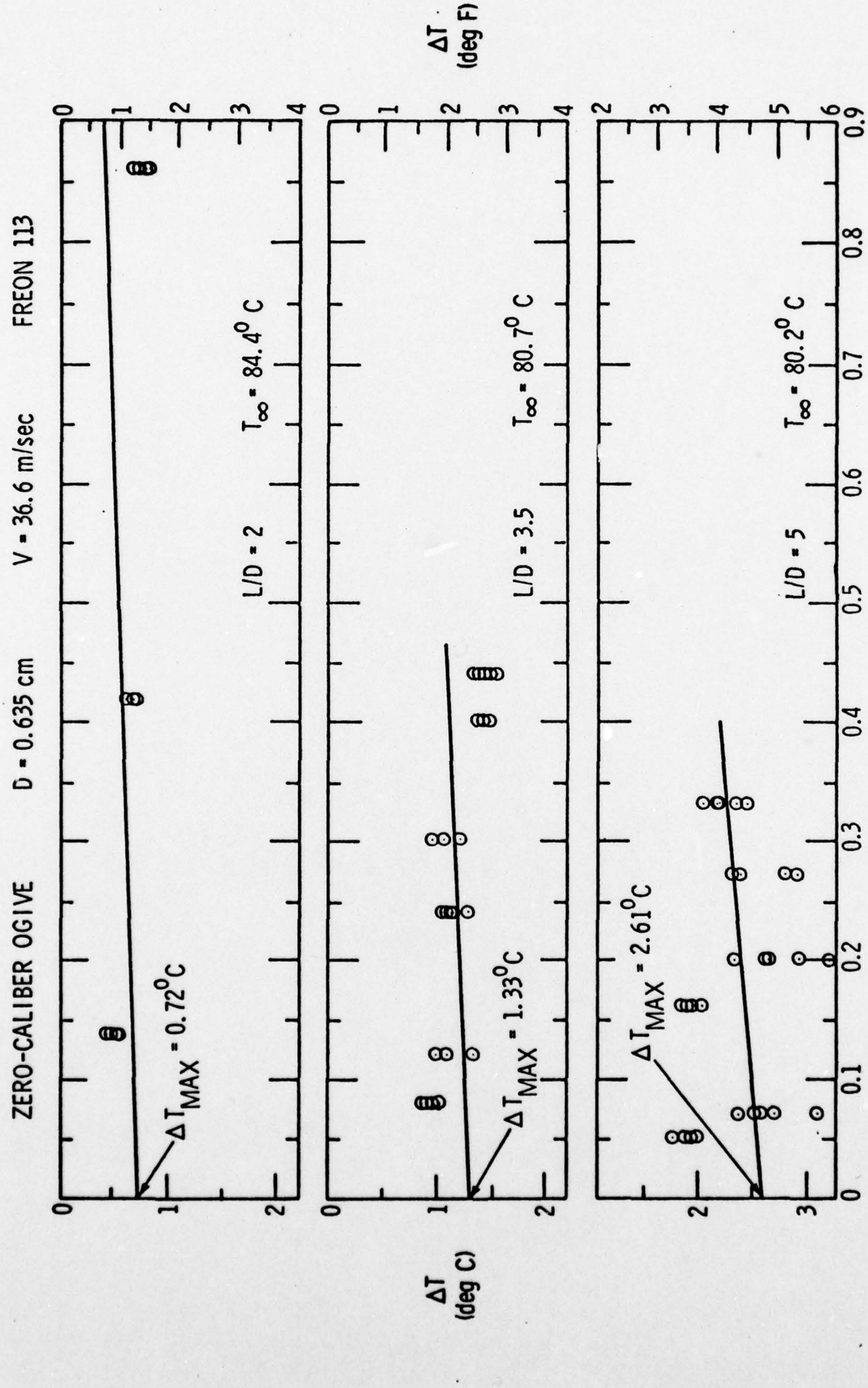

Figure 51 - ΔT vs X/L for T_∞ = 84.4, 80.7, and 80.2°C: ZCO, D=0.635 cm, V=36.6 m/sec, Freon 113

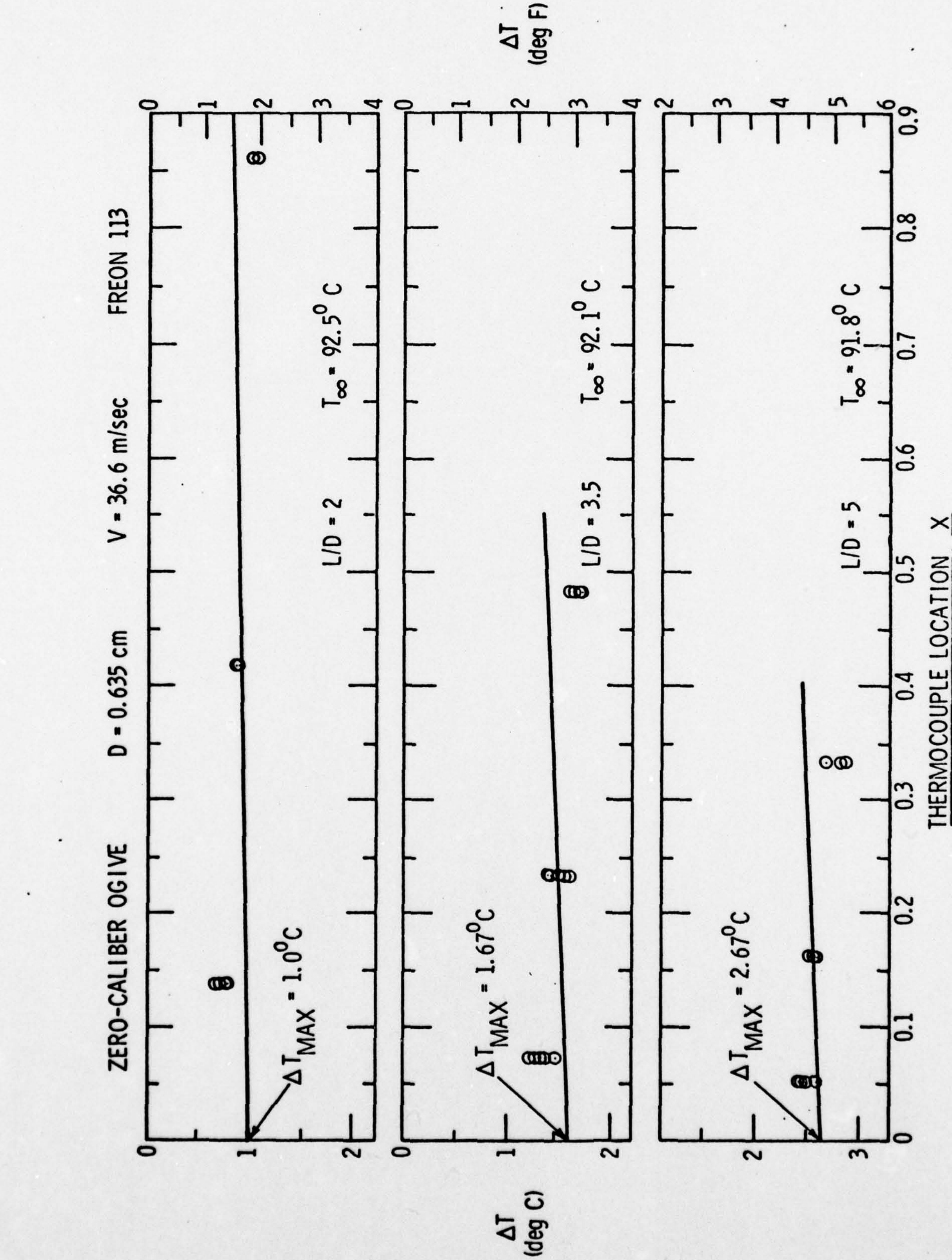

Figure 52 - ΔT vs X/L for T_∞ = 92.5, 92.1, and 91.8°C: ZCO, D=0.635 cm, V=36.6 m/sec, Freon 113

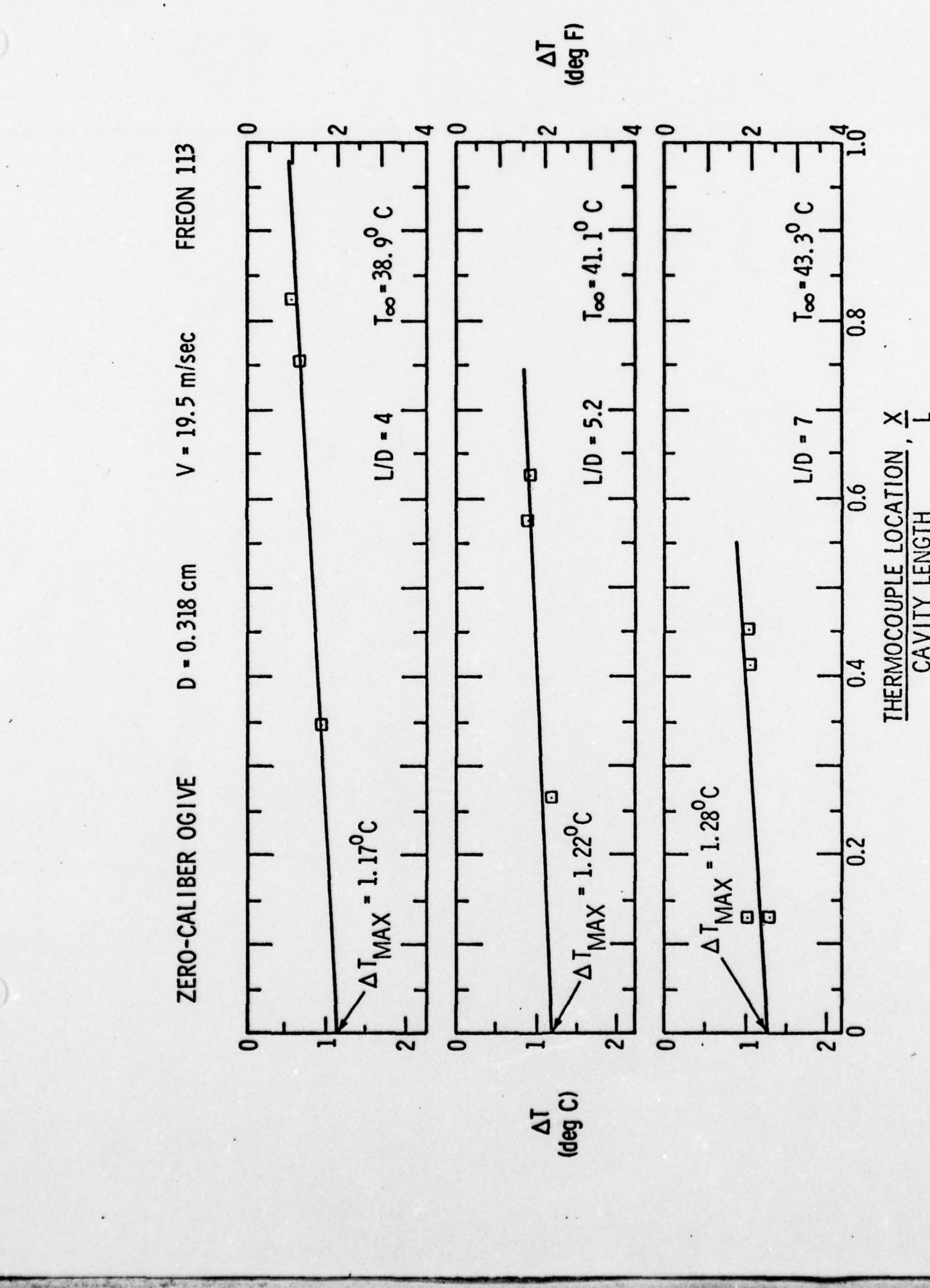

Figure 53 - ΔT vs X/L for T_∞ = 38.9, 41.1, and 43.3°C: ZCO, D=0.318 cm, V=19.5 m/sec, Freon 113

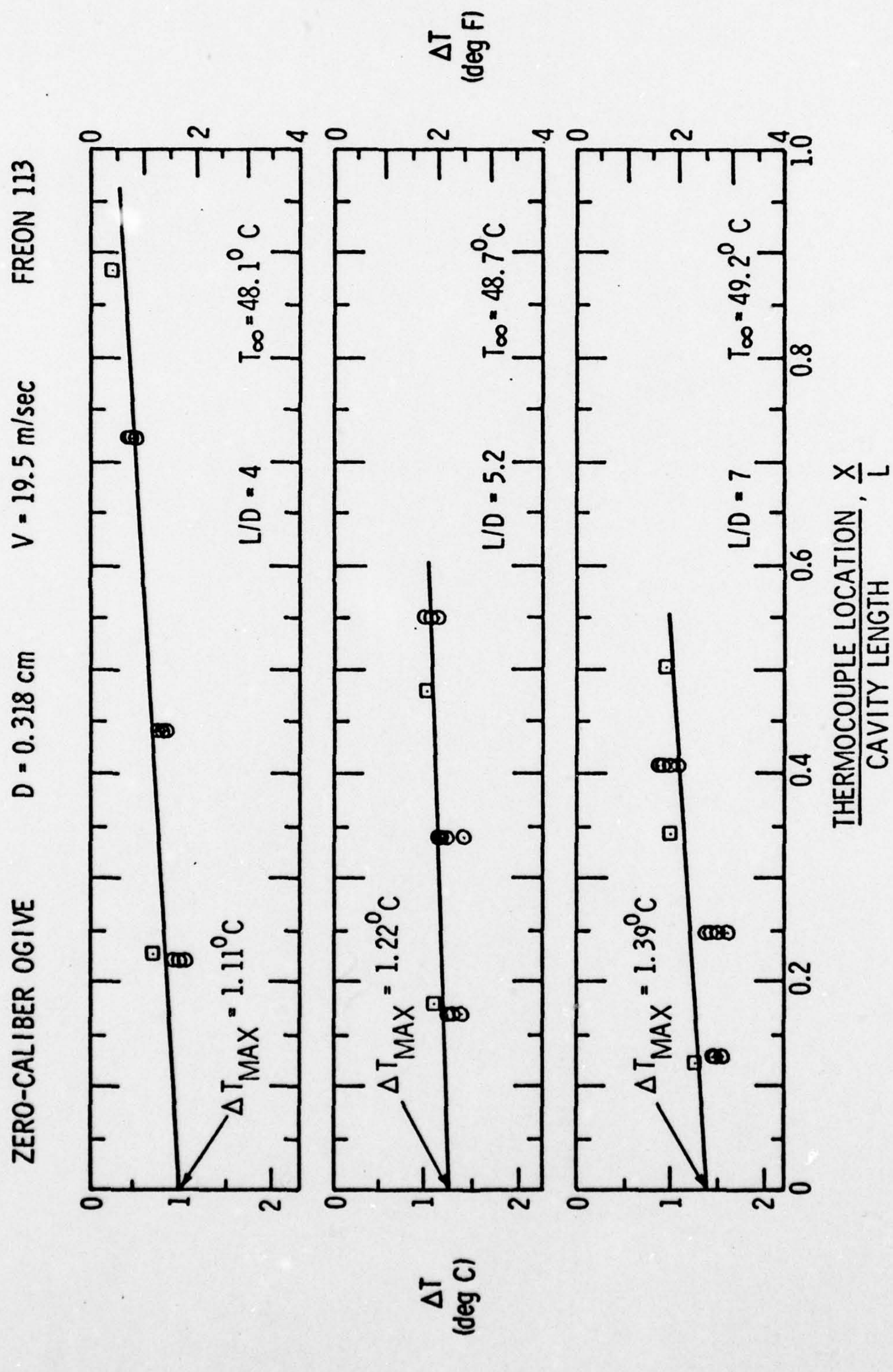

Figure 54 - ΔT vs X/L for T_∞ = 48.1, 48.7, and 49.2°C: ZCO, D=0.318 cm, V=19.5 m/sec, Freon 113

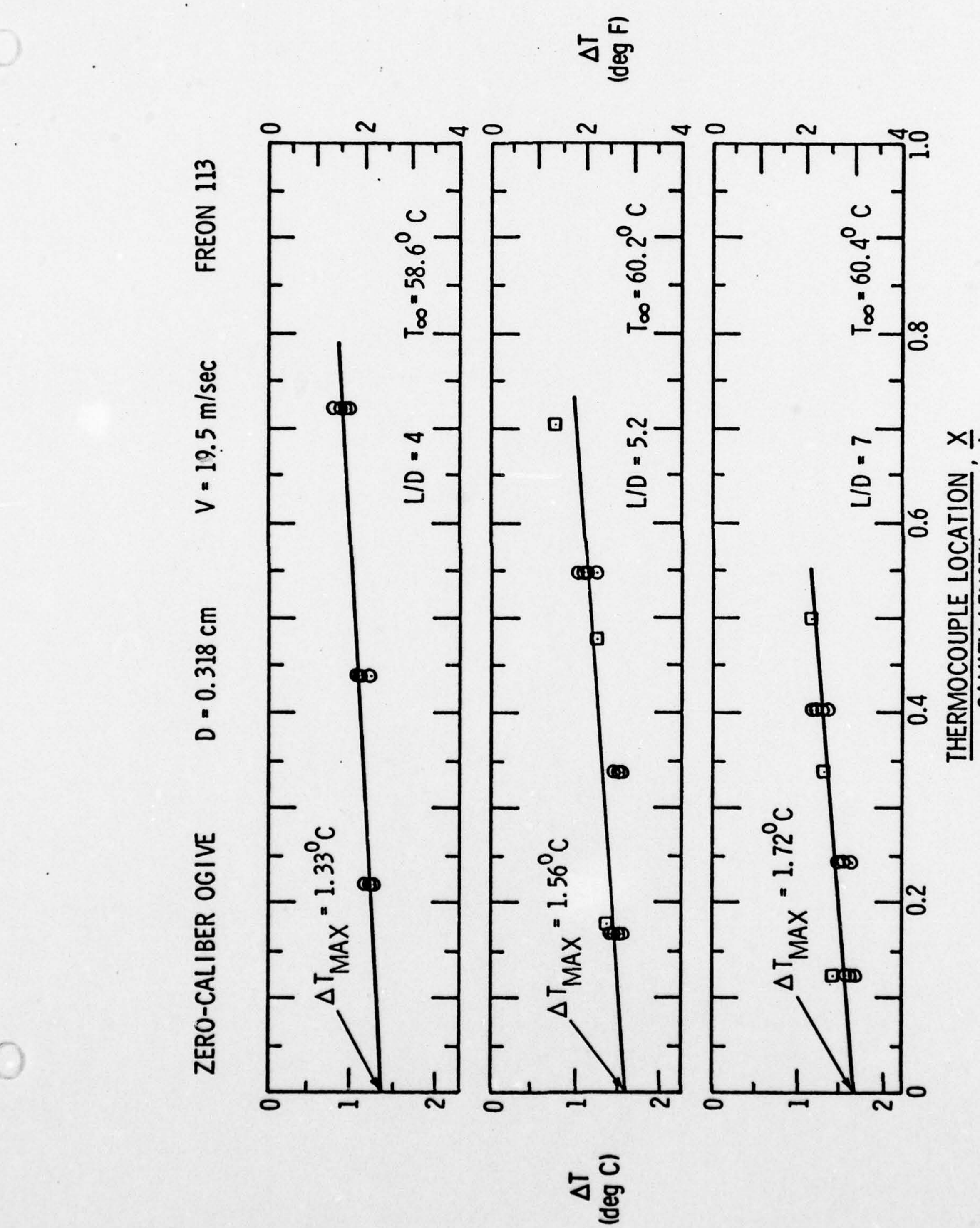

Figure 55 - ΔT vs X/L for T_∞ = 58.6, 60.2, and 60.4°C: ZCO, D=0.318 cm, V=19.5 m/sec, Freon 113

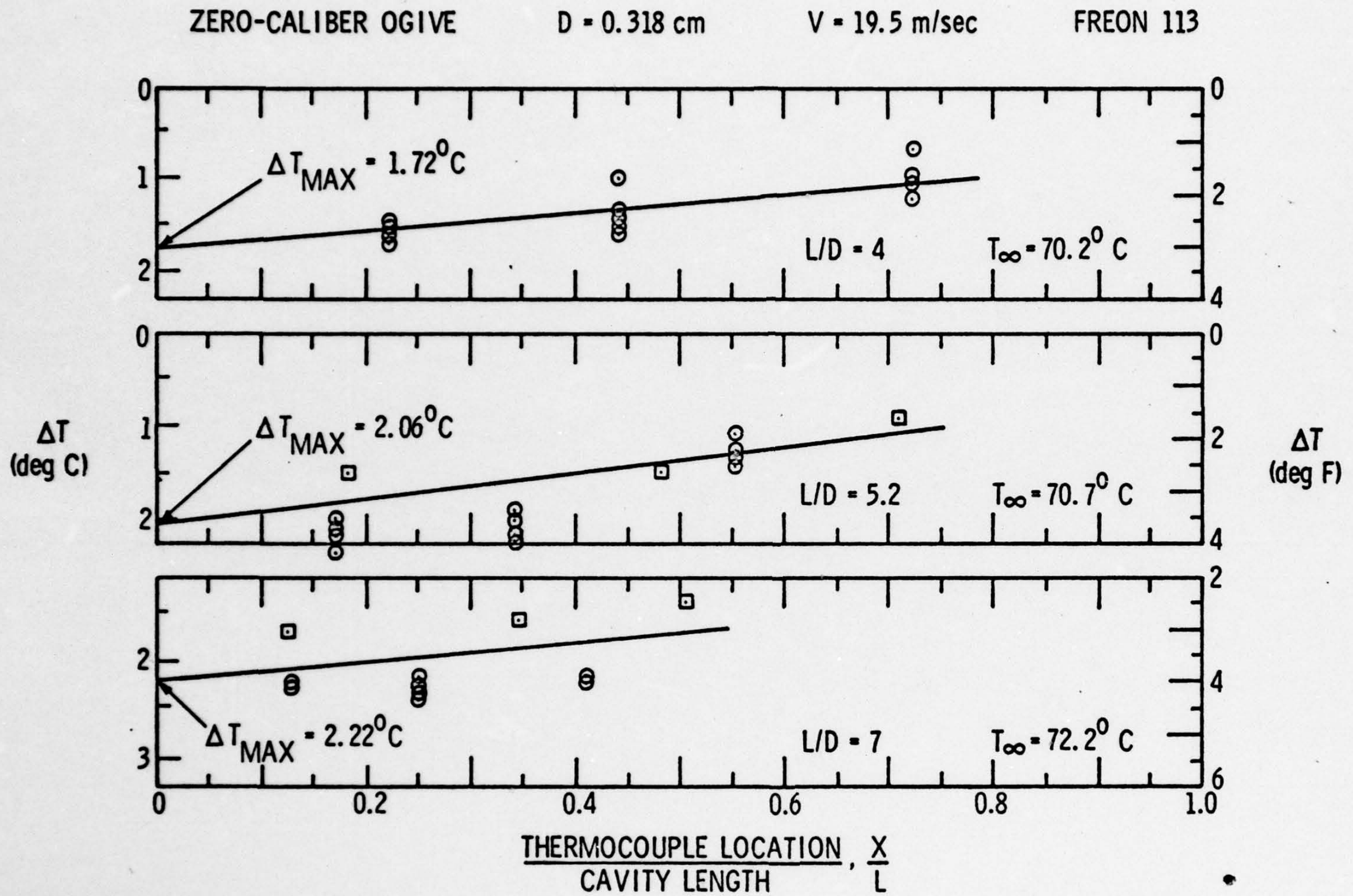

Figure 56 - ΔT vs X/L for T_∞ = 70.2, 70.7, and 72.2°C: ZCO, D=0.318 cm, V=19.5 m/sec, Freon 113

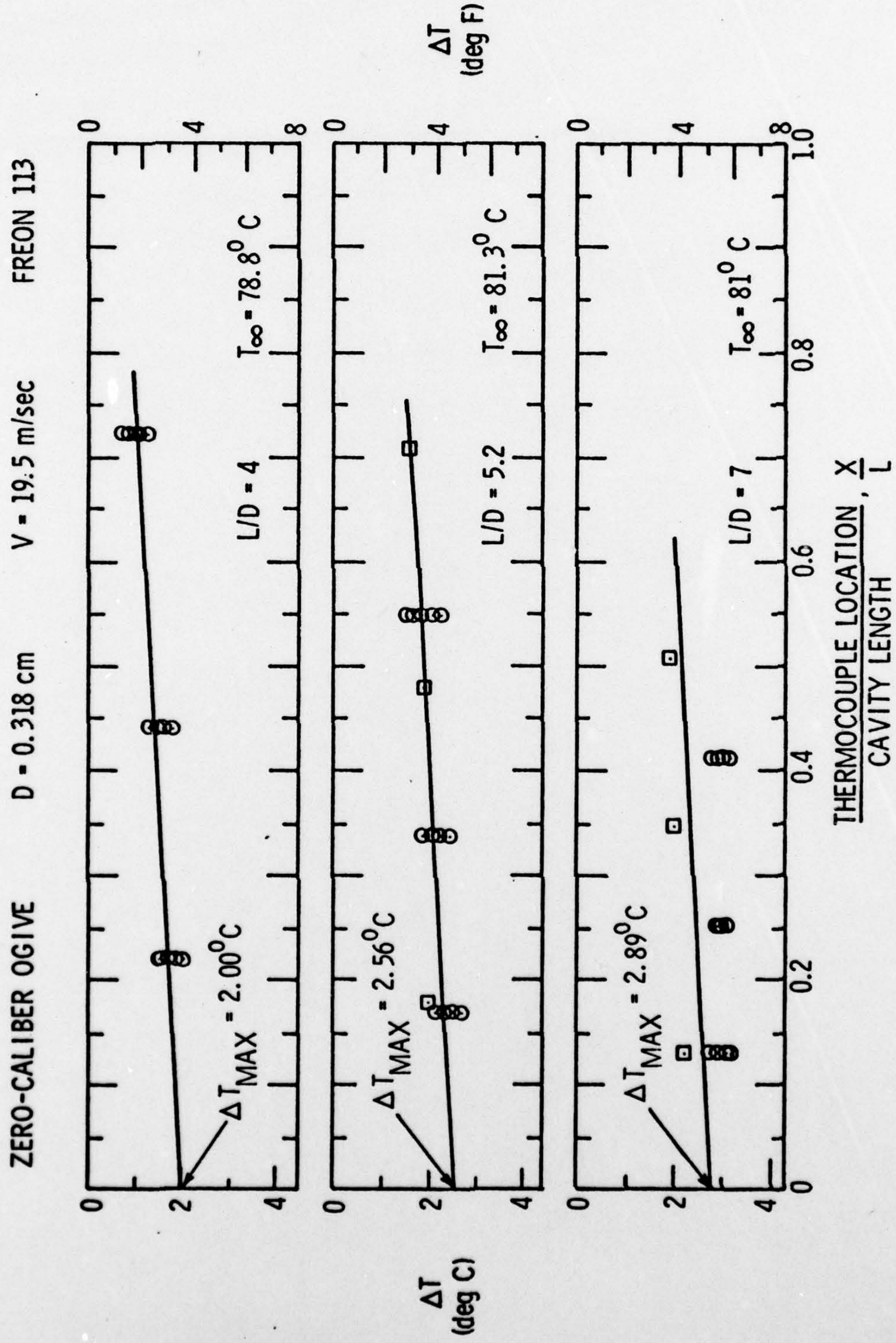

Figure 57 - ΔT vs X/L for T_∞ = 78.8, 81.3, and 81.0°C: ZCO, D=0.318, V=19.5 m/sec, Freon 113

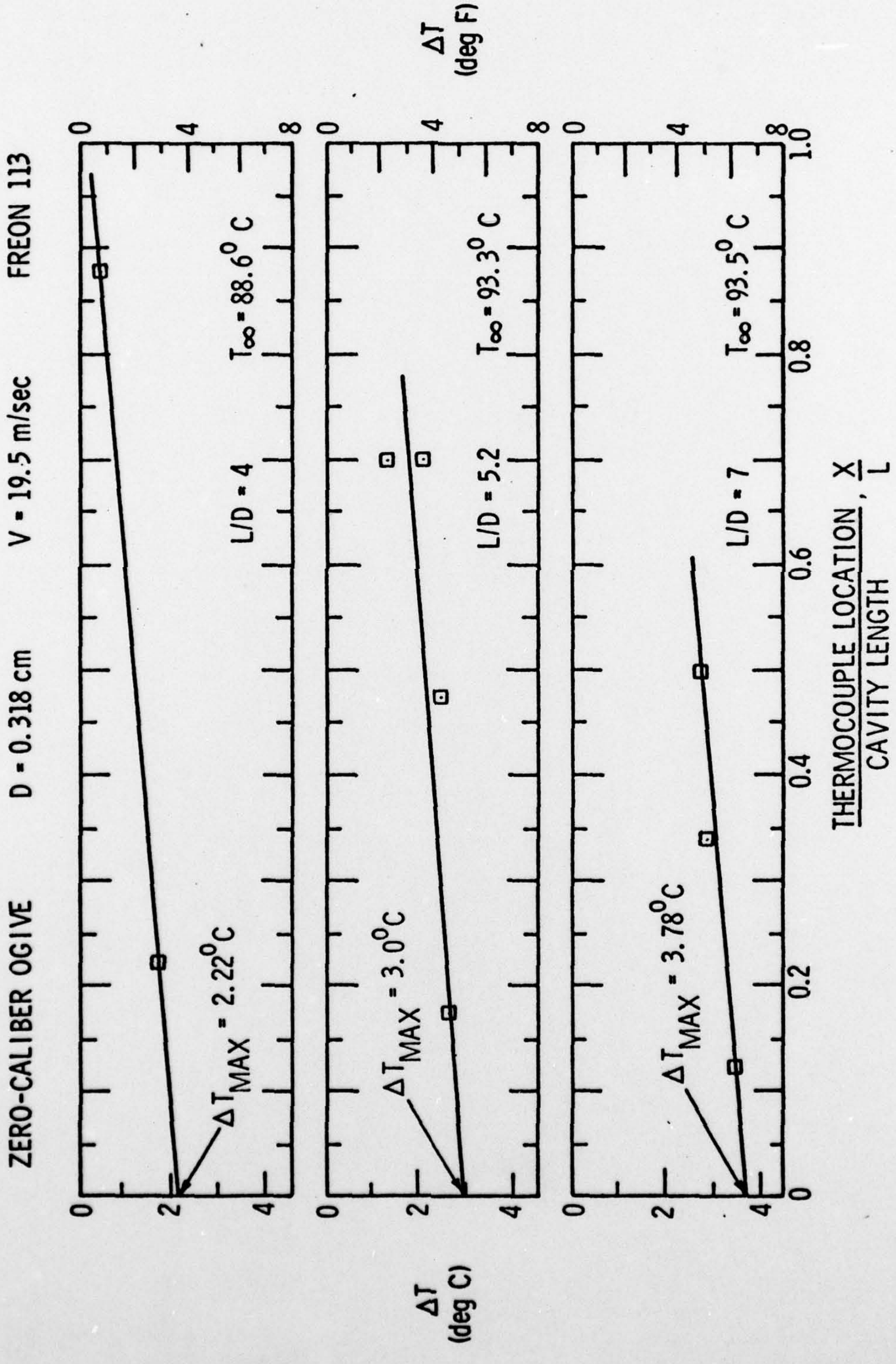

Figure 58 - ΔT vs X/L for T_∞ = 88.6, 93.3, and 93.5°C: ZCO, D=0.318 cm, V=19.5 m/sec, Freon 113

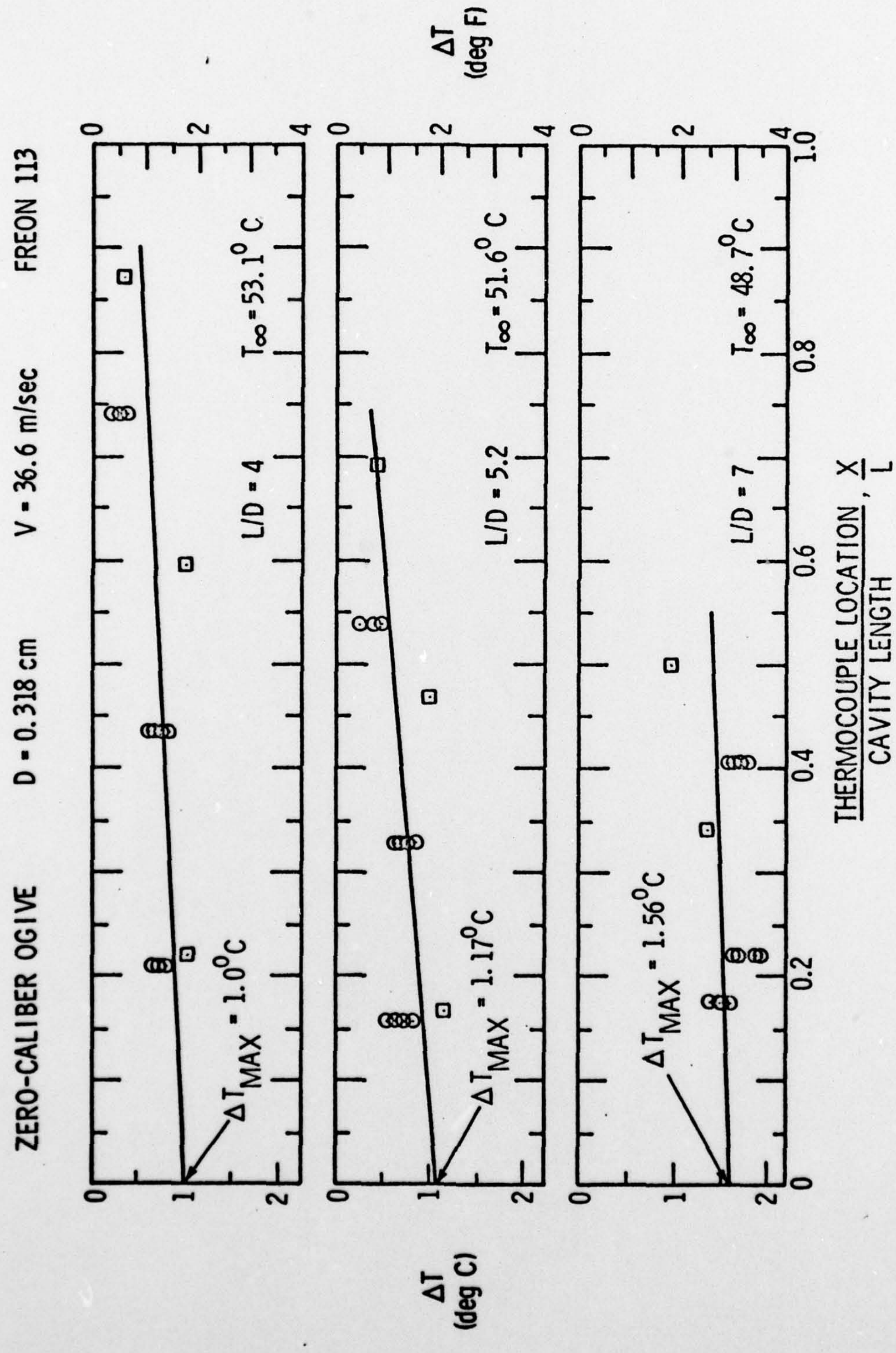

Figure 59 - ΔT vs X/L for T_∞ = 53.1, 51.6, and 48.7°C: ZCO, D=0.318 cm, V=36.6 m/sec, Freon 113

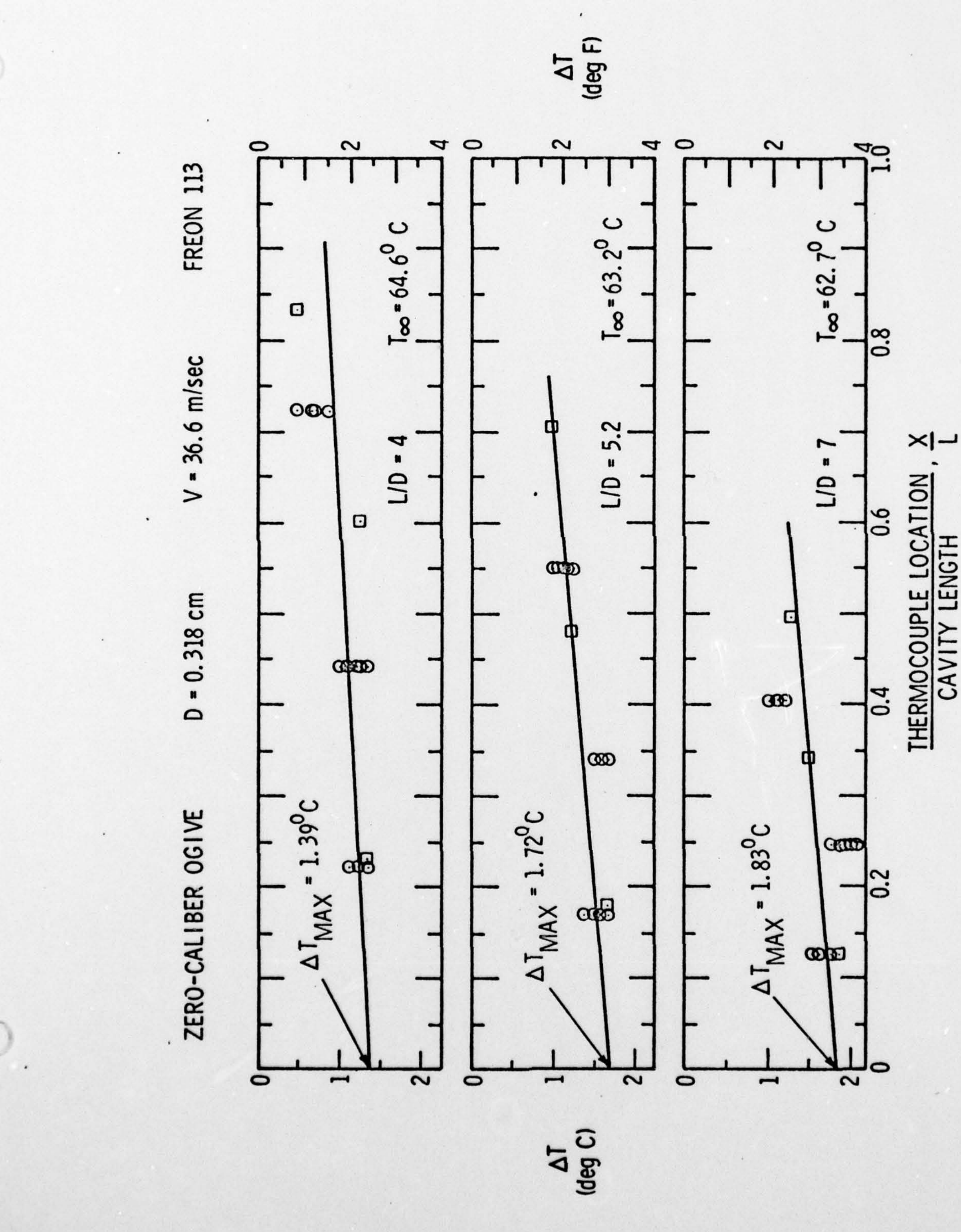

Figure 60 - ΔT vs X/L for T_∞ = 64.6, 63.2, and 62.7°C: ZCO, D=0.318 cm, V=36.6 m/sec, Freon 113

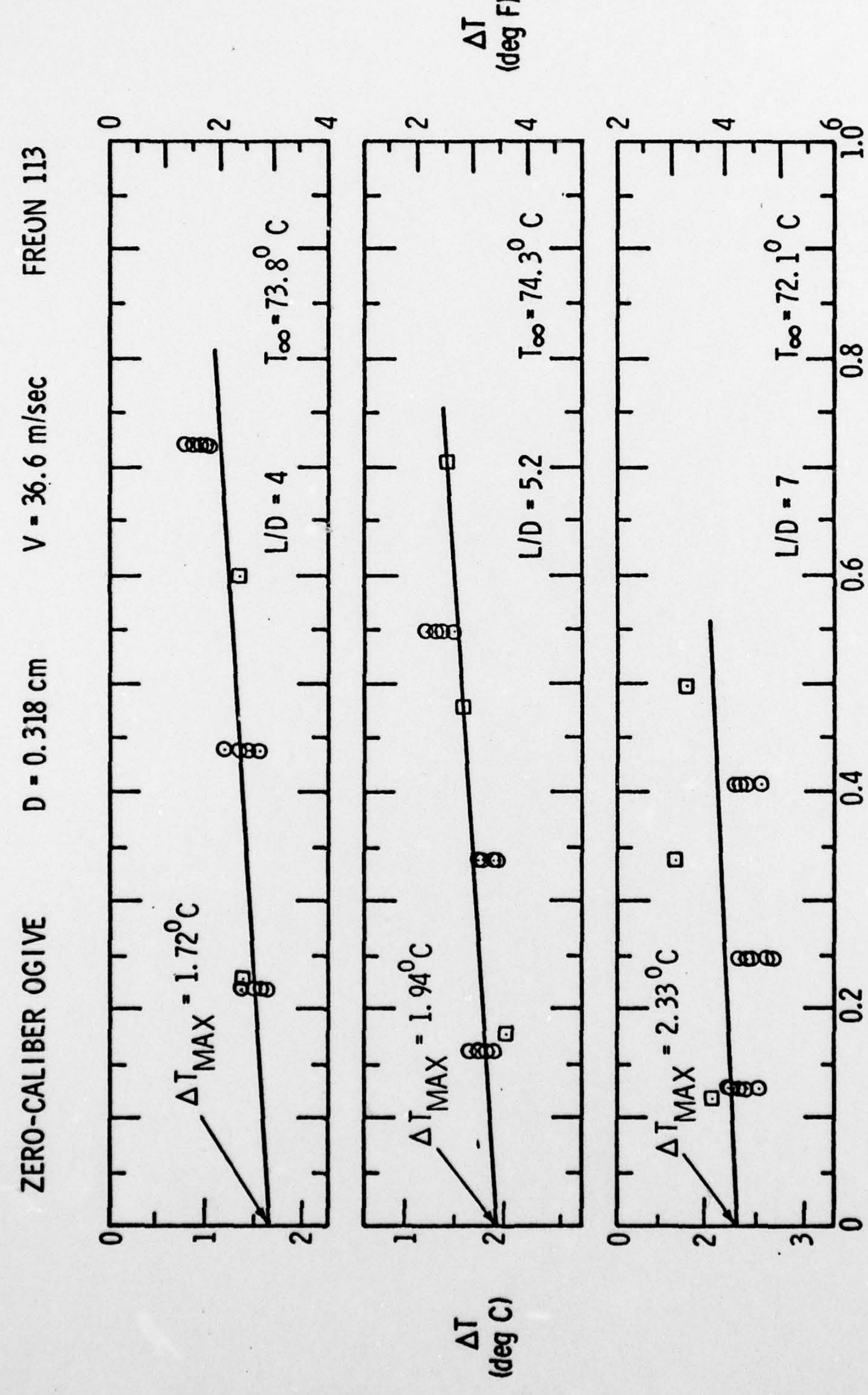

Figure 61 - ΔT vs X/L for T_∞ = 73.8, 74.3, and 72.1°C: ZCO, D=0.318 cm, V=36.6 m/sec, Freon 113

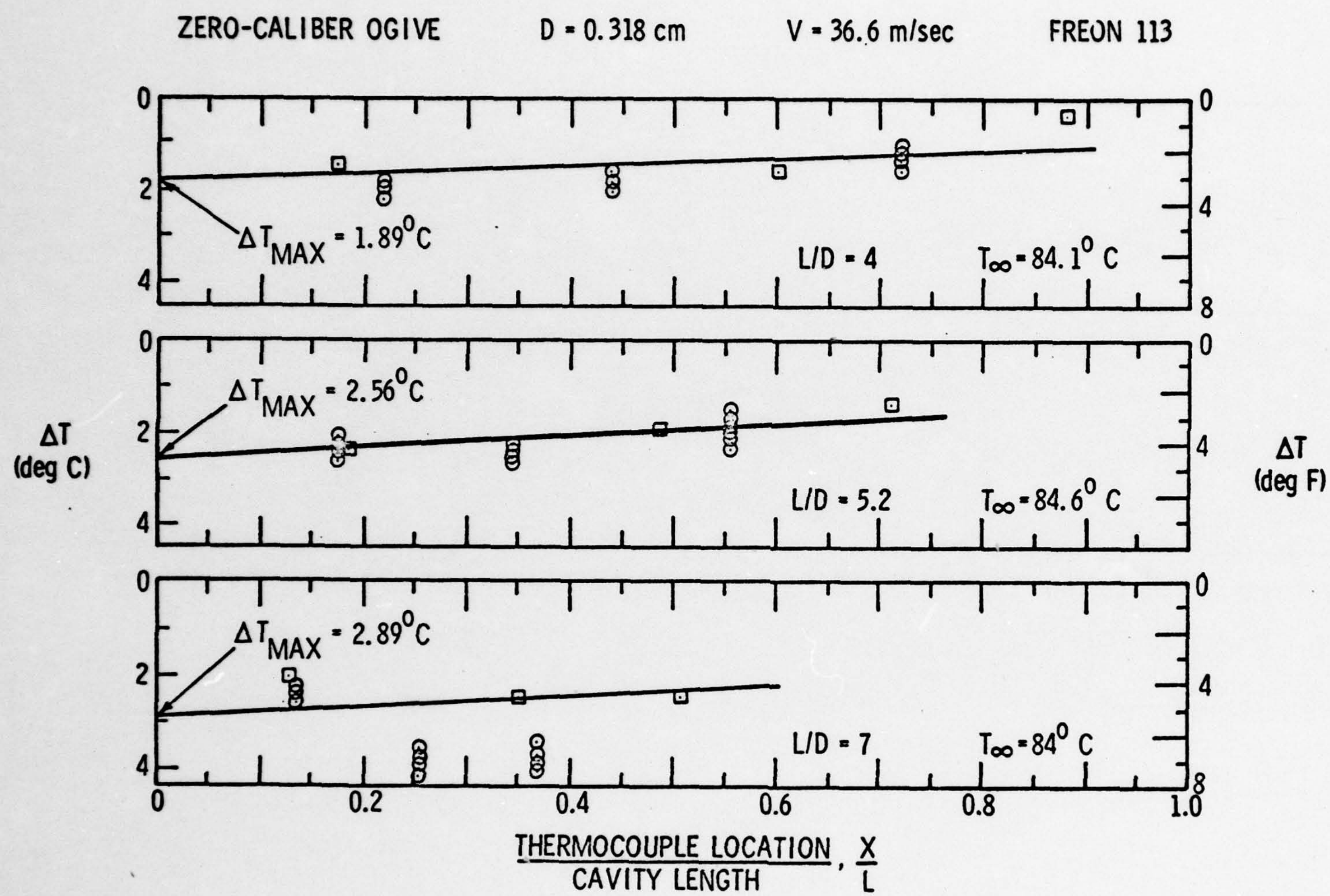

Figure 62 - ΔT vs X/L for T_∞ = 84.1, 84.6, and 84.0°C: ZCO, D=0.318 cm, V=36.6 m/sec, Freon 113

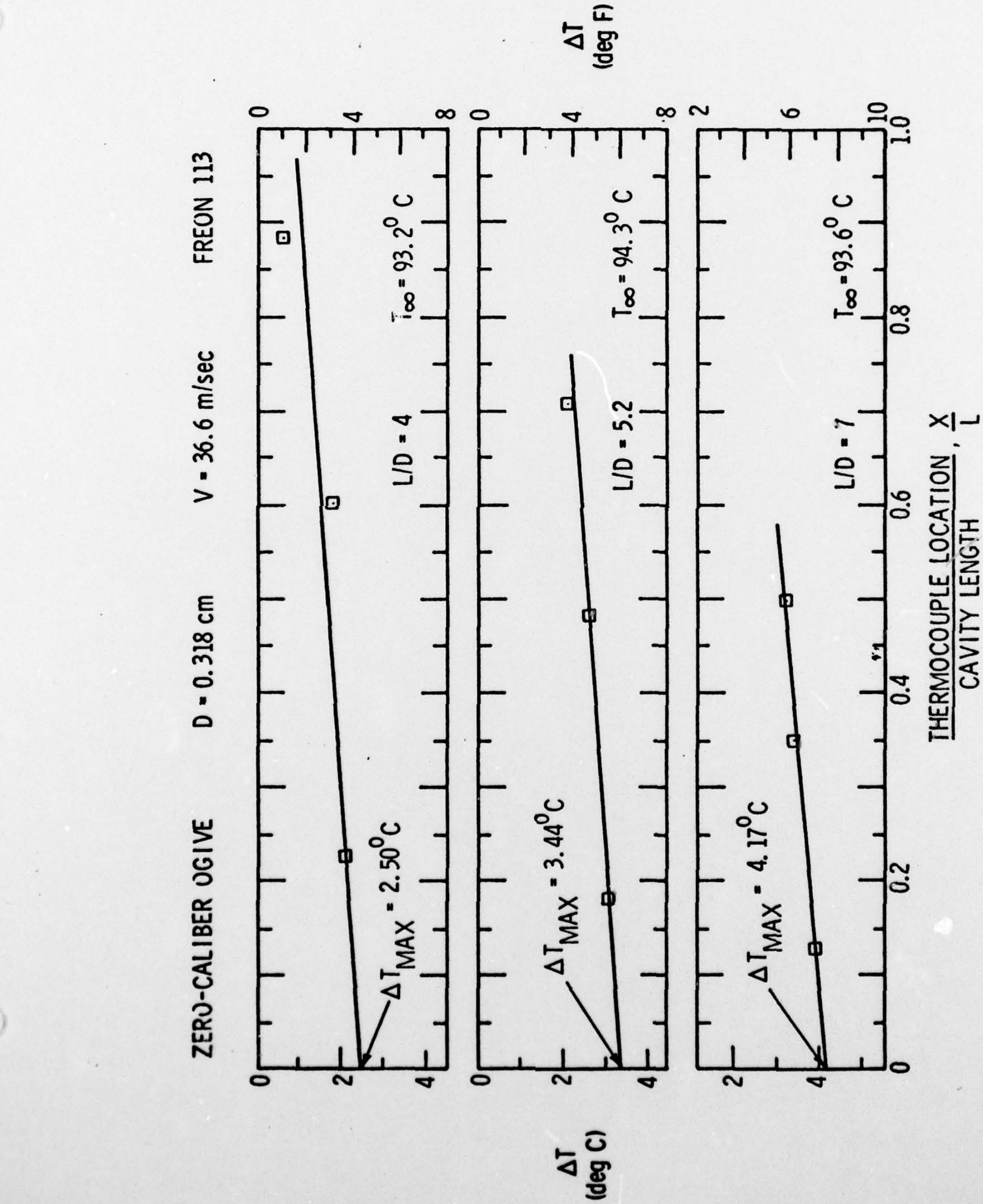

Figure 63 - ΔT vs X/L for T_∞ = 93.2, 94.3, and 93.6°C: ZCO, D=0.318 cm, V=36.6 m/sec, Freon 113

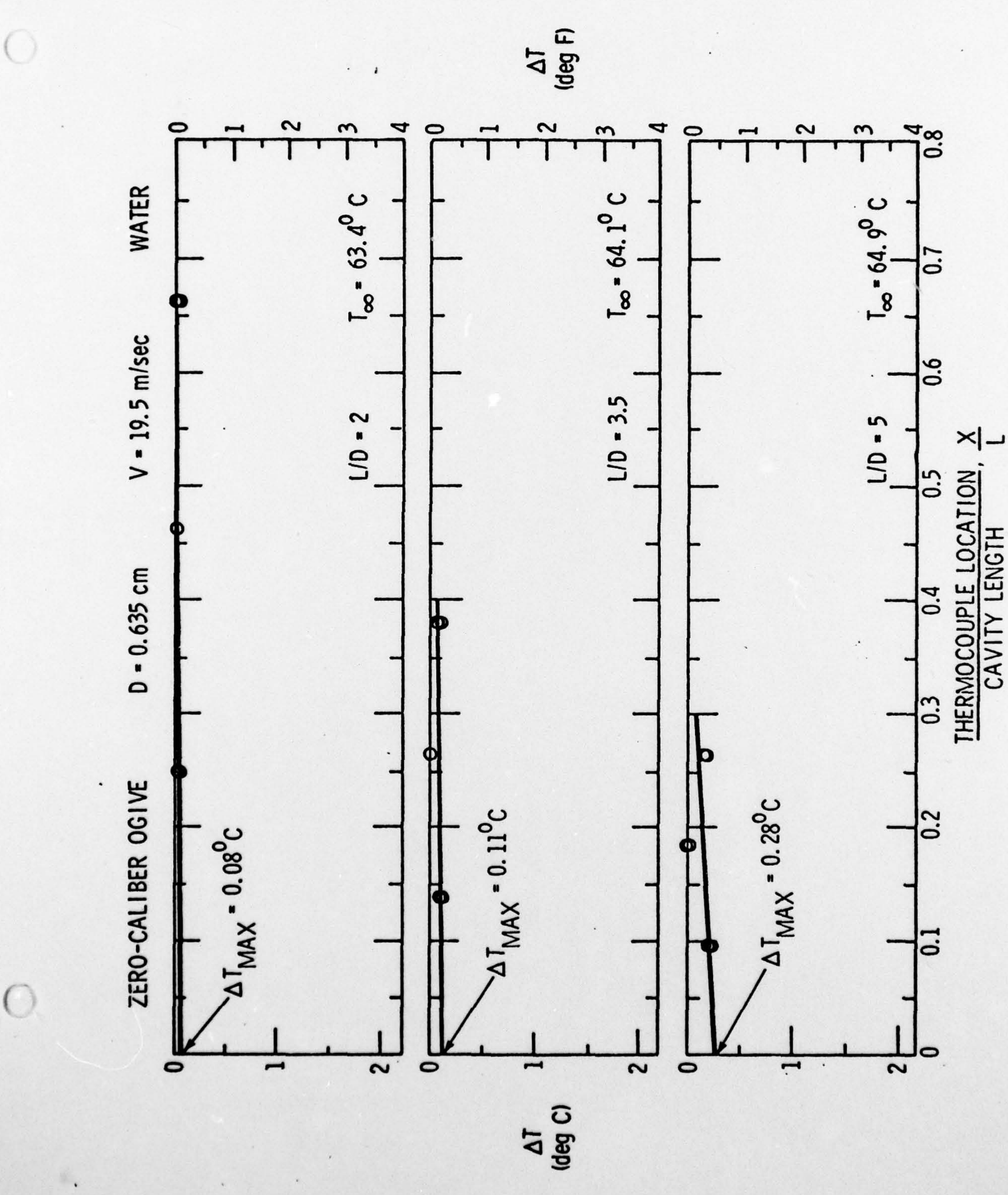

Figure 64 - ΔT vs X/L for T_∞ = 63.4, 64.1, and 64.9°C: ZCO, D=0.635, V=19.5 m/sec, Water

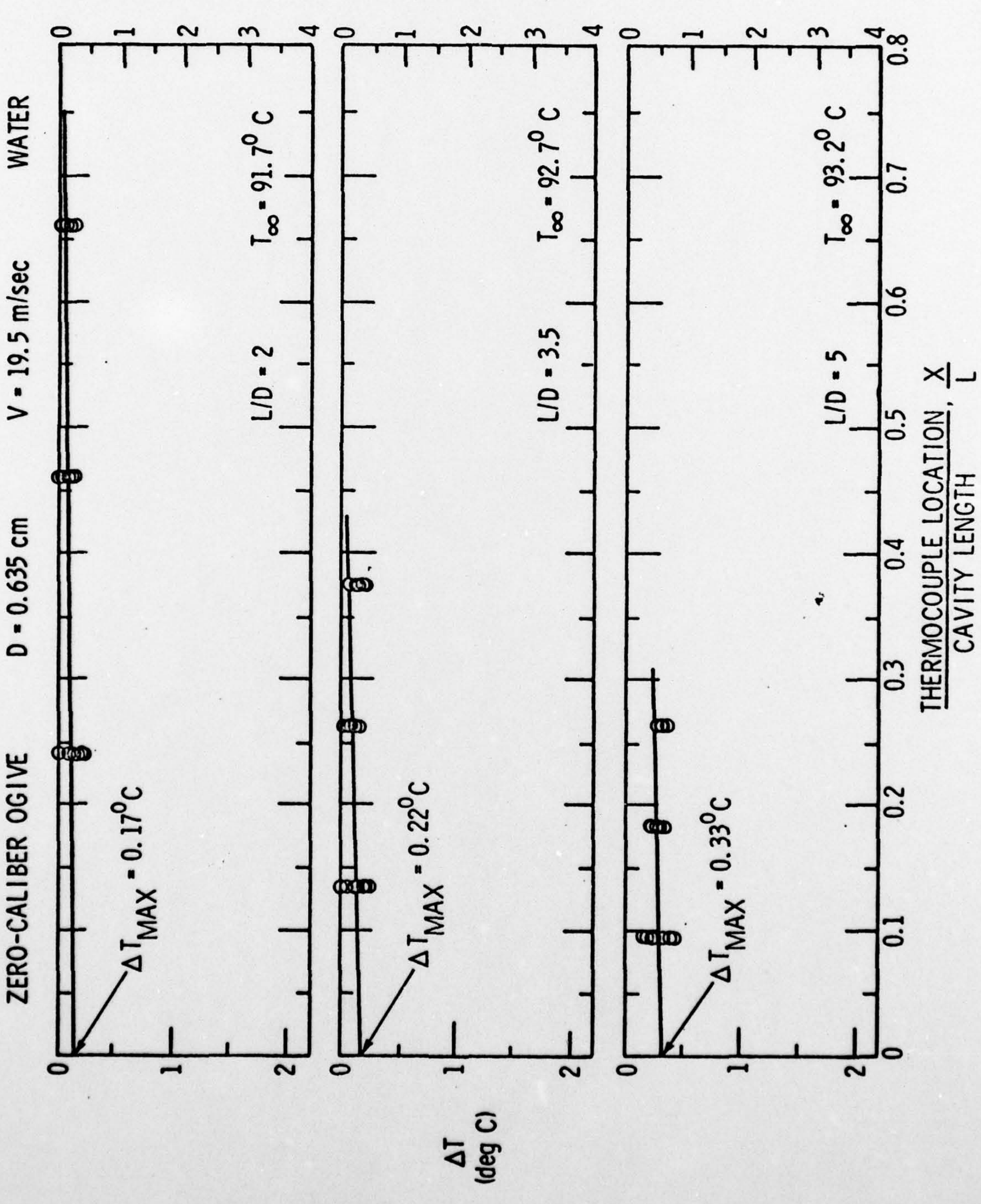

Figure 65 - ΔT vs X/L for T_∞ = 91.7, 92.7, and 93.2°C: ZCO, D=0.635 cm, V=19.5 m/sec, Water

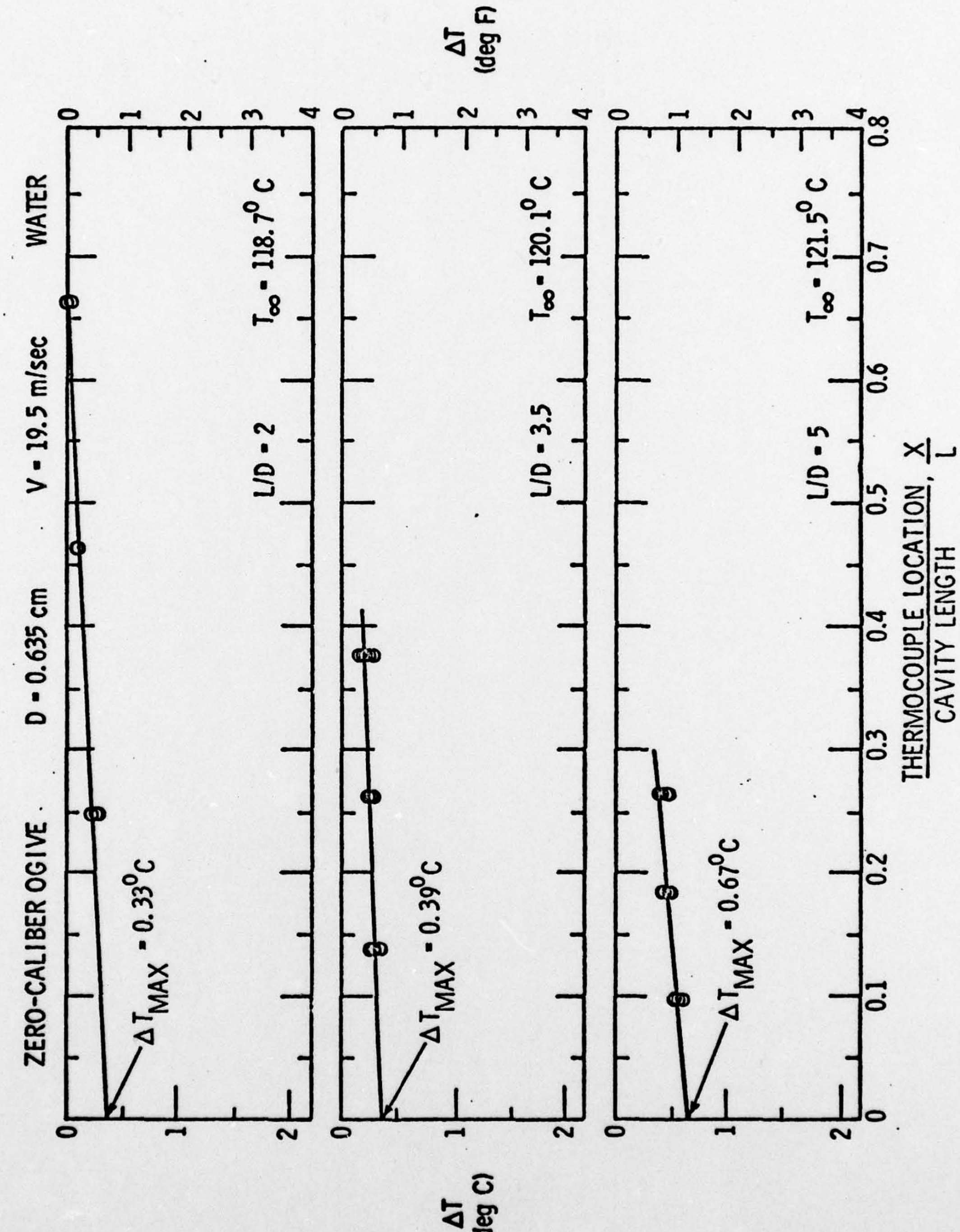

Figure 66 - ΔT vs X/L for T_∞ = 118.7, 120.1, and 121.5°C:
ZCO, D=0.635 cm, V=19.5 m/sec, Water

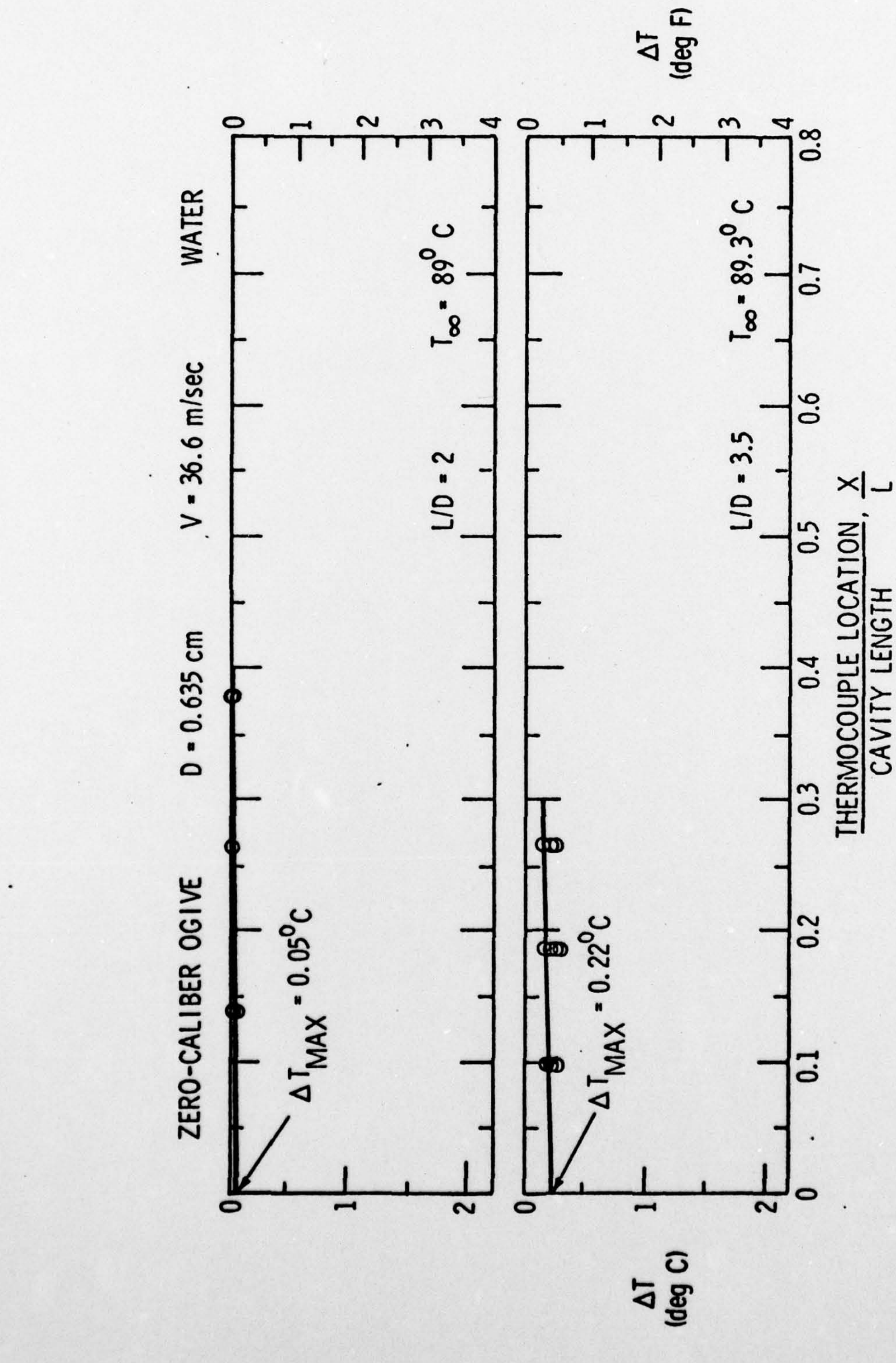

Figure 67 - ΔT vs X/L for T_∞ = 89.0 and 89.3°C: ZCO, D=0.635 cm, V=36.6 m/sec, Water

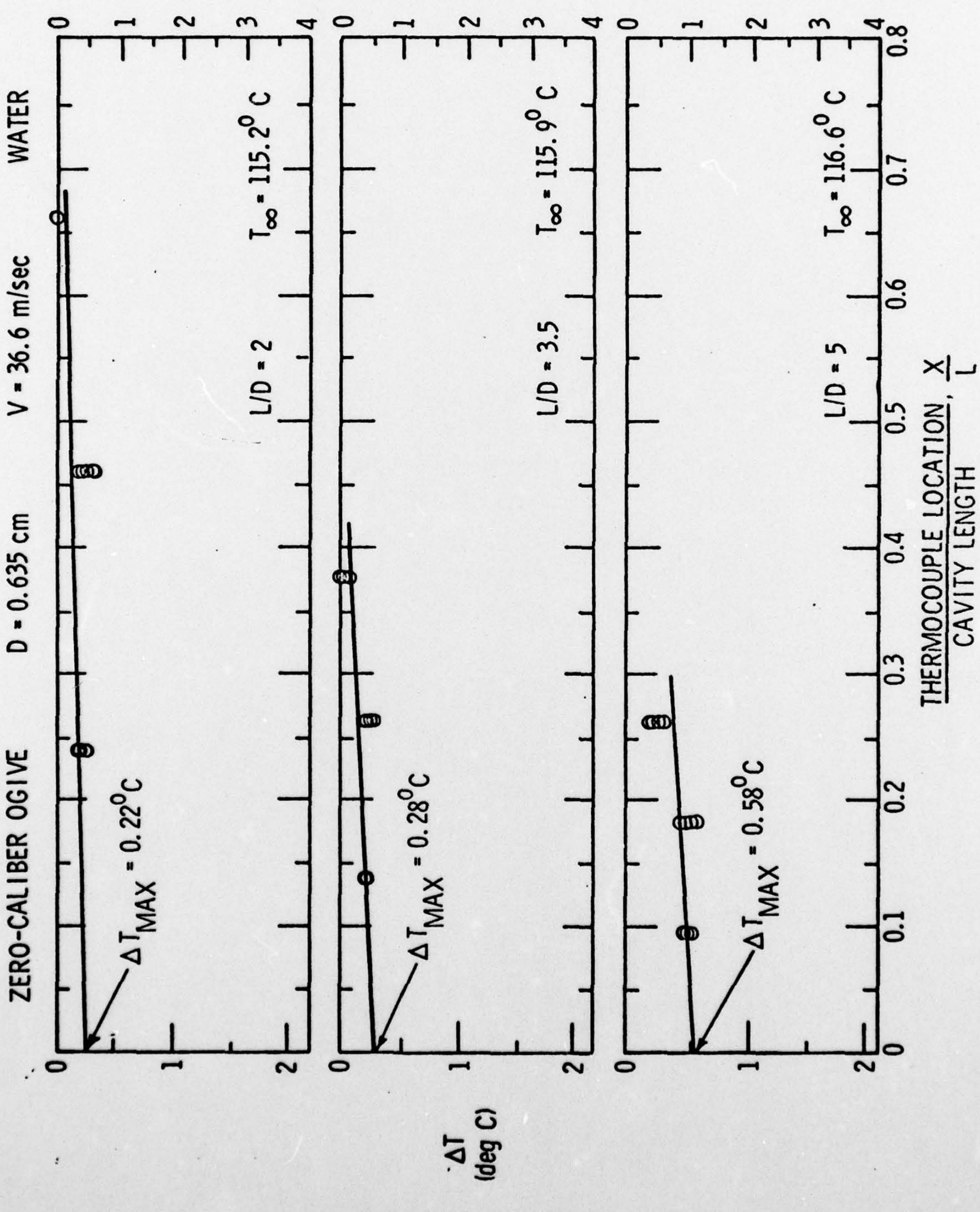

Figure 68 - ΔT vs X/L for T_∞ = 115.2, 115.9, and 116.6°C: ZCO, D=0.635 cm, V=36.6 m/sec, Water

DISTRIBUTION LIST FOR UNCLASSIFIED TM 78-18, by J. W. Holl, M. L. Billet, and D. S. Weir, dated 30 January 1978

Commander
Naval Sea Systems Command
Department of the Navy
Washington, DC 20362
Attn: Library
Code NSEA-09G32
(Copy No. 1 and 2)

Naval Sea Systems Command
Attn: T. E. Peirce
Code NSEA-0351
(Copy No. 3)

Commanding Officer
Naval Underwater Systems Center
Newport, RI 02840
Attn: Library
(Copy No. 4)

Commanding Officer
Naval Ocean Systems Center
San Diego, CA 92152
Attn: Library
(Copy No. 5)

Commander
Naval Surface Weapon Center
Silver Spring, MD 20910
Attn: Library
(Copy No. 6)

Commander
David W. Taylor Naval Ship R&D Center
Department of the Navy
Bethesda, MD 20084
Attn: Library
(Copy No. 7)

Defense Documentation Center
5010 Duke Street
Cameron Station
Alexandria, VA 22314
(Copy No. 8 - 19)

Dr. Allan J. Acosta
Prof. of Mechanical Engineering
Division of Engineering and
Applied Science
California Institute of Technology
Pasadena, CA 91109
(Copy No. 20)

National Aeronautics and Space Administration
Lewis Research Center
Mail Stop 5-9
21000 Brookpark Road
Cleveland, Ohio 44135
Attn: Mr. Werner R. Britsch
(Copy No. 21 - 23)

National Aeronautics and Space Administration
Attn: Mr. M. J. Hartman
(Copy No. 24)

National Aeronautics and Space Administration
Attn: Mr. T. Gelder
(Copy No. 25)

National Aeronautics and Space Administration
Attn: Mr. R. Ruggeri
(Copy No. 26)

Mr. L. Gross
R-P and VE
Marshall Space Flight Center
Huntsville, Alabama 35912
(Copy No. 27)

NASA Scientific and Technical Information
Facility
Post Office Box 8757
Baltimore/Washington International Airport
Baltimore, MD 21240
(Copy No. 28 - 32)

Dr. F. G. Hammitt
Professor of Mechanical Engineering
The University of Michigan
Ann Arbor, Michigan 48105
(Copy No. 33)

Institute of High Speed Mechanics
Tohoku University
Sendai, JAPAN
Attn: Library
(Copy No. 34)

DISTRIBUTION LIST FOR UNCLASSIFIED TM 78-18, by J. W. Holl, M. L. Billet and D. S. Weir, dated 30 January 1978 (continued)

Mr. Jesse Hord
Cryogenic Engineering Laboratory
U. S. Department of Commerce
National Bureau of Standards
Boulder Laboratories
Boulder, Colorado 80302
(Copy No. 35)

Dr. E. Reshotko
Case Western Reserve University
10900 Euclid Avenue
Cleveland, Ohio 44106
(Copy No. 36)

Rocketdyne Division
North American Aviation
6633 Canoga Avenue
Canoga Park, CA 91303
Attn: Library
(Copy No. 37)

Aerojet General
Post Office Box 15847
Sacramento, CA 15813
Attn: Library
(Copy No. 38)

Dr. Paul Cooper
Ingersoll Rand Research
Incorporated
Box 301
Princeton, NJ 08540
(Copy No. 39)

2LT. Donald S. Weir
5418 D Gilkey Street
Fort Knox, Kentucky 40121
(Copy No. 40)

Mr. Michael L. Billet
The Pennsylvania State University
APPLIED RESEARCH LABORATORY
Post Office Box 30
State College, PA 16801
(Copy No. 41)

Dr. J. W. Holl
The Pennsylvania State University
APPLIED RESEARCH LABORATORY
Post Office Box 30
State College, PA 16801
(Copy No. 42 - 44)

GTWT Library
The Pennsylvania State University
APPLIED RESEARCH LABORATORY
Post Office Box 30
State College, PA 16801
(Copy No. 45)